Universidade de Aveiro Departamento de Ambiente e Ordenamento
2011

GANESH K.C.

NUMERICAL MODELING OF GROUNDWATER IN KATHMANDU VALLEY, NEPAL

Funded by ERASMUS Mundus Mobility for life Project of the European Commission (EU)

Universidade de Aveiro
2011
Departamento de Ambiente e Ordenamento

GANESH K.C.

Modelação numérica das águas subterrâneas no vale de Kathmandu, Nepal

Dissertação apresentada à Universidade de Aveiro para cumprimento dos requisitos necessários realizada sob a orientação científica da Maria Teresa Condesso de Melo (orientador), Departamento de Departamento de Geociências, Universidade de Aveiro e de Celeste de Oliveira Alves Coelho (Co-Orientadora), Departamento de Ambiente e Ordenamento da Universidade de Aveiro.

Financiadas pelo Erasmus Mundus para o Projeto de Mobilidade vida da Comissão Europeia (UE))

o júri

Presidente

Ana Isabel Couto Neto da Silva Miranda
Professora Associada com Agregação no Departamento de Ambiente e Ordenamento da Universidade de Aveiro

Maria Teresa Condesso de Melo (Orientadora)
Equiparada a Investigadora Auxiliar no Centro de Geo-Sistemas do Instituto Superior Técnico de Lisboa

Celeste de Oliveira Alves Coelho (Co-Orientadora)
Professora Catedrática no Departamento de Ambiente e Ordenamento da Universidade de Aveiro (Co-Orientadora)

Tibor Stigter
Equiparado a Investigador Auxiliar no Centro de Geo-Sistemas do Instituto Superior Técnico de Lisboa

Acknowledgement

The dissertation is conducted for the master degree in Water Resouces Engineering at Tribhuvan University, Pulchowk Campus, Nepal. I would like to express my appreciation to the Erasmus Mundus Mobility for Life Project coordinated by Center for TeleInfraStruktur, Aalborg University, Denmark which gave me oppertunity to conduct my dissertation in the University of Aveiro, Portugal. I would like to gratefully acknowledge University of Aveiro for the help and support.

I am indebted to my supervisor Dr. Maria Teresa Condesso de Melo for her unceasing support, guidance and encouragement throughout my dissertation. I benefitted a lot from discussion I had with her owing to which I gained a deeper insight into and understanding of the groundwater modeling. I really appreciate her constructive critism and valuable advice which helped me to develop research and writing skills. I would like to thank co-supervisor Dr. Celeste Oliveira Alves Coelho for her valuable help during my dissertation.

I would like to express my appreciate to Prof. Dr. Bhakta Bahadur Ale, coordinator of Erasmus Mundus Mobility for Life for home university and Prof. Dr. Ana Isabel Miranda, coordinator for host university for their encouragement and support. During my dissertation, International office of University of Aveiro specially Neil Power, Marta Pereira, Helena Barbosa and Lucia Avelar helped me a lot and is highly appreciated.

I take this oppertunity to express my sincere thank to Nepal Electricity Authority for providing me study leave during this period.

To all my teacher in Water Resources Engineering Department of Institute of Engineering, Pulchowk Campus specially Prof. Dr. Narendra Man Shakya as Coordinator and Supervisor, I would like to express deep respect of the help, encouragement and providing knowledge and skills.

I am most thankful to Bishnu Prasad Pandey and Futuba Kazama of University of Yamanashi, Japan who help me by providing valuable data for my research. I would like to thank all my friends specially Ram Narayan shrestha, Tikaram Baral, Bhusan Acharya, Rupesh Mahat and Manoj shrestha for the help in collecting required data for the dissertation.

Finally I would like to express deepest gratitute to my parents and family member for their sacrifice and tenderness of a lifetime. I devote, last but never the least, gratitute to my wife, Rekha Bista and my son for her patience, love and encouragement during my absent at the time of need.

Palavras-chave modelo de fluxo subterrâneo, estado estacionário, vale de Katmandu, recarga subterrânea, balanço hídrico

Resumo

Foi desenvolvido um modelo numérico tridimensional de fluxo subterrâneo do vale de Katmandu (capital do Nepal) para avaliar o impacto da bombagem de água subterrânea sobre o padrão do fluxo de água subterrânea. Devido à escassez e contaminação da água de superfície, as águas subterrâneas constituem na região a principal fonte de água para abastecimento doméstico, agrícola e mesmo industrial. No entanto, apesar da importância local das águas subterrâneas, a hidrogeologia do vale de Katmandu ainda não se encontra bem estudada. Sabe-se que devido à recarga limitada e à captação não regulamentada de águas subterrâneas, o nível piezométrico da região tem decaído rapidamente, para valores que revelam a não sustentabilidade da captação deste recurso de água.

Dados geológicos e hidrogeológicos foram integrados para desenvolver um modelo hidrogeológico conceptual do sistema aquífero do vale de Katmandu, que foi a base para o desenvolvimento do modelo numérico. O sistema aquífero foi modelado numericamente utilizando o programa MODFLOW 4.2, em estado estacionário e definindo três camadas, duas correspondentes ao aquífero da base e ao aquífero mais superficial, e a terceira a um nível de baixa condutividade hidráulica e com um comportamento de aquitardo. Foi utilizado o programa MODPATH para simular os sentidos e direcção preferenciais de fluxo subterrâneo.

A área total do modelo é de cerca de 327 km^2 e foi dividida em células de aproximadamente 18,330 m^2. Os limites do modelo foram delimitados com com base em mapas topográficos e o modelo digital do terreno extraído a partir de uma imagem raster. Os parâmetros hidráulicos do sistema aquífero foram atribuídos com base nos valores de estudos anteriores e foram ajustados durante a calibração do modelo. O mecanismo de recarga foi considerado como principal entrada directa de água no aquífero e dá-se por infiltração da água das chuvas. Utilizou-se o método do balanço hídrico recomendado pela FAO para determinar o valor de recarga anual de água subterrânea. O modelo foi calibrado a partir de valores de níveis água subterrânea medidos nos furos de bombagem e que são monitorizados.

A modelação do fluxo subterrâneo em estado estacionário permitiu determinar gradientes hidráulicos, velocidades aparentes e padrões de fluxo no interior da área de estudo. O modelo foi utilizado para simular em regime estacionário as condições de bombagem em 2001 e 2009, pretendendo-se com este exercício demonstrar o impacto da captação de água subterrânea na região. As análises da sensibilidade permitiram determinar quais os parâmetros mais importantes para o modelo e quais aqueles que necessitam de serem melhor estudados. Este modelo de fluxo tem associadas uma série de incertezas resultantes da simplificação de dados de entrada e condições de contorno que foi preciso fazer para poder simular um caso de estudo tão complexo, da utilização de dados com pouca qualidade e da falta de caracterização detalhada das condições hidrogeológicas. É por isso importante ter em conta estas limitações a quando da interpretação e extrapolação dos resultados deste exercício de modelação.

Keywords model of groundwater flow, steady state, the Kathmandu valley, groundwater recharge, water balance

Abstract

We developed a three dimensional numerical model of groundwater flow in the valley of Kathmandu (capital of Nepal) to assess the impact of groundwater pumping on the flow pattern of groundwater. The scarcity and contamination of surface water, groundwater in the region constitute the main source of water supply for domestic, agricultural and even industrial. However, despite the importance of local groundwater hydrogeology of the Kathmandu valley is still not well studied. It is known that due to limited recharge and unregulated abstraction of groundwater, the groundwater level in the region has declined rapidly to values that show the unsustainability of the capture of this water resource.

Geologic and hydrologic data were integrated to develop a conceptual hydrogeologic model of the aquifer system of the Kathmandu valley, which was the basis for the development of the numerical model. The aquifer system was modeled numerically using the program MODFLOW 4.2, steady state and defining three layers, two corresponding to the aquifer base and the more shallow aquifer, and the third level of a low hydraulic conductivity and with an attitude of aquitard. MODPATH program was used to simulate the sense and direction of preferential groundwater flow.

The total area of the model is approximately 327 km2 and is divided into cells of about 18.330 m2. The boundaries were marked with the model based on topographic maps and digital terrain model extracted from a raster image. The hydraulic parameters of the aquifer system were assigned based on values from previous studies and were adjusted during model calibration. The reloading mechanism was considered as the main direct entry of water into the aquifer and occurs by infiltration of rainwater. We used the water balance method recommended by FAO to determine the value of annual recharge of groundwater. The model was calibrated with values measured groundwater levels in boreholes and pumping stations that are monitored.

The modeling of groundwater flow in steady state allowed us to determine hydraulic gradients, apparent velocities and flow patterns within the study area. The model was used to simulate steady state conditions of pumping in 2001 and 2009, intending with this exercise to demonstrate the impact of abstraction of groundwater in the region. The sensitivity analysis allowed to determine what the most important parameters for the model and which ones need to be better studied. This flow model has an associated range of uncertainties arising from the simplification of input data and boundary conditions that we had to do in order to simulate a very complex case study, using data with poor quality and lack of detailed characterization of the conditions hydrogeological. It is therefore important to consider these limitations when interpreting and extrapolating the results of this modeling exercise.

This thesis is dedicated to my parents,

Beloved Wife Rekha

And my son

TABLE OF CONTENTS

List of Figures

List of Tables

Acronyms

BBWMS – Bagmati Basin Water Management Strategy

BDFID - British Department for International Development

BGS – British Geological Survey

DEM – Digital Elevation Model

DFID – Department of International Development (UK)

DMG – Department of Meteorology and Geology

DOI – Department of Irrigation (Nepal)

DSMW – Digital Soil Map of the World

FAO – Federation of Agriculture Organization

GCN – Gosainkund Crystalline Nappe

GIS – Geographical Information System

GWD – Groundwater District

GWDB – Groundwater Development Board

GWRDP – Groundwater Resources Development Project

HHC – Higher Himalayan Crystalline

ISET-Nepal- Institute of Social and Environmental Transition Nepal

JICA – Japan International Cooperation Agency

KCN – Kathmandu Crystalline Nappe

KMC – Kathmandu Metropolitan City

KUKL – Kathmandu Upatyaka Khanepani Limited

LSGA – Local Self Governing Act

mbgl – meter below ground level

MCT – Main Central Thrust

MLD – Million Liters per day

NGO – Non Governmental Organization

NWSC – Nepal Water Supply Corporation

RME – Residual Mean Error

RMS – Root Mean Squared

SMEC – Snowy Mountain Engineering Corporation

USGS – United States Geological Survey

WSSC – Water Supply and Sewerage Corporation

List of Symbols

A – area

B(m) – Soil moisture balance for the month

Eta (m) – Actual evapotranspiration for the month

Eto – Reference evapotranspiration for the month

ft – feet

h – Hydraulic head

K – hydraulic conductivity

m – Metre

MCM – million cubic meters

mm – millimeter

^{o}C – Degree Celsius

^{o}F – Degree Fahrenheit

P(m) – Precipitation for the month

pF – Suction pressure

Prd – Period of evapotranspiration reduction

qx, qy, qz – Velocity component in x, y and z direction respectively

RP – Reduction point

s – second

S – Storage coefficient

Sav (m) – Available soil moisture for the month

Seav – Easily available soil moisture

Smax – Maximum soil moisture storage capacity

T – Transmissivity

1

INTRODUCTION

Different myths are famous about the draining of the Kathmandu valley. Hindus believe that lord Krishna drained the lake by cutting the gorge at Chobhar, south of the Kathmandu valley with its weapon known as “Sudarshan Chakra”. He came to Kathmandu valley with other cow herders from Dwarika (a palce in the India which is believed to have been sunk in the ocean). Buddhist claim that the Bodhisattva Manjushree came to Nepal from Tibet for the meditation at a place Called Nagarjun hill. Then he cut the mountain at Chobhar with one blow of his sword and the lake was drained.

1.1 Background

Groundwater is the subsurface water that occurs beneath the water table in the soils and geological formations that are fully saturated. Groundwater is one of the key natural resources of the world. Many major cities and small towns in the world depend on groundwater for water supplies, mainly because surface water has been impacted by human activities and surface water is not adequate in some places. Also quality of groundwater is more stable than surface water. Groundwater use has fundamental importance to meet the rapidly expanding urban, industrial and agricultural water requirements where surface waters are scarce and seasonal. Uneven distribution of surface water resources resulted in an increased emphasis on development of groundwater resources.

An important objective of most groundwater studies is to make a quantitative assessment of the groundwater resources in terms of the total volume of water stored in aquifer or long-term average recharge. Groundwater recharge is determined to a large extent as an imbalance at the land surface between precipitation and evaporative demand. When precipitation exceeds evaporative demand by an amount sufficient to replenish soil, water storage, any further excess flows deeper into the ground and arrives at the water table as recharge.

Groundwater abstractions that exceed the average recharge results in a continuing depletion of aquifer storage and lowering of the groundwater table. Hence safe groundwater abstraction and proper groundwater management is crucial for sustainability of the resource. Safe yield is the amount of naturally occurring groundwater that can be withdrawn from an aquifer on a sustained basis, economically and legally, without impairing the native ground water quality or creating undesirable effects, such as environmental damage (Fetter, 2001).

Groundwater systems have been studied by the use of computer based mathematical models (Brassington, 1998). These essentially comprise a vast array of equations, which describe groundwater flow and the water balance in the aquifer. Finite difference method is a commonly used method to solve the equations. The equations are solved for each node and the movement of groundwater from one node to its neighbor is calculated. As discussed by Scanlon *et al.* (2003), numerical groundwater models are one of the best predictive tools available for managing water resources in aquifers. These models can be used to test or refine different conceptual models, estimate hydraulic parameters and, most importantly for water-resource management, predict how the aquifer might respond to changes in pumping and climate.

Kathmandu valley is the most densely and haphazardly populated city in Nepal. Hence Kathmandu valley is facing the water scarcity particularly in dry season. Due to the complex geological setting with the renewal rate of ground water resources is very low. Unplanned urbanization and rapid growth of population in the study area lead to the over pumping of the groundwater which leads to the over exploitation of the groundwater resources.

1.2 Problem statement

The major resource of water in the Kathmandu valley is ground water and is facing water scarcity problems particularly during the dry season. The major resource of water in the Kathmandu valley is ground water but due to its complex geological setting, the renewal rate of ground water resources is very low. Unplanned urbanization and rapid growth of population in the study area lead to the over pumping of the groundwater which lead to the over exploitation of the groundwater resources.

The main source of the surface water in the Kathmandu valley is Bagmati river and its tributaries which flows downstream in the middle of the settlements suffering gradual deterioration of the quality of water.

Due to the rapid population growth and unplanned urbanization, a number of pumping wells as well as groundwater abstraction has been increasing to meet the demand (Fig 1.1 & Fig 1.2). The demand of water for domestic as well as industrial use is growing fast and hence the pressure on the field will be even more serious in the future. Abstraction of the groundwater has an associated impact on the water balance and hence on the availability of the water resources. It has been reported that the water table of the Kathmandu valley is continuously declining (Shrestha, 2002). The hydrogeological setting of the valley is more complex and groundwater flow pattern is not well defined. Thus understanding of the aquifer system and assessment of the water balance component of the groundwater basin is crucial for the sustainability of the resources. To understand the effect of abstraction and other forces on the groundwater flow system, it is worthwhile to develop a groundwater flow model simulating not only the groundwater flow but also the impact of abstraction.

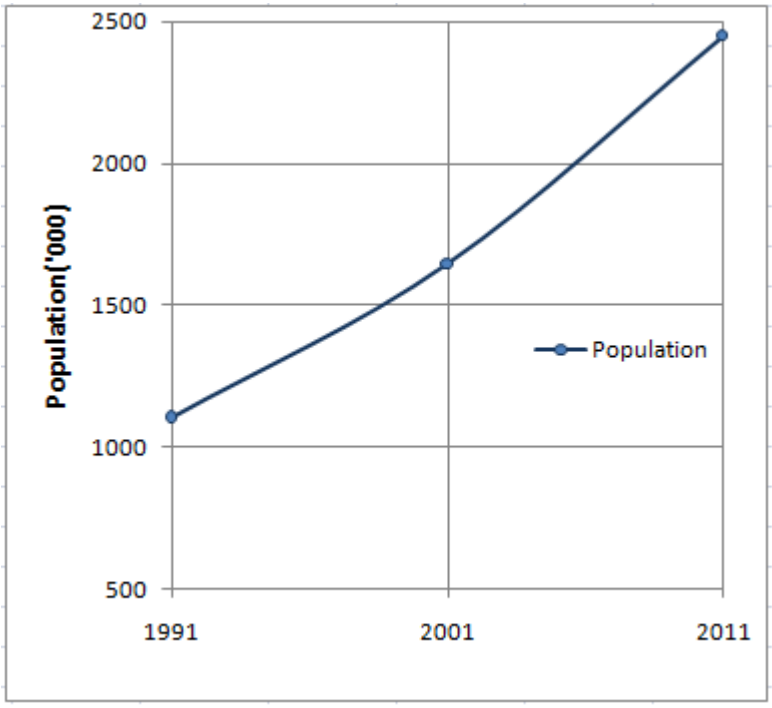

Fig 1.1: Graph showing the population trend in the Kathmandu valley (Population at 2011 is projected value)

The hydrogeological setting of the Kathmandu valley is complex and groundwater flow pattern is not well defined nor well understood. Thus understanding of the aquifer system and assessment of the water balance component of the groundwater basin is crucial for the sustainability of the resources. To understand the effect of abstraction and other human and environmental impacts on the groundwater flow system, it was decided to develop a groundwater flow model simulating not only the groundwater flow but also the impact of abstraction.

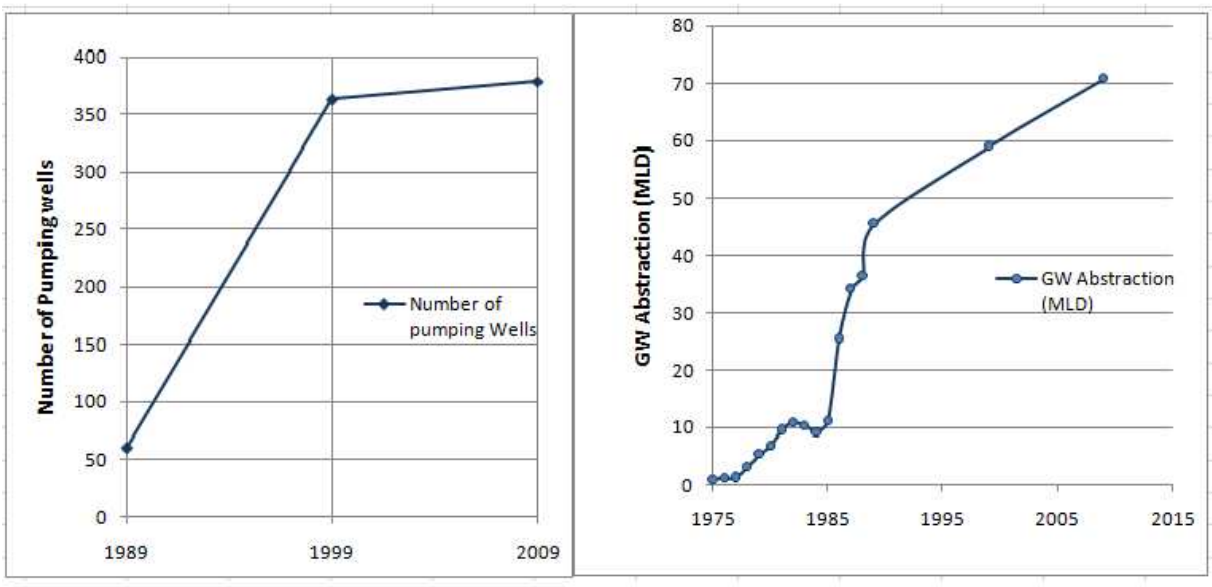

Fig 1.2: Graph showing the cumulative number of pumping wells and groundwater abstraction.

1.3 Research objectives

Groundwater systems in the Kathmandu valley are affected through increased withdrawal rates and low recharge. Groundwater is the source of drinking water as well as water for domestic use. Increased withdrawal rates, combined with the increase in impervious surfaces associated with urban areas may eventually over-stress the groundwater system.

There is an increasing number of public and private companies and industries which are exploiting the groundwater by pumping water with shallow and deep wells. This results in the lowering of groundwater table in Kathmandu valley which creates a great concern to the region. There have been already few hydrogeological studies but still the components of the

water balance are not yet well understood and not considered in the design of the well field. Hence it is necessary to carry researches to identify the main impacts of abstraction on the groundwater resources.

Also it has been found that the monitoring of groundwater level in the study area is very limited and discontinuous. There have been yet detailed modeling works of groundwater systems of the Kathmandu valley. Hence the necessity of a modeling study regarding the groundwater resources have been realized which will help to present the groundwater condition and to predict the effect of the abstraction.

Considering the above mentioned evidences, the main objective of the study is to assess groundwater resource of the well field and to improve the understanding of groundwater flow pattern in response to recharge and abstractions using groundwater flow model.

The specific objectives of the study are:

a) to develop a conceptual model representing the hydrogeological condition of the Kathmandu valley based on ground observations and data analysis;
b) to assess the water balance components of Kathmandu Valley;
c) to estimate groundwater recharge;
d) to model and simulate the groundwater of the Kathmandu valley;
e) to find the impact of groundwater abstraction on the decline of the groundwater.

1.4 Scope of work

The main tasks involved in this study include:

a) Collection and review the Quaternary geology and borehole data to develop the model for the study area.
b) to build the groundwater model for the study area.
c) to estimate the recharge of the study area using water balance method
d) to run the built groundwater model in the steady state condition.
e) to try to calibrate the model with respect to the measured water level at different well locations in the study area.
f) to use the calibrated model for the analysis of the outcomes of the model and thus to estimate the groundwater decline in the study area due to abstraction

g) to simulate the steady state groundwater model using different properties and hence conduct the sensitivity analysis.

h) to verify the outcomes of the model with respect to different stresses (pumping, recharge, boundaries, etc).

1.5 Related studies at regional level

Several investigations have been carried out in the Kathmandu valley by different researchers.

Sharma & Singh (1966) studied the groundwater condition of the Kathmandu valley under the groundwater exploration program carried out by Nepal Government and Geological Survey of India. They conducted a detailed hydrogeological investigation followed by drilling and compiled a number of exploratory drilling results from the Kathmandu valley. They concluded that the total thickness of the sediments varies in different parts and also that water quality is not good since it is contaminated with methane gas, hydrogen sulphide and iron and silica content. They also concluded that the quantity of water is better in the area further north.

Binnie & Partner (1973) had carried out groundwater investigation on Kathmandu water supply and sewerage scheme. They classified the aquifer layers in seven types as interbedded, linear, bedrock, basal gravel, river deposit, gravel fans and surface gravel. According to the research, the aquifer of the Northern Valley are highly stratified and contains layers of all gradations of sediments from boulders through mixed sand to silt and impermeable clay. They have calculated the transmissivity value between 92 to 301 m^3/day/m and hydraulic conductivities ranges from $1.4x10^{-4}$ to $1.7x10^{-5}$ m/s.

Yamanaka (1982) studied the geology of Kathmandu Valley. He divided the fluvio-lacustrine sediments of the Kathmandu Valley into Pyangaon terraces, Chapagaon terraces, Boregaon terraces, Gokarna formation, Upper Thimi formation, Upper Patan formation, Patan formation, Lower terraces and Flood plain.

Yoshida & Igarashi (1984) studied the lacustrine as well as fluvial deposits of the Kathmandu Valley. The fluvio-lacustrine of the Kathmandu Valley consists of peat, clay, carbonaceous clay, sand and gravel. They have divided these sediments into eight stratigraphic units.

Dangol (1985,1987) divided the fluvio-lacustrine deposit of the Kathmandu valley into four groups according to their geological components as Kalimati clay, Chhampi Itaiti gravel, Nakhu Khola mudstone and Keshari Nayakhadi lignite and Tarephir Basal.

JICA (1990) carried out the research project on the topic “Groundwater Management Project in Kathmandu Valley”. According to the research, availability of the groundwater recharge is controlled by widespread distribution of the lacustrine deposits interbedding impermeable black clay which prevents easy access to water. In the research, historical data on well hydrograph have been used to assess seasonal fluctuation of groundwater level and recharge into the main aquifer. Trial and error method has been applied in order to make calculated groundwater level of main aquifer layers to coincide with the observed ones. They have divided the Kathmandu valley into three groundwater districts (GWD) - Northern GWD, Central GWD and Southern GWD. The research states that the northern groundwater district contains permeable sediments whereas southern and central groundwater district consists of low permeable sediments.

Gautam & Rao (1991) carried out a study on the evaluation and estimation of the total groundwater resources within the Kathmandu valley. They had classified the study area into four aquifer zones as unconfined aquifer zone, two aquifer zones, confined aquifer zone and no groundwater zone. The unconfined aquifer zone and the two aquifer zone lies in the northern part of the Valley. The confined aquifer zone lies in the central part of the valley and no groundwater zone lies in the southern part (Sunakhothi and Lubhu area) of the Kathmandu valley.

Department of Meteorology and Geology, Nepal (1998) prepared the engineering and environmental geological map of the Kathmandu valley and divided fluvio-lacustrine of the study area into seven formation as basal boulder bed, Lukundol formation, Kabgaon formation, Kalimati formation, Chapagaon formation, Gokarna formation and Tokha formation.

Metcalf and Eddy (2000) in association with CEMAT Consultant designed and initiated groundwater monitoring in 1999 under a project “Urban Water Supply Reforms in Kathmandu Valley”. Some wells were selected for the groundwater levels and for water quality monitoring. They concluded that the groundwater levels have been declining due to abstraction. After completion of the project in 2001, Groundwater Resources Development Project (GWRDP) under Department of Irrigation (DOI) took the responsibility of monitoring.

Sakai (2001) made a detailed study of the valley fill sediment deposits. Three bore holes were drilled in different places and detailed investigation carried out. Based on drill core study and field observations, Sakai divided the southern part into three groups as Itaiti formation, Lukundol formation and Tarebhir formation whereas central part into three groups as Kalimati formation, Basal lignite member and Bagmati formation.

Shrestha (2002) studied about the assessment of effects due to the landuse change in the groundwater storage of the Kathmandu Valley. He selected the twelve deep tube wells for the study considering its coverage and availability of the drawdown data and created the thiessen polygon. It is assumed that the drawdown calculated for the well points will be uniform within the polygon area. The calculated drawdown data by JICA (1990) are used in this study. The drawdown is taken as aerial average and multiplied by Thiessen polygon coefficient for all well points and summed up to calculate equivalent drawdown for the basin. The author concluded that the groundwater storage is found to be decreasing and drawdown is found to be increasing. He exposed that the drawdown at Kathmandu Valley was 0.3 m in 1976 and increased up to 1.826 m in 1990.

A report (Dixit &Upadhya, 2005) has been prepared as a contribution to the project entitled “Augmenting groundwater Resources through artificial recharge”. The British Department for International Development (BDFID) commissioned the British Geological Survey (BGS) to undertake this project which runs from July 2002 to July 2005 through a program of collaborative studies with the Institute of Social and Environmental Transition Nepal (ISET-Nepal) and other NGO’s and universities of India. The project’s objective is to summarize existing knowledge on groundwater condition of Kathmandu valley and also identifying the potential avenues for enhancing groundwater availability to meet the water demand. The report has been prepared with an intensive survey of previous published and unpublished reports and accessible data with field visits. The study concluded that substantial opportunities may exist for groundwater recharge and water harvesting to supplement the water supplies at Kathmandu Valley. These opportunities may exist in the northern portion of the Kathmandu valley where the permeable nature of the valley fill and upper aquifer could allow both storage and recovery. This report also states that through carefully designed well field potentially enhanced by specific recharge facilities, it might be possible to operate this portion of aquifer as a reservoir. The report recommends for the actual evaluation with much more detailed analysis based on new field data on groundwater condition.

Pandey *et al* (2009) undertook a study for the evaluation of groundwater environment of the Kathmandu valley. This study attempts to evaluate current state of the groundwater environment considering the natural and social system together to better understand the origin of stresses eg their state, expected impact and response made to restore healthy groundwater environment. The methodology consists of collection of published and unpublished reports, papers, data and information related to the groundwater resources in the valley and analyze under the established framework. The study reveals that different stresses such as increase in population and urbanization which resulted in the increase in the groundwater abstraction. The abstraction rates (21.56 m^3/year) exceed the recharge (9.6 m^3/year) which resulted in the decrease in the groundwater by 13-33 m during 1980 to 2000(Metcalf and Eddy ,2000) and 1.38 to 7.5m during 2000 to 2008. He laos produced the gradual deterioration of groundwater quality.

Pandey & Kazama (2010) studied the hydrogeologic characteristics of groundwater aquifers in Kathmandu valley. The study uses GIS to map the spatial distribution of hydrogeologic characteristic such as aquifer thickness, transmissivity, and hydraulic conductivity of shallow and deep aquifer in the Kathmandu Valley. They collected different data from different sources such as borehole lithology, hydrogeology data (transmissivity, storage coefficient, discharge, and drawdown), and physical data. They established an empirical relationship between transmissivity and specific capacity for the shallow and deep aquifer and thus estimated the hydraulic conductivity and mapped hydraulic characteristics of shallow and deep aquifers. They classified the lithological information as shallow aquifer, aquitard and deep aquifer. Thus the thickness and spatial extent of the hydrogeologic layers over the entire area of the groundwater basin were delineated using ArcGIS 9.2 technique. They concluded that the conductivity of shallow aquifer layer ranges from 12.5 to 44.9 m/day whereas for deep aquifer, it ranges from 0.3 to 8.8 m/day.

Groundwater systems in the Kathmandu valley are effected through increased withdrawal rates and low recharge. Groundwater is the source of drinking as well domestic use. Increased withdrawal rates, combined with the increase in impervious surfaces associated with urban areas may eventually over-stress the groundwater system. Also it has been found that the monitoring of groundwater level in the study area is very limited and discontinuous. There is not detailed modeling works of groundwater of the Kathmandu valley. Hence the necessity of a modeling study regarding the groundwater has been realized which will help to present the groundwater condition and to predict the effect of the abstraction.

There is increasing number of public and private companies and industries which are exploiting the groundwater by extracting with shallow and deep wells. This results in the lowering of groundwater table in Kathmandu Valley which creates a great concern to the region. There has been already few hydrogeological studies but still the components of the water balance are not yet well understood and not considered in the design of the well field. Hence it is necessary to carry researches to identify the main impacts of abstraction on the groundwater resources.

1.6 Methodology and materials

The methods followed in the study are based on the objectives formulated. The methodology used in this study included several steps which are summarized in the flow chart shown in Fig 1.3.

First the objectives of the study were defined properly. Several groundwater flow models used in the different parts of the world were studied to understand the general concept about the groundwater model. Available studies of the Kathmandu Valley were collected and reviewed. This included geological, topographical, hydrogeological and different modeling studies on the study area.

The data needed for the study were collected from the local Water Authorities and company, government, published reports and papers. The data includes meteorological data, hydrological data, geological and hydrogeological data. Also water level monitoring data from March 2001 up to 2005 for some wells were collected which are discontinuous. Water withdrawal data from the groundwater basin were collected from the related authorities and reports. There are a lot of borehole logs in the study area but only around 49 borehole logs were collected which seemed to be inadequate. To better represent the real aquifer, some control points which consists of different aquifer thickness were collected from Digital Elevation Model (DEM) prepared by Pandey (2010). All the data are stored in the form of excel sheet, maps and charts.

These data were analyzed and processed so that they could be properly and accurately inputted to the model. Surfer 8 ® was used for the spatial integration of data such as preparation of contour maps of different layers of aquifer, contour map of initial groundwater level etc which could be directly inputted to the model.

The recharge to the groundwater in the Kathmandu Valley was estimated flowchart of which is presented in Fig 3.7.

For the modeling the conceptual model had been prepared for the aquifer system. It includes the delineation of aquifer layers in the area, rivers and boundary conditions.

After constructing the conceptual model, the software MODFLOW® had been selected as the computer code, which is the modular three dimensional finite difference groundwater model developed by U.S. Geological Survey (McDonald & Harbaugh, 1988; Harbaugh & McDonald, 1996). The model was designed consisting of grid design, assigning the aquifer parameters to each layer, selecting and defining suitable boundary condition, defining initial heads etc.

After completion of the model design, the model was run. Model was calibrated with the help of trial and error procedure. Calibration was performed in steady state condition and error analysis was done. After the model was calibrated, sensitivity analysis was done with changing the aquifer parameter and recharge with certain fraction to identify the sensitive parameters in the model. Model results were evaluated and drew conclusion along with future recommendations.

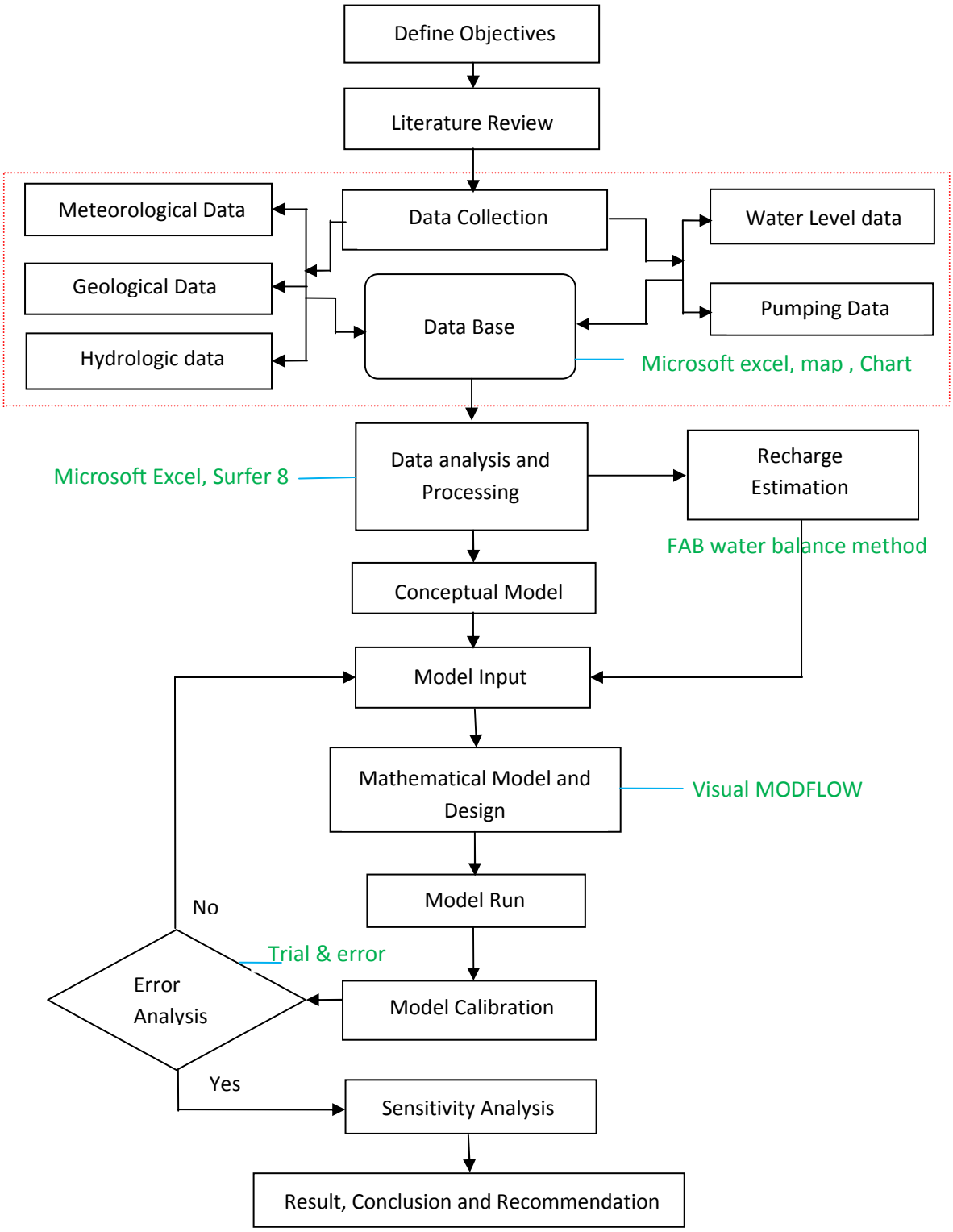

Fig 1.3: Flow chart showing the methodology of the study

1.7 Organization of the thesis

The thesis is divided in six chapters and the contents are outlined briefly as:

Chapter 1. Introduction: Describes the introduction of the research that includes the problem statement, the objective of the research which the research will solve on the basis of the available data and applied methodologies. Methods followed and materials used are also discussed in this introductory chapter. It includes the review of previous studies in the study area and literature review related to principle of groundwater modeling applied globally.

Chapter 2. Study area: General description of the study area. The Kathmandu valley is describer in this chapter in relation to location, climate, land use and soil cover, among other details.

Chapter 3. Geology and Hydrogeology: This chapter will describes about the geology of the study area. It includes the general geology and hydrogeological units of the study area. . Recharge to the aquifer is also estimated

Chapter 4. Groundwater Flow Modeling: This chapter is devoted to the processing and analysis of data (primary and secondary data) and involved in synthesizing and screening collected field data and translating the data to model input. It also includes the development of conceptual model of the area by defining the hydrostratigraphy and boundary condition. The selection of computer code and its description are included in this chapter. This chapter is also mainly designed to discuss the model design, model calibration and sensitivity analysis. Illustration and discussion of the modeling results are described in this chapter.

Chapter 5. Conclusion and recommendation: Conclusion and recommendations. Conclusions and recommendations will be made on the basis of the analysis result. In this final chapter, matters which cannot be addressed fully or partially are out lined and limitation of the research and possibilities of further research are indicated.

2

STUDY AREA

Kathmandu, Nepal's capital city, sits in a circular valley. It lies between the latitudes 27^{o} 32' 13" and 27^{o} 49' 10" north and longitudes 85^{o} 11' 31" and 85^{o} 31' 38" east and is located at a mean elevation of about 1,300 meters (4,265 feet) above sea level.

2.1 The Kathmandu valley

Kathmandu valley covers 656 km^2 and is surrounded by the Mahabharat Hills. The central part consists of gentle hills and flat lands at elevations of 1,300-1,400 m. The surrounding hills rise to about 2,000 m or more in elevation. Phulchoki to the south of the valley has the highest elevation at 2,762 m. East of the valley contains Nagarkot peak with an elevation of 1,895 m. Chandragiri peak in the west with elevation of 2,356 m and Shivapuri peak in the north with an elevation of 2,732 m surround the valley. The study area includes three major cities: Kathmandu, Bhaktapur and Lalitpur (also known as Patan).

2.2 Administrative division

Kathmandu valley comprises of three districts, Kathmandu, Lalitpur, and Bhaktapur, together which cover an area of 899 km^2, whereas the area of Kathmandu valley as a whole is 656 km^2. It encloses the entire area of Bhaktapur district, 85% of Kathmandu district and 50% of Lalitpur district (Pant & Dangol, 2009).

The three districts have a total of 150 local administrative units (Village Development Committees and Municipalities) out of which five city governments have the highest population and economic activities. Hence the Kathmandu valley is the most important urban concentration The Kathamndu valley has 1.6 million populations. Among them, Kathmandu district has 1.0 million, Lalitpur district has 0.33 million and Bhaktapur district has 0.22 million people. Being a capital city, Kathmandu valley in comparison to the rest of Nepal, possesses

basic amenities like water supplies, electricity, gas, telecommunications, roads, sanitation, education, security, and transportation. New technologies and interventions come to the capital first, and this technological sophistication along with other amenities is an important pull factor for rural to urban migration.

Kathmandu valley is the urban center of Nepal and includes five major cities: Kathmandu, Lalitpur, Bhaktapur, Kirtipur, and Thimi (Fig 2.1). Kathmandu Metropolitan City (KMC) is the largest city in Nepal and the cosmopolitan heart of the Himalayan region. With a history and culture dating back 2,000 years, the city, along with the other towns in the valley, ranks among the oldest human settlements in central Himalaya. Old Kathmandu corresponds to the current city core, encompassing a compact zone of temple squares and narrow streets.

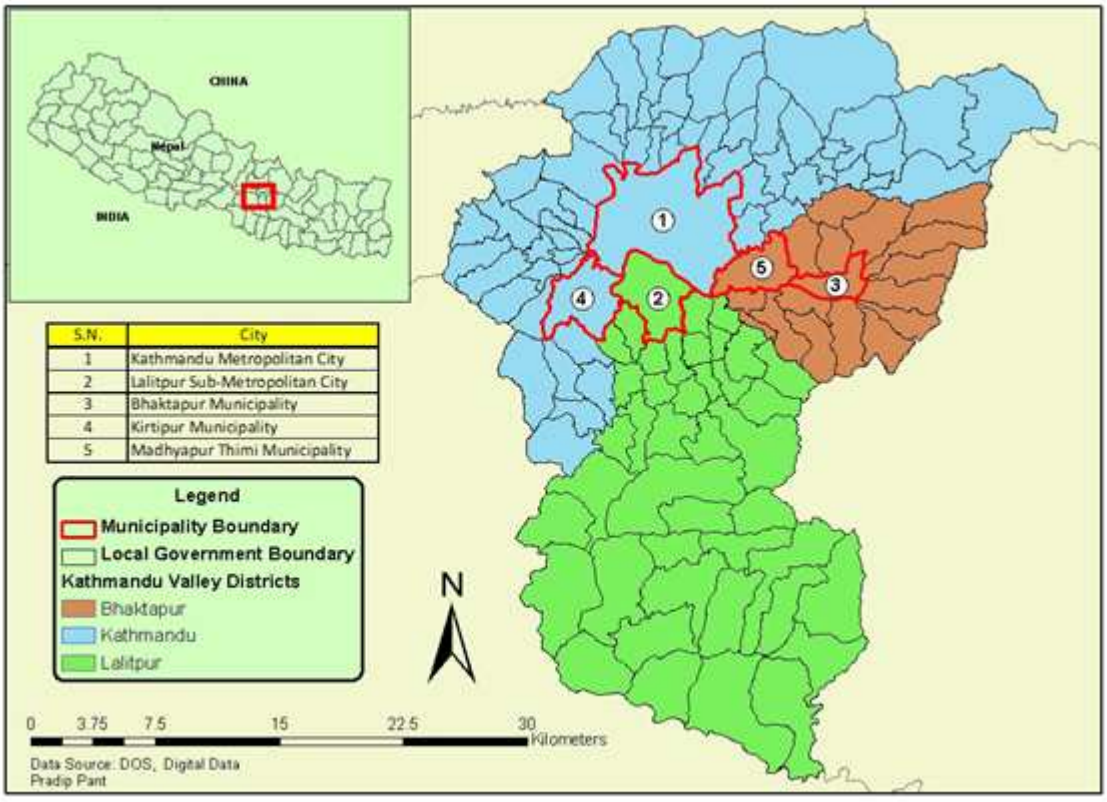

Fig 2.1: Location map of the Kathmandu valley

2.3 Population

Kathmandu valley has both urban and rural residents. Most of the rural population is engaged in agriculture as its primary source of livelihood. This is also the case with some families living in urban areas. Both push and pull factors have led to an increase in the population of the valley. It is difficult to estimate the actual rate of population growth though it has increased in each inter census period since 1951.

The core area of the Kathmandu valley is densely populated. The valley has 1.6 million people. Among them, Kathmandu district has 1 million, Lalitpur has 0.33 million and Bhaktapur district has 0.22 million population. The expansion of rural areas into adjacent urban areas is likely to continue without regulation.

Past studies have provided different estimates of the population and the rate of population growth has varied in different decades. After the Maoist insurgency began in 1996, security in most of rural Nepal deteriorated and those that could afford to migrated to Kathmandu valley. The resultant change in the rate of growth in Kathmandu has, therefore, made estimating the actual rate difficult. In recent years, migration from rural to urban areas has significantly increased due to economic opportunities in the city and to the deteriorating political conditions and ongoing violence in rural areas. The capital's population, currently estimated at over one million, will undoubtedly increase rapidly in the coming years**.** The expected growth rate of urban population is about five percent (Table 2.1). In the face of rapid growth, it has become increasingly difficult to meet the water needs of the population.

Table 2.1: Population growth rate predictions, 1994

District	1991 (nos)	2001 (nos)	Annual growth rate (%)
Kathmandu	675,341	1,081,845	4.71
Lalitpur	257,086	337,785	2.73
Bhaktapur	172,914	225,461	2.65
Total	1,105,379	1,645,091	4.06

Source: Central Bureau of Statistics, 2003

According to the census of 2001, the population of the districts of Kathmandu, Lalitpur and Bhaktapur was 1,645,091 people (including 42,826 people of the hilly area of Lalitpur that lies outside the valley) and that of the five municipalities within the area was 995,966. The total population in the Kathmandu valley was 1,602,265. With the average annual growth rate of 4.06%, the predicted population at 2011 will be 2.5 million.

Table 2.2: Population and density of the three districts of Kathmandu valley and their urban areas, 2001 (in number)

District	Total Population	Municipality population	Density (per km^2)
Kathmandu	1.081.845	Kathmandu: 671,846	13,586
		Kirtipur: 40,835	2,767
Lalitpur	337,785	Lalitpur: 162991	10,758
Bhaktapur	225,461	Bhaktapur: 72,543	11,058
		Madhyapur Thimi: 47,751	4,298
Total	1,645,091	995,966	
Total Population: 1,602,265			

Source: HMG, Central Bureau of Statistics 2002

Compared to Kathmandu district, there have been few changes in the size of the rural populations of Bhaktapur and Lalitpur districts as these comprise large rural areas. Table 2.2 does not include the transient population that comes to Kathmandu: short-term migrants from the hills, the Tarai and even from north India who come to work as daily wage laborers. Kathmandu Valley is like a hub for the wider population. The enactment of the Local Self Governing Act (LSGA) 1999 is expected to decrease the flow of the transient population to some extent (ICIMOD 2007). Large pockets of the population move in the valley for different purposes, mainly seeking services and institutional activities. Uneven allocation of resources for development and institutionalisation in the valley has given rise to this movement of population. The transient population is distributed sporadically throughout the valley, determined by the objectives of their visits. The main reasons for coming to the valley are higher education, medical check-ups, pilgrimages, bureaucratic formalities, visiting relatives, internal tourism, and official visits.

In early years before 1980s, the water supply needs of the city's residents were met using springs, rivers and shallow dug wells because of low population. Due to the increase in population, transient polpulation and haphazard settlement, surface water as wells as shallow well sources was getting polluted which in turn results in the increased abstraction of the groundwater resources especially by deep wells. This causes in the overstress in the groundwater resources and decline in the groundwater level.

2.4 Land Use

The Kathmandu valley floor is found to be extensively farmed. The land use type is mixed. The urban areas are covered with houses and pavings whereas rural areas are not so much inhabited. The rural areas consist of cultivated land, forest and water bodies. The landuse of the Kathmandu has not changed in rural areas but extensively changed in urban areas. The area that is currently being absorbed into urban Kathmandu is undergoing changes in land use practices. The city has grown in all directions, but it is denser to the north. Kathmandu has also encroached on the adjacent districts of Bhaktapur and Lalitpur. The conversion of rural land into urban has a disproportionate impact on the groundwater situation. It has led to increased pumping in many areas and, probably more importantly, extensive pollution of both surface streams and the upper aquifer. Most development activities are located along rivers, which probably serve as recharge zones where pumping has lowered groundwater levels in the upper phreatic aquifer. As residential areas have expanded, trails and footpaths have been converted into poor quality roads. Riverbanks, once used as footpaths to access farmland along rivers, have also been converted into roads. The trend of converting agricultural areas into residential properties has been increasing. All major rivers in the valley have roads and housing complexes on either side of them. Table 2.3 shows that over 56 percent of the area within metropolitan Kathmandu is residential.

Table 2.3: Land use pattern in municipalities of Kathmandu valley (value in the bracket denotes percentage)

Land use type	Kathmandu (ha)	Kirtipur (ha)	Lalitpur (ha)	Bhaktapur (ha)	Madhyapur (ha)
Built up	2592.7 (48.89)	163.05 (10.31)	673.06 (43.6)	145.46 (21.5)	183.73 (16.02)
Cultivation	891.18 (16.8)	944.08 (59.71)	395.12 (25.59)	383.97 (56.76)	712.26 (62.10)
Open area	571.17 (10.77)	37.85 (2.39)	57.54 (3.73)	19.87 (2.94)	17.03 (1.48)
Road	386.89 (7.29)	41.33 (2.61)	95.29 (6.17)	33.61 (4.97)	51.93 (4.53)
Plantation	190.72 (3.6)	194.13 (12.28)	17.12 (1.11)	79.03 (2.15)	47.56 (4.15)
Others	671.0 (12.65)	200.58 (12.7)	305.64 (19.80)	93.59 (11.68)	134.37 (11.72)

Source: Kathmandu valley profile, Pant & Dangol (2009)

Village Development Committees in the study area, a significant percent of land use is cultivation land.

With urbanisation, the pattern of land use is constantly and rapidly changing. As previously mentioned, rural land once used for agriculture is being converted into residential area. The expected annual rate of conversion of rural land to urban area, measured by the Bagmati Basin Water Management Strategy (BBWMS) of 1994, is shown in Table 2.4.

Table 2.4: Conversion of rural land into urban uses

District	1991-2001	2001-2011
Kathmandu	2%	3%
Lalitpur	0.5%	2%
Bhaktapur	0.5%	2%

Source: HMG (1994)

Changes in land use affect the regional hydrological regime, which in turn causes a social response. With increasing urbanization, more area comes under construction, which may be reducing the permeable area. As a result, less rainwater probably infiltrates into the ground, thereby reducing groundwater recharge. In addition, with an increase in impervious areas, more runoff is generated when it rains. Such runoff scours channels and increases the rate at which water flows out of the Kathmandu valley, probably further reducing groundwater recharge. Building foundations and sewer drainage block subsurface flow. Although no detailed studies have been done, some studies suggest that less infiltration, blockage of subsurface flow and increased runoff reduces soil moisture and affects the groundwater situation.

2.5 Climate

Climatic conditions vary to a large extent in view of several geographical factors (topography and altitude). Five major climatic regions have been deciphered in Nepal, out of which Kathmandu valley falls under the Warm Temperate Zone (elevation ranging from 1,200–2,300 meters (3,900–7,500 ft)) where the climate is fairly pleasant, atypical of the region. This zone is followed by the Cool Temperate Zone with elevation varying between 2,100 meters (6,900 ft) and 3,300 meters (10,800 ft). Portions of the city with lower elevations features, a mild form of a humid subtropical climate while portions of the city with higher elevations generally feature a sub tropical highland climate. In the Kathmandu valley, which is representative of its valley's climate the average temperature during the summer season varies from 28–30 °C (82–86 °F). During the winter season the average temperature is 10.1 °C (50.2 °F) (Table 2.5)

Table 2.5: Temperature data for Kathmandu valley

Month	**Average high (°C)**	**Average low (°C)**
January	18.0	2.1
February	20.2	3.8
March	24.3	7.5
April	27.4	11.3
May	28.2	15.5
June	28.3	19.0
July	27.7	20
August	28.0	19.7
September	27.2	18.2
October	25.8	13.0
November	22.7	7.4
December	19.4	3
Yearly	24.8	11.7

Source: World Weather Information Service-Kathmandu

The city generally has a salubrious climate with comfortable warm days followed by the cool mornings and nights. Unpredictability of weather is expected as during winter, temperatures during the winter months have dropped to 3 °C (37 °F). The rainfall which is mostly monsoon based (about 65% of the total concentrated during the monsoon months of June to August), which decreases (100 cm to 200 cm) substantially from eastern Nepal to western Nepal (Pant & Dongol, 2009). It has been recorded as about 1689 millimeters average annual precipitation for the Kathmandu valley. On an average Humidity is 75%.

3

GEOLOGY AND HYDROGEOLOGY

3.1 Geological Setting

Kathmandu valley is surrounded by high rising mountains ranges. Several low hills are aligned in the southwestern part. They connect the towns of Naikap, Kirtipur, Chovar, Thanagau, and Magargau from the northwest to the southeast. In a southeasterly extension of this line, there are low hills near Banegau. The surface of the Kathmandu valley is almost flat but it has buried bedrock surface with irregular shapes and high relief.

Geologically, Kathmandu valley comprises of basin fill fluvio-lacustrine sediments underlying the basement rocks of Pre-Cambrian to Devonian ages (Piya, 2004). The basement rocks mainly consists of phyllite, sandstones, slates, meta-sandstones, quartzite, siltstones, shales and crystalline limestone in the east, west and south of the valley whereas in the north and north-east site of the valley, it consists of gneiss, schist, granite etc. (Stockin and Bhattarai, 1977; Stocklin, 1980). The basin fill sediments are divided into two series of sediments namely Quaternary unconsolidated Sediment and Plio-Pleistocene slightly consolidated sediment (DMG, 1998).

The quaternary unconsolidated sediments are grouped into four formations; recent alluvial soil, residual soil, colluviums and alluvial fan deposit (Shrestha, 2010).

According to the type and distribution of Plio-Pleistocene sediment, it is grouped in to seven formations, namely- Tokha Formation, Gorkarna Formation, Chapagoan Formation, Kalimati Formation, Kobgoan Formation, Lukundol Formation and Basal Boulder Bed (Shrestha *et al*, 1998).

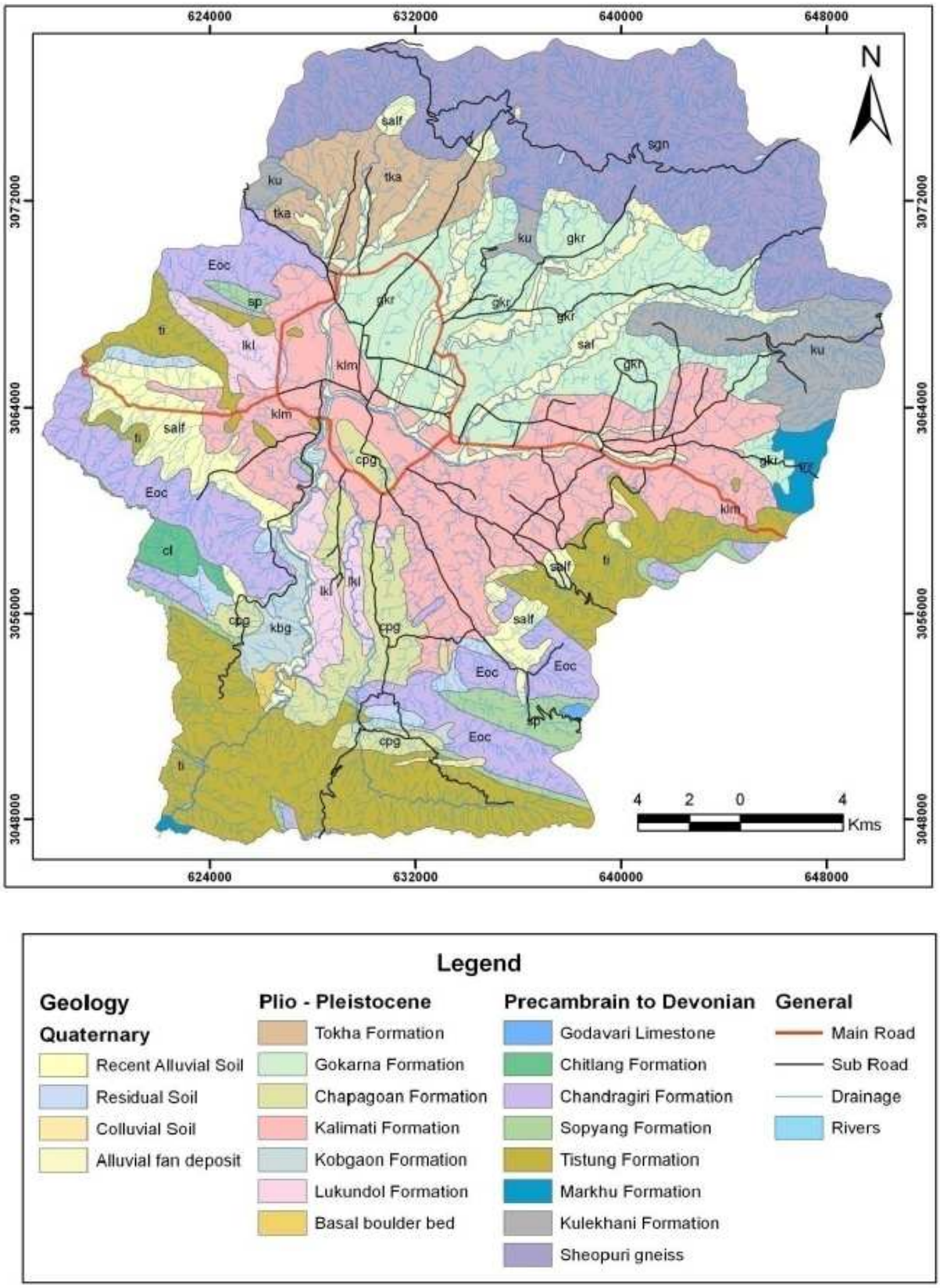

Fig 3.1: Geological map of the study area (modified from Stocklin and Bhattarai, 1977; Stocklin, 1980; DMG, 1998)

3.2 General basin fill sediment classification

The thick semi-consolidated fluvio-lacustrine sediment of Pliocene to Pleistocene age overlies the basement rock of the Kathmandu valley. The maximum depth of the valley sediment is more than 550 m on the basis of different borehole located on the central part of the valley (Piya, 2004). The source of the thick sediment is the surrounding hills. The sediment consists of Arenaceous sediments and argillaceous sediments. Aranaceous sediments composed of fine to coarse grained sand with a small quantity of rock fragments from northern gneiss rocks. Argillaceous sediments composed of clay and silt resulting from the erosion of limestone and phyllite in the eastern, southern and western mountainous areas. It also consists of agglomerate of boulder and gravel with a clayey and silty in the southern basin.

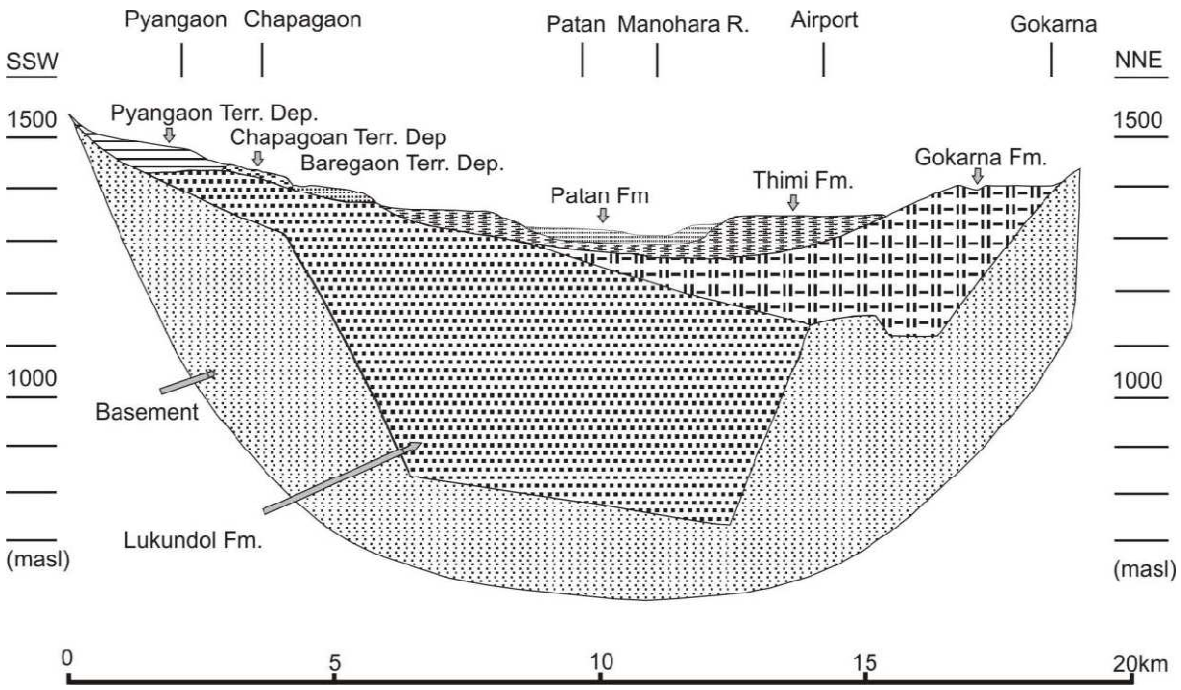

Fig 3.2: Schematic geological section of the Kathmandu Valley (after Yoshida and Igarashi, 1984; modified). The topography of the basement is after Moribayashi and Maruo (1980) in Grad (2009)

Different workers have worked on the classification of the Kathmandu valley basin fill sediments. The classification made by Yashida & Igarashi (1984) consists of seven stratigraphic units. Dangol (1985, 1987) classified the fill into four groups (Table 3.1). In the

classification of Dangol (1985, 1987) , Patan Formation, Thimi Formation and Gokarna Formation of Yoshida & Igarashi (1984) are combined into Kalimati clays, which are mainly distributed in the central part of the basin. Similarly all the terrace Formations and upper part of Lukundol formation of Yoshida & Igarashi (1984) are included by Dangol into three groups; Champi-itaiti gravel, nakhu khola mudstone and Keshari Nayakhandi lignite. Dangol (1985, 1987) made more simplified classification. The classifications and modifications made by different authors are summarized in Table 3.1. All the workers classified the basin fill according to the evidences obtained from the field work observations without any evidences of borehole log information. Hence Sakai (2001) has proposed a new classification based on the evidences from borehole log information as well as field observation. The schematic geological section of the Kathmandu valley has been shown in Fig 3.2.

Table 3.1: Correlation of stratigraphy of the Kathmandu Basin Fill by different workers

<table>
<tr><th rowspan="2">Yoshida &Igarashi (1984)</th><th rowspan="2">Dangol (1985,1987)</th><th rowspan="2">Shrestha et al (1998)</th><th colspan="2" rowspan="2">Sakai et al (2001)</th><th colspan="2">Sakai 2001</th></tr>
<tr><th>Southern part</th><th>Central part</th></tr>
<tr><td rowspan="2">Patan Fm</td><td rowspan="3">Kalimati Fm</td><td rowspan="3">Gokarna Formation

Tokha Formation</td><td rowspan="2"></td><td rowspan="2"></td><td rowspan="5">Itaiti Formation</td><td>Patan Fm</td></tr>
<tr><td rowspan="4">Kalimati Formation</td></tr>
<tr><td>Thimi Fm</td></tr>
<tr><td>Gokarna Fm</td></tr>
<tr><td>Boregaun Terrace deposit</td><td rowspan="4">Champi Itahari Gravel</td><td rowspan="6">Kalimati Formation

Chapagaon Formation</td><td rowspan="6">Lukundol Formation</td><td rowspan="3">Upper member</td></tr>
<tr><td>Chapagaun Terrace deposit</td></tr>
<tr><td>Pyangaun Terrace deposit</td></tr>
<tr><td></td></tr>
<tr><td rowspan="3">Lukundol Formation</td><td rowspan="2">Nakhukhola mudstone & keshari Nayakhandi lignite</td><td rowspan="2">Middle member</td><td rowspan="2">Lukundol Formation</td><td rowspan="2">Basal lignite member</td></tr>
<tr><td rowspan="2">Lukundol Formation & Kobgaon Formation</td></tr>
<tr><td rowspan="2">Tarebhir basal gravel</td><td rowspan="2">Basal boulder bed</td><td rowspan="2">Lower member</td><td rowspan="2">Tarebhir Formation</td><td rowspan="2">Bagmati Formation</td></tr>
<tr><td></td></tr>
</table>

Based on the lithological variation, sediments within the valley basin can be divided into three main groups: Southern, Central and Northern groups.

3.2.1 Southern group

The sediments in the southern group can be subdivided into three formations

3.2.1.1 Tarebhir formation

According to Sakai (2001), it is the oldest fill sediments and is unconformably overlying Pre-Cambrian Tistung Formation. It consists of mainly boulder and cobbles with minor sand beds. It is fluvial in origin. The thickness of this formation varies from 1 to 350 m. The age of this formation is believed to be from late Pliocene to early Pleistocene (Yashida & Igarashi, 1984).

3.2.1.2 Lukundol formation

The Lukundol Formation conformably overlying the Tarebhir Formation. The formation is exposed to the south of the Kathmandu valley. It consists of black to grey organic mud, clay, silt and sand beds with lignite layers. The clay and silt bed are sometimes carbonaceous and hence occurrence of the vertebrate fossils may be noticed (Sakai, 2001). The formation attains a total thickness of more than 100 m. In the central part, the formation is correlated with the Kalimati Formation of Sakai (2001). The age of this formation is believed to be from early to mid Pleistocene (Yashida & Igarashi, 1984).

3.2.1.3 Itaiti formation

It is the cliff forming thick gravel dominant sequence resting on the Lukundol Formation. This formation consists of alternating sequence of gravel, fine sand and silty clay. It consists of base of the pebble and cobble of meta-sandstone of southern hills. The Itaiti Formation is correlated with Terrace deposits of Yoshida & Igarashi (1984). The age of this formation is believed to be middle Pleistocene (Yoshida & Igarashi, 1984).

3.2.2 Central group

The sediments group is sub divided into three formations - lower part, middle part and upper part (Sakai, 2001) defined them as Bagmati Formation, Kalimati Formation and Patan formation.

3.2.2.1 Bagmati formation

It is the lower part of the central basin of the valley. It rests on the base rock. The name Bagmati formation is given because it was the sediment deposited by Bagmati river during lake. It mainly consists of medium to coarse sand, gravels and boulders. The sediments of this formation were derived from the surrounding hills i.e. Shivapuri hill in the northern part of the Kathmandu valley. The thickness of this formation varies from few meters up to about 135 m.

3.2.2.2 Kalimati formation

The kalimati means black clay in local language. Hence it consists of dark grey carbonaceous and diatomaceous beds of open lacustrine facies (Sakai 2001). This type of sediment is extensively distributed beneath the central portion of the Kathmandu valley. This formation was formed during the lacustrine period between 2.5 million to 29,000 years B.P. (Yoshida & Igarashi 1984). The lower part of it contains lignite and bituminous pebbles in some places. Varying thickness of medium to coarse grained sand is found to be inter bedded in some places. The thickness of this formation varies from few meters up to 300m at Harisiddhi. The formation is correlated with the Lukundol Formation in the southern part.

3.2.2.3 Patan formation

Sakai (2001) and Yoshida & Igarashi (1984) both defined the upper part as Patan Formation. It is mainly distributed in and around the Kathmandu and Patan city. It mainly consists of fine to medium sand and silt intercalated with clays and fine gravel in some places. It is fluvial in origin. The sediments of this formation that overlie the Kalimati Formation may have been developed after lake started drying up and fluvial process became active. The age of this formation is determined as 19000 to 10000 B.P. (Yoshida & Igarashi 1984). The thickness of this formation ranges from few meters up to more than 50 m in Bansbari.

3.2.3 Northern group

This formation consists of terrace forming sand from fluvio-deltaic and is extensively distributed in the northern and north eastern part of the Kathmandu valley. The formation found in the northern part is named as Gokarna Formation and the formation found in the north eastern part is named as Thimi Formation. According to Yoshida & Igarashi (1894) and Sakai (2001), Thimi Formation is younger than Gokarna Formation. The age of the Gokarna Formation is determined as 28000 to 30000 years B.P. and that of the Thimi Formation is

determined as 23000 to 28000 years B.P. The borehole data of the northern part shows that it contains sand and silt without clay. The Kalimati formation diminishes its thickness and pinches out in the northern area of Dhapasi and Bansbari and also in the eastern part in the Mulpani village.

3.3 Basement rock

Stocklin & Bhattarai (1977) described the basement geology of the Kathmnadu valley in detail. According to them, it consists of Phulchowki group and Bhimphedi group of the Kathmandu Complex. It is formed by Precambrian to Denonian rocks (Table 3.2).

The Kathmandu Complex has been divided into Bhimphedi Group and Phulchowki Group.

Table 3.2: Stratigraphic sequence of basement rocks of Kathmandu basin

Unit			Main Lithology	Approx. Thickness (m)	Age
Kathmandu Complex	Plulchowki Group	Godavari Limestone	Limestone, dolomite	300	Devonian
		Chitlang Formation	Slate	1000	Silurian
		Chandragiri Limestone	Limestone	2000	Cambrian to Ordovician
		Sopyang Formation	Slate, calc-phyllite	200	Cambrian
		Tistung Formation	Metasandstone, Phyllite	3000	E. Cambrian or Lower Precambrian
	Transition				
	Bhimphedi Group	Markhu Formation	Marble, Schist	1000	Precambrium
		Kulekhani Formation	Quartzite, Schist	2000	Precambrium
		Chisapani Quartzite	Quartzite	400	Precambrium
		Kalitar Formation	Schist, Quartzite	2000	Precambrium
		Bhainsedobhan marble	Marble	800	Precambrium
		Raduwa Formation	Garnet-schist	1000	Precambrium

Source: Stocklin & Bhattarai, 1977

Similarly, the Phulchowki Group comprises of the unmetamorphosed or weakly metamorphosed sediments containing fossils of the early middle Palaeozoic age. It consists of about 6 km thick sequence of rocks, and is divided into five formations (Table 3.2). The rocks consists of intensively folded and faulted meta-sediments such as phyllite, schist, slates, limestones and marble covering the southern, eastern and western part and granite and gneiss known as Shivapuri complex in the northen part of the valley. Some isolated rock outcrops of Tistung Formation and Chandragiri Formation can also be observed in some parts of the basin such as Balkhu, Pashupatinath, Swayambhu and Chobar.

Table 3.3: Geological Succession of the Kathmandu valley (modified after Stocklin & Bhattarai 1977)

Cenozoic	Holocene		Fan Gravel, Soil, Talus, Fluvial deposits (gravel , sand, silt)
	Pleistocene		Lake deposits (gravel, sand, silt, clay, peat, lignite & diatomite)
	Late Pliocene Early Pleistocene		Fluvial deposits (boulder, gravel, sand, silt)
Unconformity			
Lower Paleozoic	Devonian	Phulchowki Group	Godavari Limestone-limestone, dolomite
	Silurian		Chitlang Formation - slate
	Cambrian - Ordovician		Chandragiri Limestone-limestone, phyllite
	Cambrian		Sopyang Formation-slate, Calcareous phyllite
	Early Cambrian		Tistung Formation-meta sandstone, phyllite
Unconformity			
Pre-Cambrium		Bhimphedi Group	Markhu Formation- marble, schist
			Kulekhani Formation- quartzite, Schist
Intrusion			Metamorphic-Sheopuri gneiss
			Igneous Rocks- pegmatite, granite, basic intrusive

3.4 Sedimentation and draining of the paleolake

Tha Kathmandu valley is filled with unconsolidated clay, silt, sand and gravel from upper Pliocene to Quaternary age (Yashida & Gautam, 1988; Fort & Gupta, 1981) which overlay

consistent the Precambrian Bhimphedi group and early Paleozoic Phulchoki group (Stocklin & Bhattarai, 1981).

The sediment can be divided into three facies types, an open lacustrine facies in the central part of the basin, mainly marginal fluvio deltaic facies in the north and an alluvial fan facies in the southern part. All these originate from the lake which once filled the basin; therefore it is called Paleo-lako Kathmandu.

There are many faults running in the basin. Kalphu khola fault system segmented the basin and produced a faulted topography. According to the Sakai (2001), Chandragiri fault and Chobhar fault are the active faults cutting the colluvial slopes and terraces of the late Pleistocene. Kalphu khola fault is the active fault cutting the late Pleistocene gneiss boulder beds to the north-west of the valley (Nakata *et al*, 1984). Hence it can be said that the sedimentation of the Kathmandu basin group must have been controlled by these faults. The main source of the basin is the surrounding mountains from where sediments were carried by the drainage system. Metamorphic sedimentary rock which is argillaceous type was carried from the southern hills Chandragiri and Phulchowki hence called southern sediments. Intrusive rocks (gneiss and granites) ware carried from northern Shivapuri hills and hence called northern sediments. The unconsolidated sediments that occupy the Kathmandu valley consist of the fluvial-lacutrine sequences with many local variations. The sediments from the northern part are generally poorly sorted, thin to medium bedded highly micaceous coarse sands, gravel and silts inter bedded with clays in some places. In the southern half, the sediments mainly consists of a thick sequence of cohesive sediments consisting of dark grey to black highly plastic clay and silts that is usually overlain and underlain by sequence of coarse sediments. The plastic clay locally called kalimati is exposed at the surfaces in some places. The clay is assumed Pliocene to Pleistocene in age (Yoshida & Igarashi 1984). Its thickness is greatest along the central part of the valley. The Kathmandu valley also comprises of alluvial deposits which are Holocene age (Yashida & Igarashi 1984). The sediments in this area have been described as highly micaceous coarse grained sand and silt and have been derived from bedrock areas.

According to the Sakai (2001), Danuwaargaon fault in the southern part of the Kathmandu valley is responsible for the draining of the paleo lake of Kathmandu. Sakai (2001) and Saijo (1995) both believe that the Chandragiri fault and Chobhar faults in the south, which are active faults, may have played an important role for the basin development of the valley.

3.5 Tectonic setting

The tectonics of the Kathmandu region were first studied by Hagen (1969) who recognized the Kathmandu Nappe in the vicinity of Kathmandu, and the Khumbu Nappe farther to the north near Langtang Himal. Many authors consider the rocks of the Kathmandu area to represent the rocks in the hanging wall of the Main Central Thrust (MCT) (Le Fort, 1975; Stocklin, 1980). On the basis of lithology and metamorphism, Upreti & Le Fort (1997) recognized two thrust packages in the Kathmandu transect. The section north of the Kathmandu valley is named the Gosainkund Crystalline Nappe (equivalent to the Higher Himalayan Crystallines (HHC) or the Tibetan Slab) and the crystalline rocks to the south, the Kathmandu Crystalline Nappe (KCN). The boundary between these two units is marked by the MCT which passes through the north of Kathmandu valley. North of the MCT, the Gosainkund Crystalline Nappe (GCN) corresponds to the southward continuation of the HHC of the Langtang area. To the south, the KCN represents an out-of-sequence thrust sheet in the Lesser Himalaya (Upreti & Le Fort, 1997). The KCN was mainly mapped by Hagen (1969), Arita *et al* (1973), and Stocklin (1980). The frontal part of the nappe reaches almost to the Main Boundary Thrust (MBT) to the south.

According to Nakata (1982), fault system in Kathmandu valley is classified into four system.

i) Main central active fault system
ii) The active fault system in the lower Himalaya
iii) The main boundary active fault system
iv) The active fault system along the Himalayan frontal thrust

These faults are produced by the collision of the Indian Plate with the Eurasian plate.

According to the Sakai (2001), the Kathmandu complex occupies the core of the synclinorium, the axes of which trends in WNW-ESE direction. The main fold axis lies on the line connecting the peak of the Phulchowki and Chandragiri. Many longitudinal faults run parallel to the fold axis and the northern and southern margins of the basin are bounded by the Kalphu Khola fault and Chandragiri fault respectively. Both active faults cut the late Pleistocene sediments. Saijo *et al* (1995) and Yagi et al (2000) also reported the existence of the active fault in the southern part of the Kathmandu basin such as Chobar fault and Chandragiri fault. According to Saijo et al (1995), these faults are cutting the late Pleistocene sediments and hence have vertical displacement of 1mm/yr.

Sakai (2001) reported Danuwaargaon fault in the southern part of the Kathmandu valley and stated that it was very active in the late Pleistocene and hence might have been responsible for the draining of the Paleolake of the Kathmandu. It was also believed that Chandragiri and Chobhar fault in the south may have played an important role for the draining of the lake.

3.6 Hydrogeological setting

Sedimentation in the Kathmandu valley is thought to have taken place in two main fluvio-lacustrine phases separated by an interval of tectonics and erosion (Yoshida & Igarashi, 1984). The development of the present ground water system is thought to date from the draining of the younger Kathmandu lake in the Middle – Late Pleistocene when the proto-Bagmati river eroded the southern margin of the basin and flowed out southwards (Yoshida & Igarashi 1984). The deep aquifer may have filled gradually since the Late Pleistocene period with restricted flow to the southwards. The basin contains up to 550 m of Pliocene-Quaternary fluvio-lacustrine sediments (Yoshida & Igarashi 1984). These sediments were deposited into different layers consisting of different hydrogeological properties (Fig 3.3).

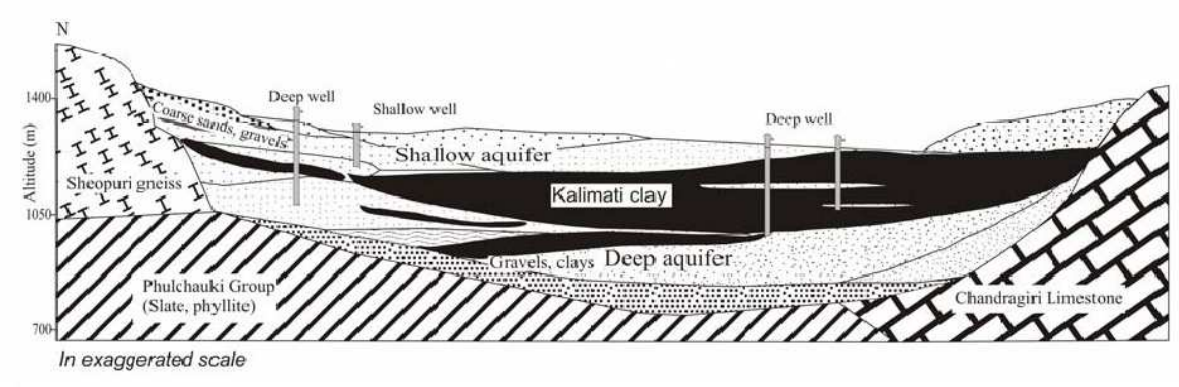

Fig 3.3: Schematic cross section (N-S) indicating shallow aquifer, aquitard and deep aquifer layer of Kathmandu valley (Source: Gurung *et al* 2007)

Well log data has a great importance to develop better understanding of subsurface aquifers and groundwater flow direction. In other words, the information from well log data contributes for proper characterization of the hydrogeological condition at a site which is necessary to understand the relevant flow process. Drilling log data (Appendix A) of the

boreholes in the wellfield are collected from different drilling organizations and applied to demarcate the hydrostratigraphic zones of the area.

3.6.1 Principle hydrogeological unit

The subdivision of the geological formations into hydrogeological units for analysis is based on the borehole logs to identify the layers with different sediments types and properties. The approximate thickness of the principle hydrogeological units was assessed based on the analysis and interpretation of borehole logs for the study area. Borehole logs showed the different layers of sediments. The well log data show that the geologic units in the area are not uniform and are highly heterogeneous in lateral and vertical extent. There are interlayers of permeable and low permeable geologic units (clay). The geological heterogeneity mainly results from the existence of clay layers interbedded into permeable layers. According to the similarity in the hydrogeologic properties of these layers and simplification required, they are divided into three principle hydrogeological units whose formations and sediments types are summarized in Table 3.4.

Table 3.4: Classification of principle hydrogeological units

Hydrogeological units	**Geological Formations**	**Sediment types**
Shallow Aquifer	Itaiti Formation	Gravel, sand, silty sand
	Patan Formation	Sand, gravel, sandy clay, gravelly clay
	Thimi and Gokarna Formation	Sand, sandy silt
Aquitard	Lukundol Formation	Clay, clayey sand, silty clay
	Kalimati Formation	Clay, clayey sand, lignite, silt, gravelly clay
Deep Aquifer	Tarebhir Formation	Sand, sandy gravel, sandy silt
	Bagmati Formation	Sand, gravel, gravelly clay, sandy silt, gravelly silt,

3.6.1.1 Shallow aquifer

The shallow aquifer corresponds to Itaiti, Thimi, Patan and Gokarna Formation (Pandey & Kazama, 2010). It is the upper unconfined aquifer which consists of discontinuous Quarternary sand, silt and clay lenses. It is up to 85 m thick in some places. The shallow aquifer is thicker towards the northern part of the basin. In the southern and some central part of the Kathmandu valley, the thickness of the aquifer is very small or null. In this aquifer, standing water levels are between 1 m to 20 m below ground level, increasing towards the southwest (Sharma 1981).

3.6.1.2 Aquitard

The aquitard corresponds to the Kalimati Formation and Lukundol formations. It consists of black clay with grey carbonaceous and diatomaceous beds of open lacustrine facies. The aquitard layer varies from less than few meters to more than 200m. The thickness of the clay layer is more than 200m in the central part of the valley and deceases towards north and southeastern part of the valley. At the northern part of the valley (Gokarna and Manohara) and small southern part (Chapagaon), there is no evidence of the existence of the clay layers and these are the major recharge zones for the deep aquifer. It may contains clay interbedded with silt and sand in some part. It also contains peat and lignite bands.

3.6.1.3 Deep aquifer

The deep aquifer corresponds to Bagmati and Tarebhir formation. It consists of a sequence of Pliocene sand and gravel beds, intercalated with clay, peat and lignite. These sand and gravel beds collectively comprise the deep, confined aquifer. This aquifer thickens more than 300m beneath the Kathmandu and Patan cities in the center of the basin. It becomes thinner to the margins where it is in hydraulic contact with the upper aquifer.

3.6.2 Hydraulic properties

Hydraulic properties including both horizontal and vertical hydraulic conductivities are key components for calibrating the groundwater model. The hydraulic property data for the Kathmandu aquifer system is derived from data published in previous studies. Hydraulic properties of the different geologic units have been reported by Pandey & Kazama (2010). The hydraulic conductivity of shallow aquifer ranges from 12.4 to 44.9 m/day with the average value of 23.7 m/day. The shallow aquifer has higher conductivity than deep aquifer.

The hydraulic conductivity of the deep aquifer is reported to be 0.3 to 8.8 m/day with the average value of 4.5 m/day. The hydraulic conductivity of shallow aquifer is found to be 5 times higher than that of deep aquifer. The transimssivity of shallow aquifer varies from 163.2 to 1056.6 m^2/day with average value of 609.9 m^2/day whereas that for deep aquifer varies from 22.6 to 737 m^2/day with average value of 379.9 m^2/day. The transmissivity of shallow aquifer is found to be 1.6 times higher than deep aquifer. The storage coefficient of the shallow aquifer is almost constant through the study area with value 0.2. The storage coefficient of the deep aquifer varies from 0.00023 to 0.07.

Table 3.5: Hydrogeologic properties of the aquifers of the Kathamandu valley

S.No.	Parameters	Shallow aquifer	Deep aquifer
1	Surface area, A (km^2)	241	327
2	Transmissivity, T (m^2/day)	163.2 – 1056.6	22.6 - 737
3	Hydraulic conductivity, K (m/day)	12.5 – 44.9	0.3 – 8.8
4	Permeability, k (m^2)	1.48E-11 to 5.32E-11	3.74E-13 to 1.04E-11
5	Storage coefficient (S)	0.2	0.00023 – 0.07
6	Total aquifer volume (MCM)	7261.27	56813.70

Source: Pandey & Kazama (2010)

3.6.3 Estimation of groundwater recharge

For the purpose of this study, water surplus has been defined as the part of the precipitation which does not evaporate and therefore contributes to the water resources (surface and groundwater flow). Based on a (vertical) soil water balance, the notion of surplus represents the contribution of all elementary areas to the overall water resources produced in a given river basin. Water surplus either infiltrates to recharge aquifers or runs off into rivers. As soon as water starts flowing, it is subject to losses by evaporation, resulting in a reduction of the available water resources.

The time distribution of the data used for the model may also induce an underestimation of the actual amount of surplus water, available for surface and groundwater. When rainfall is characterized by a few events scattered over the rainy season, the model, made on a monthly basis, cannot reproduce surplus issued from heavy rainfall. In humid areas, where rainfall is more evenly distributed, this underestimation of surplus is less significant. The methodology for the estimation of the recharge (Fig 3.7) is based on FAO publication on Irrigation Potential in Africa (FAO, 1997).

3.6.3.1 Precipitation

Precipitation in Nepal occurs due to the southeast monsoon which lasts between the months of June to September. The humid monsoon air stream blowing from the Bay of Bengal is forced to rise as it meets the Himalaya. Rainfall is concentrated, and more than 75% of the annual rainfall occurs during the months of June to September (Shrestha, 2010). The months of October to May are dry and the rainfall occurs is sporadic.

The main form of precipitation in the Kathmandu valley is rainfall. Total 19 rainfall gauging stations within and in the vicinity of the catchment area of the Kathmandu Valley are analyzed (Appendix D). These data are used for the computation of annual average. The annual average for the study area calculated from the data of rainfall gauging stations is 1689. The isohytal map of 34 years annual average precipitation has been prepared by Shrestha (2010) (Fig 3.4) and shows the highest precipitation occurs around the hills surrounding the valley. And the north-western and north-eastern part receives highest precipitation, and around Budanilkantha area receives highest precipitation of 2300-2400 mm average annual precipitation. And precipitation gradually decreases towards the central part and the Khumaltar area received lowest annual average precipitation of around 1200-1300 mm.

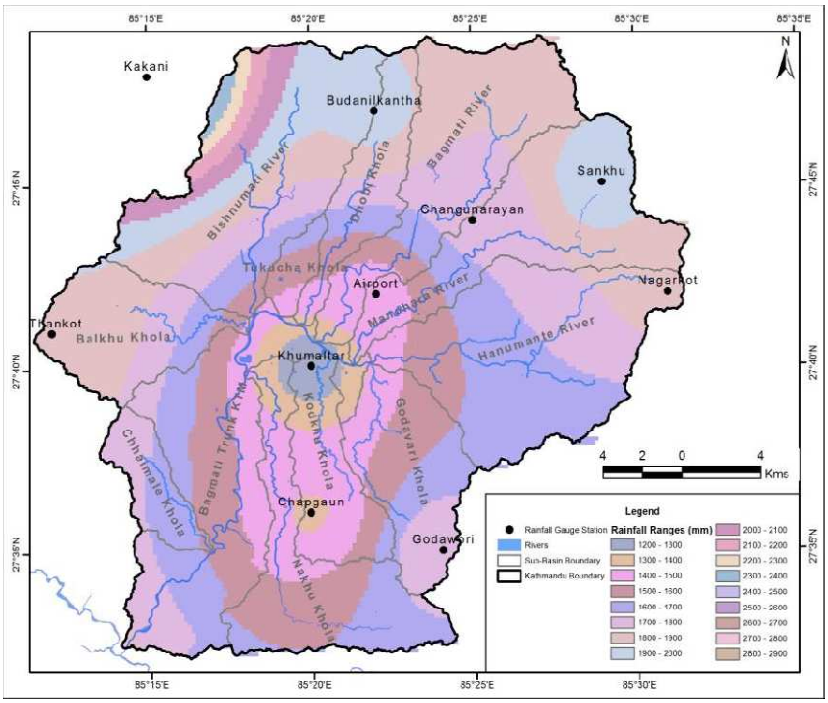

Fig 3.4: Isohytal map of average annual precipitation (Source: Shrestha, 2010)

The rainfall trend results that, the rainfall pattern is gradually changing. The amount of precipitation received by the rainfall gauge stations within the study area is gradually decreasing (Shrestha, 2010) which directly impact on the hydrology of Kathmandu valley. Hence it affects on the groundwater recharge.

3.6.3.2 Evapotranspiration

Monthly mean evaporation data has been collected from Department of Hydrology and Meteorology recorded at two stations at Tribhuvan Internation Airport and Khumaltar which is included in Appendix D.

3.6.3.3 Discharge:

The main river draining the Kathmandu valley is Bagmati river. It originates in Bagdwar of Shivapuri Danda (hill) in the north of Kathmandu valley. The river is fed by number of tributaries originating from Mahabharat and Chure Ranges before it reaches Terai at Karmaiya and to the Gangetic plain. The Bagmati River is a perennial river fed by storm and spring flow. And river flow is generally governed by the surface runoff flow during rainy sessions and depends upon groundwater flow when the river does not receive rainfall. Hydrograph of average annual precipitation and average annual discharge of the watershed shows that there is a positive correlation between precipitation and discharge (Shrestha, 2010). The average monthly discharge at gauging station located at the outlet of the study area is given in Table 3.6.

Table 3.6: Average monthly discharge (m^3/s) at Chovar of Kathmandu valley

Jan	Feb	Mar	Apr	May	June	July	Aug	Sep	Oct	Nov	Dec
2.3	1.6	1.7	1.9	1.8	6.5	43.2	50.0	28.5	14.0	6.8	3.6

Source: Singh *et al* (2008)

3.6.3.4 Recharge area

The ground water basin of the Kathmandu valley covers 327 km^2 of 656 km^2 of total watershed area. According to the JICA (1990), the watershed is divided into three parts; Northern, Central and Southern.

The total area of the northern part is 157 km^2 out of which 59 km^2 is the recharge area. The upper part of deposits in the northern part is composed of unconsolidated, highly

permeable materials consisting of micaceous quartz, sand and gravel. The most rechargeable areas are high plain and low alluvial regions.

The central part is composed of thick, stiff black clay with some lignite to the depths of more than 300 m. The unconsolidated, low permeability, coarse sediments underlie the thick black clay. The total area of the central part is 114 km^2. About 6 km^2 of this part near Chapagaun is covered with sand and gravel and is the only recharge area.

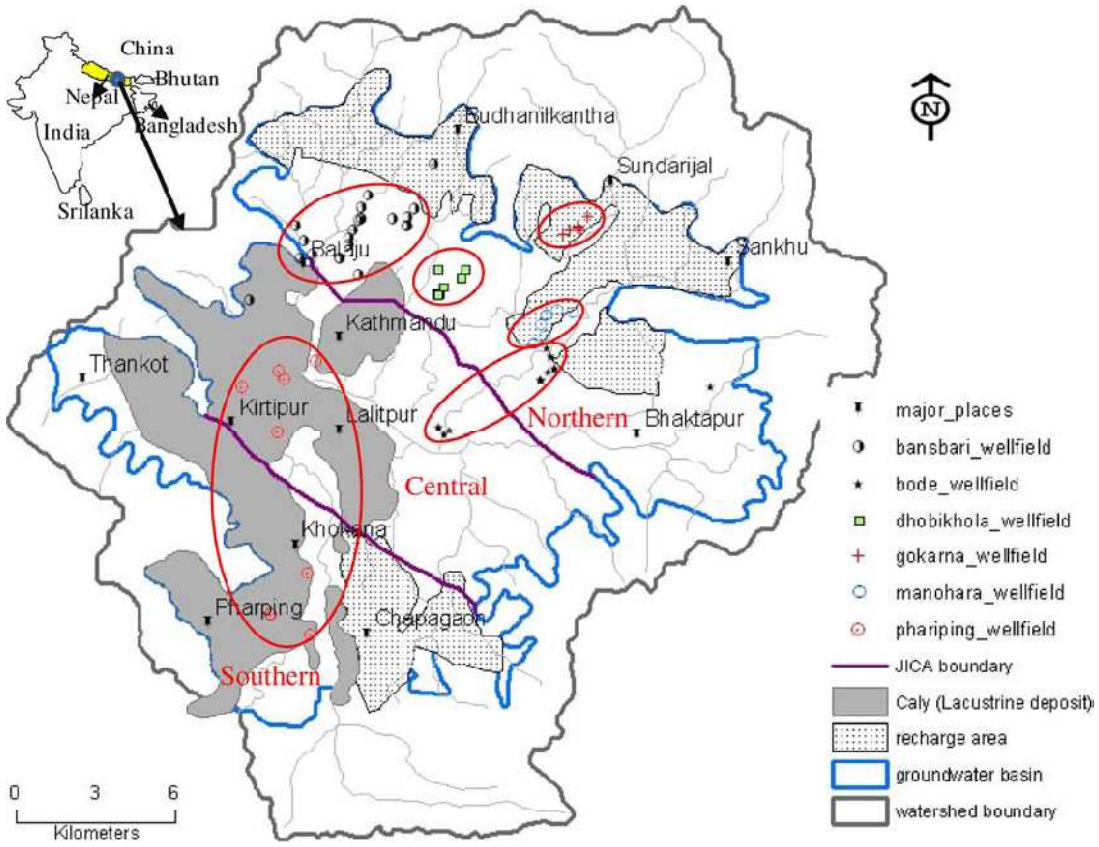

Fig 3.5: Surface area, groundwater basin and recharge area in Kathmandu valley aquifer (Source: groundwater basin boundary and recharge area (JICA 1990)

The southern part is characterized by a thick clay formation. The eastern area of the southern part is covered with sand and gravel deposits. Out of the total area of 55 km^2, recharge takes place in 21 km^2. Hence total recharge area of the Kathmandu valley is about 86 km^2 (JICA 1990).

3.6.3.5 Groundwater recharge estimation method

The method used in the estimation of the groundwater recharge in this study is water balance method. The method yields natural groundwater recharge on a monthly basis, evaluated as the difference between the inflows (rainfall) and the outflows (evaporation, surface runoff).

The soil water balance is calculated on a monthly basis with the following as input parameters:

- precipitation (P);
- reference evapotranspiration (ETo);
- maximum soil moisture storage capacity (Smax);
- easily available soil moisture (Seav).

The Digital Soil Map of the World and Derived Soil Properties (DSMW) distinguishes the following classes regarding soil moisture (Table 3.7):

Table 3.7: Table showing the relation between Smax and Seav

Class	Smax (mm)	Seav (mm)
A	<20	<20
B	20 – 60	20 – 40
C	60 – 100	40 – 60
D	100 – 150	60 – 100
E	150 – 200	100 – 120
F	>200	>120
W	Wetlands	Wetlands

If one considers the amount of water available in the soil at different suction pressures, the maximum soil moisture storage capacity (Smax) can be defined as the amount of water held in the soil between 0.05 and 15 bar suctions (pF 1.7 and pF 4.2 respectively). Easily available soil moisture (Seav) is defined as the amount of water held in the soil between 0.05 and 2 bar suctions (pF 1.7 and pF 3.3 respectively) (FAO, 1997).

The amount of water available at pF 1.7 is the maximum amount of water that the soil can retain; this is the situation of field capacity. Above this limit, water cannot be retained by the soil and percolates. When the amount of water falls below pF 4.2, the vegetation is no

longer able to extract water from the soil. This is called 'wilting point'. Between pF 1.7 and pF 3.3, the vegetation can easily extract the moisture from the soil to satisfy its evapotranspiration needs. The available soil moisture at pF3.3 is called "reduction point"; when the suction pressure becomes higher than this limit, the evaporative capacity of plants is reduced and evapotranspiration is less than potential. The reduction in the evapotranspiration between the reduction point and the wilting point depends on the available soil moisture. In this model, the reduction in evapotranspiration was assumed to vary linearly with available soil moisture in the range between reduction point and wilting point (Fig 3.6) (FAO, 1997).

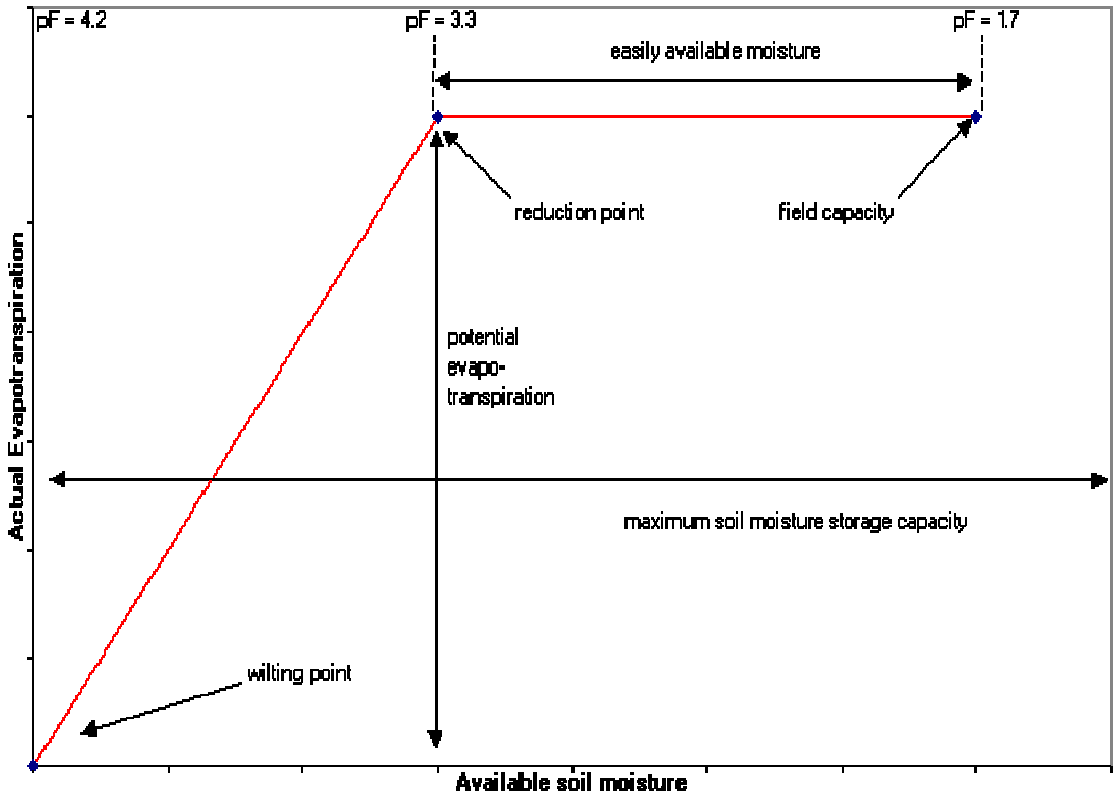

Fig 3.6: Reduction in evapotranspiration as a function of soil moisture (FAO, 1997)

3.6.3.6 Water balance for basin

The water surplus is calculated as the difference between precipitation and evaporation. It can either be positive or negative:

$S(m) = P(m) - ETo(m)$ [3.1]

where:

S(m) = water surplus for the month m

P(m) = precipitation for month m

ETo(m) = reference evapotranspiration for month m.

With the assumption that water is always present in the water bodies, the actual evapotranspiration ETa(m) is equal to ETo(m):

$$ETa(m) = ETo(m) \quad [3.2]$$

The calculation of the actual evapotranspiration is carried out with FAO water balance method.

The computational steps are organized according to the following flowchart:

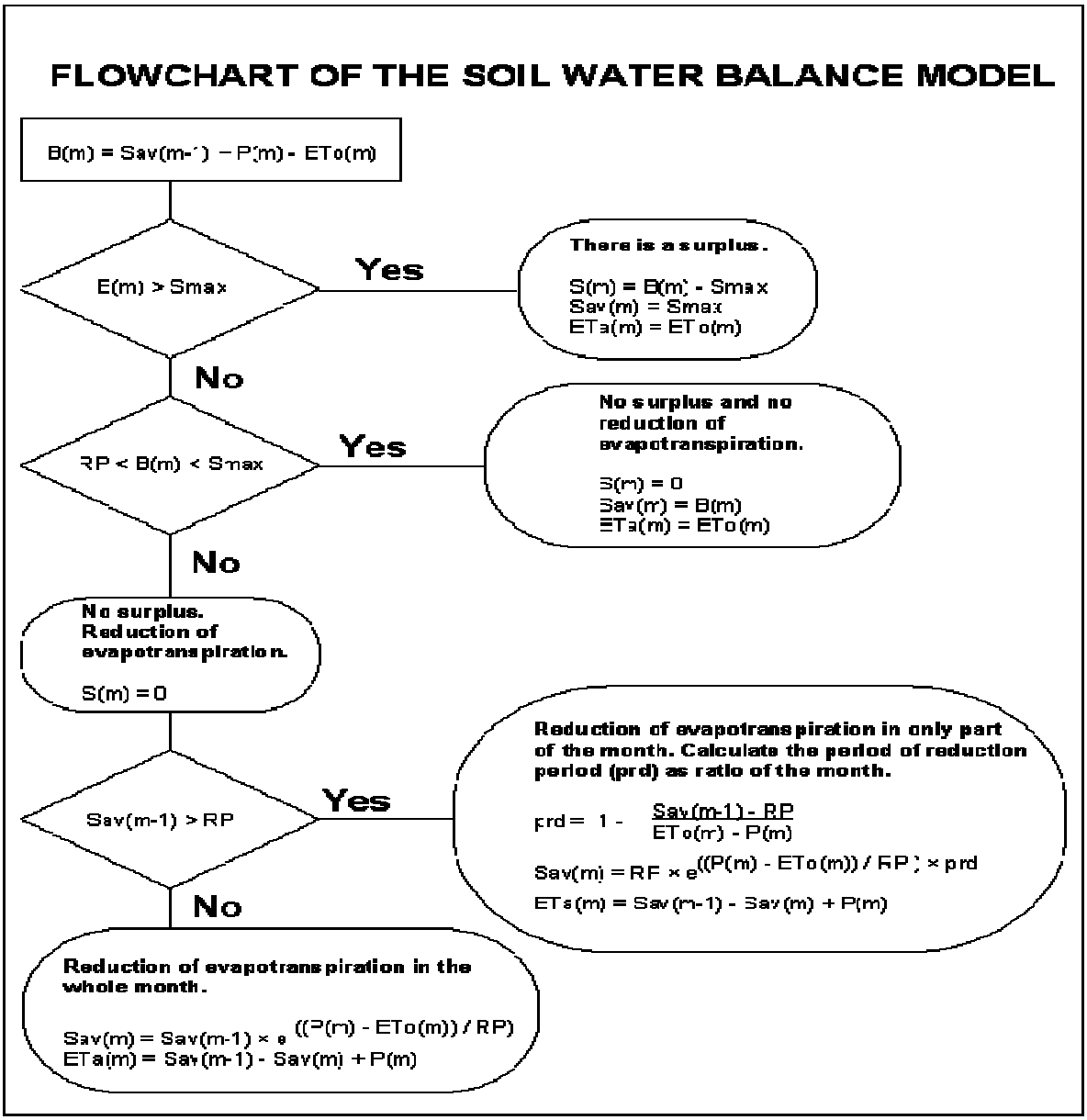

Fig 3.7: Flow Chart showing the computation of the water balance in the basin (FAO, 1997)

Where:

S(m) = Surplus of month m, P(m) = Precipitation of month m

ETo(m) = reference evapotranspiration Seav = Easily available moisture

Eta(m) = Actual evapotranspiration RP = reduction point =(Smax-seav)

Prd = Period of evapotranspiration reduction Smax = maximum soil storage capacity

Sav(m) = Available soil moisture on month m B(m) = soil moisture balance of month m

Annual groundwater recharge is estimated by deducting annual runoff from the annual surplus.

3.6.3.7 Computational Steps

Following steps were carried out in order to estimate the groundwater recharge.

i) First select the dry hydrological month of the year. For this study, the dry hydrological year is taken March to start the computation.

ii) Historical monthly data for potential evapotranspiration of the basin for the period of 10 years is collected and average monthly value is calculated.

iii) The recharge model is calibrated with changing the Smax and Seav.

iv) For each month, a monthly balance is computed by adding precipitation to the soil moisture content of the previous month and subtracting potential evapotranspiration. If this balance exceeds Smax, the excess is the monthly surplus. If the balance is less than Smax, but still larger than the reduction point, there is no surplus and no reduction in evapotranspiration. When the balance falls below the reduction point, evapotranspiration is less than the potential. The actual evapotranspiration for each month is calculated and summed up to find the annual evapotraspiration for the basin. Again the surplus of each month is calculated and summed up to find the annual surplus. The computations are shown in Table 3.8.

v) The mean monthly discharge data at Chovar station of the Kathmandu valley is collected .

vi) The baseflow of the Bagmati river has been determined and runoff value for each month is calculated. The runoff value is summed up to determine the annual runoff of the basin (Table 3.9).

vii) The above procedure has been repeated until the calculated runoff value properly calibrated with the observed runoff.

viii) The annual runoff is subtracted from the annual surplus to determine the annual recharge to the groundwater of the basin.

Table 3.8: Water balance calculation for the Kathmandu valley (all units are in mm)

S.N.	Month	P(m)	Eto(m)	B(m)	S(m)	Sav(m)	Eta(m)	Remarks
1	Mar					0		assumed
2	Apr	60.2	151.0	-90.8	0	0	60.2	
3	May	139.1	153.6	-14.5	0	0	139.1	
4	Jun	263.8	144.1	119.7	0	119.7	144.7	
5	Jul	454.9	132.5	442.1	242.1	200	132.5	
6	Aug	409.3	142.8	466.6	266.6	500	142.8	
7	Sept	215.2	114.8	300.4	100.4	200	114.8	
8	Oct	56.2	112.5	143.7	0	143.7	112.5	
9	Nov	7.4	94.8	56.3	0	27.2	44.8	
10	Dec	12.5	75.1	-3.12	0	27.2	44.8	
11	Jan	18.8	82.6	-36.7	0	12.2	33.7	
12	Feb	19.1	98.9	-67.6	0	4.5	26.8	
13	Mar	33.35	142.4	-104.1	0	1.2~0	38.3	verified
Total		1689			609			

Table 3.9: Calculation of the recharge for the Kathmandu valley

Month	Surplus (mm)	Measured discharge (m^3/s)	Base flow (m^3/s)	Runoff (m^3/s)	Eq. Depth (mm)	Remarks
January	0.0	2.3	2.3	0.0	0.0	
February	0.0	1.6	1.6	0.0	0.0	
March	0.0	1.7	1.7	0.0	0.2	
April	0.0	1.9	1.7	0.2	0.6	
May	0.0	1.8	1.8	0.0	0.0	
June	0.0	6.5	1.9	4.6	18.4	
July	242.1	43.2	1.9	41.3	170.0	
August	266.6	50.0	2.0	48	198	
September	100.4	28.5	2.1	26.4	105.4	
October	0	14.0	2.1	11.9	49.1	
November	0	6.8	2.2	4.6	18.5	
December	0	3.6	2.3	1.3	5.3	
Total	609.1				565.7	

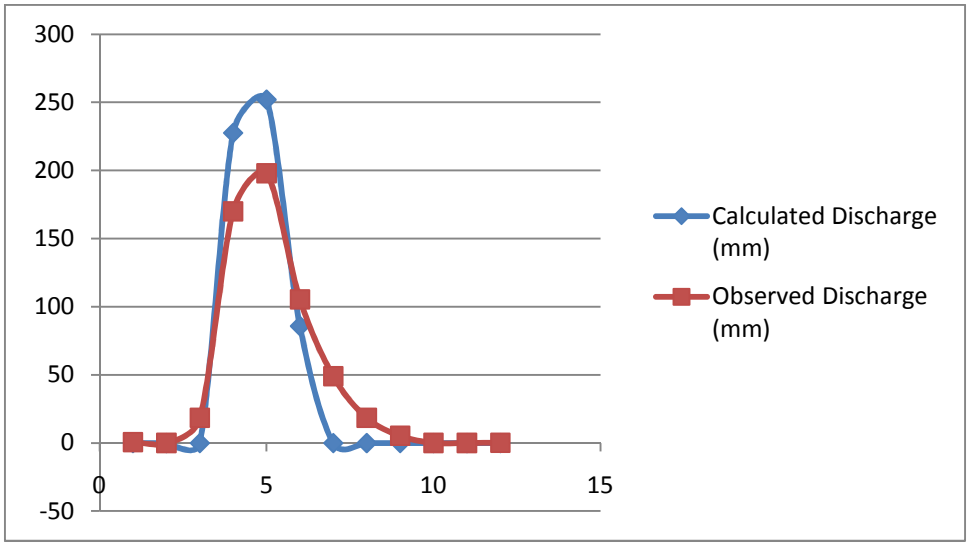

Fig 3.8: Calibration of the calculated discharge and observed discharge

The calibration result show that the calculated discharge and the observed discharge closely matched (Fig 3.8) and hence is considered calibrated. The graph shows that the calculated discharge is slightly higher than the observed monthly value. This is due the fact that the calculation is on monthly basis and rainfall occurs in the month. The peak runoff will be diffused slowly in the other months due to time lag of the groundwater flow which is not considered in this study. The peak runoff should be routed to get the exact runoff value of the other month which is not the scope of the study. The volume of the calculated and the observed discharge is found be equal.

The output of the model consists of the following data:

- monthly actual evapotranspiration;
- monthly surplus;
- available soil moisture at the end of each month.
- annual recharge to groundwater

From the calculation, it is found that the annual recharge to the groundwater of the Kathmandu valley is 43 mm/year.

The value of the annual recharge to the Kathmandu groundwater basin calculated by different authors and method has been summarized in Table 3.10. It is found that the annual recharge value calculated is seemed to be comparable estimated by other methods.

Table 3.10: Comparison of recharge estimates

Calculation method	Estimated recharge (mm/yr)
Water balance	51
Base flow separation	55
Specific yield	38
Chloride balance	59
Groundwater flow	41

Source: Gupta *et al* (1990)

3.6.4 Surface - groundwater interaction

As rainfall occurs, some will flow as surface runoff and some will flow into ground. Kathmandu valley is drained by the Bagmati river which originates in the Shivapuri hills to the north. The river flows southwest, cutting through the valley at Chobhar and dissecting the Mahabharat range at Katuwaldaha. The origin of the Bagmati lies almost completely within the Shivapuri National Park. The Bagmati River has nine major tributaries: Nakhu, Kodku, Godavari, Balkhu, Bisnumati, Dhobi, Manohara, Hanumante and Manamati. The Bisnumati, Bagmati and the Manohara originate in the northern and northeastern watersheds and flow southwest, meeting at the valley floor. The Hanumante river flows west joining the Manahara while the Balkhu flows to the east, joining the Bagmati in the central part of the area. The tributaries of these three rivers, originating in the south of the watershed, are the Godavari, the Kodku and the Nakhu. They flow from the south to the north to join the Bagmati in the central part of the Kathmandu valley (Fig 3.9).

Recharge to the shallow aquifers occurs mostly along the basin margins, directly from precipitation and by supply from a number of small rivers. However, recharge to the deeper aquifers is considered to be limited, due to the presence of clay beds that significantly restrict downward percolation Because the Kathmandu Valley is a closed basin with gentle slopes toward the center, groundwater flow is assumed to be slow, particularly in the deeper aquifers (Gurung et al, 2006).

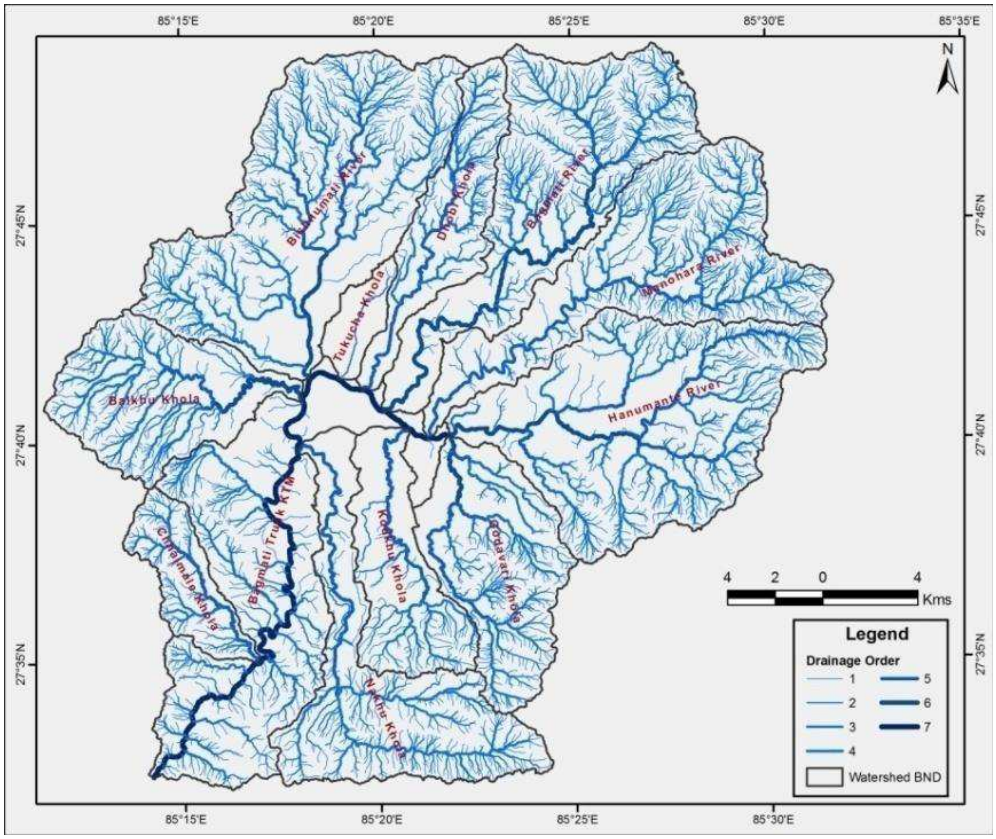

Fig 3.9: Showing the rivers in the Kathmandu Valley (Source: Shrestha, 2010)

3.6.5 Groundwater abstraction

The increase in use of groundwater in Kathmandu has to be analysed in relation to the development of the water supply system. A modern piped water supply system was introduced in Kathmandu in 1891 to serve people. The common people were served with public stand-posts. In the 1950s, the pace of building new systems increased, and in 1960 water from the Bagmati River (the tailrace of the Sundarijal hydropower plant) was used to meet the growing needs of the valley population. This nucleus has expanded over the decades into a large municipal supply system, currently operated and managed by the Nepal Water Supply Corporation (NWSC). The system exploits water from rivers as well as from a network of wells tapping the lower, confined or unconfined aquifers of the valley. Municipal water production from surface sources has always remained in short supply in the valley.

To meet domestic water needs, tubewells were installed at Balaju and Bode in 1961. These abstracted 1.7 million and 1.96 million litres of water per day (MLD) respectively (Dixit & Upadhya, 2005). Since then, the rate of groundwater abstraction has gradually increased

to meet domestic as well as commercial needs. Increasing abstraction has, however, proved insufficient to meet the demand. The abstraction of groundwater by NWSC has been starting from 1979. Before 1979, only private wells were in operation. It has been shown that there was huge rise in abstraction from year 1986 onwards by NWSC. Abstraction increased to 54.5 MLD in the year 1989 and to 70.9 MLD in year 2009. The estimated groundwater abstraction by the WSSC (Water Supply and Sewarage Corporation) and other private tube wells between 1975 and 2009 is shown in Table 3.11 which includes the estimate of groundwater abstraction at 2009 which is estimated by Dhakal (2010)

Table 3.11: Estimated groundwater abstraction in Kathmandu valley

Year	Estimated abstraction in MLD			Total
	NWSC tubewell	Private tubewell	DMG tubewell	
1975	0	1	0	1
1976	0	1.2	0	1.2
1977	0	1.4	0	1.4
1978	0	3.2	0	3.2
1979	2.4	3	0	5.4
1980	3.6	3.24	0	6.84
1981	5.8	3.4	0.4	9.6
1982	6.8	3.4	0.6	10.8
1983	5.8	3.5	1	10.3
1984	4.4	3.6	1.2	9.2
1985	5.3	4.5	1.4	11.2
1986	17.6	6.6	1.4	25.6
1987	26.2	6.4	1.6	34.2
1988	28.7	6.3	1.6	36.6
1989	36.4	7.3	1.8	54.5
2002				61.0
2009				70.9

Source: Japan International Cooraporation Agency JICA (1989)

The annual groundwater abstraction from these and private wells was estimated to be about 20 million cubic meter. A study conducted by the Japan International Cooperation Agency, JICA, in 1990 estimated that the static groundwater level fell 10 m annually after the WSSC wells were developed. According to the Snowy Mountains Engineering Corporation (SMEC, 1992), the upper limit of groundwater abstraction should be about 40.1 MLD. Estimated abstraction levels in 1989 were, however, already much higher than that. In 2002, the NWSC's Optimizing Water Use in Kathmandu valley Project found that the amount of groundwater abstracted by NWSC and private wells for domestic use was about 47 MLD. In addition, it is estimated that bulk abstraction for other domestic and private use is 13.2 MLD, yielding a total abstraction of about 61 MLD, a figure much higher than the upper limit of abstraction calculated by SMEC in 1992.

The groundwater modeling in this study has been performed for the year 2001 and hence by the interpolation, groundwater abstraction from the Kathmandu valley was estimated 61 MLD.

3.6.5.1 Pumping wells and screens

In the Kathmandu valley, pumping wells are being developed haphazardly and unregulated. There is no need of provision of permit hence there is not the proper database of pumping wells. Hence it is difficult to know the number of pumping wells in the study area. It has been reported that more than 700 pumping wells were established (GWDB, 2009). Due to the lack of proper monitoring, documentation and licencing, the exact positions of the screens in the tube wells are also difficult to find. The report prepared by GWDB (2009) has collected the data of tubewells established within the valley and also collect the screen data only for some of them.

In the investigation carried out in 1999 by Melamchi Development Board, it has reported that there are 363 tube wells in which 320 deep and 43 deep tube wells. In 2009, KUKL reported 379 tube wells in the Kathmandu valley.

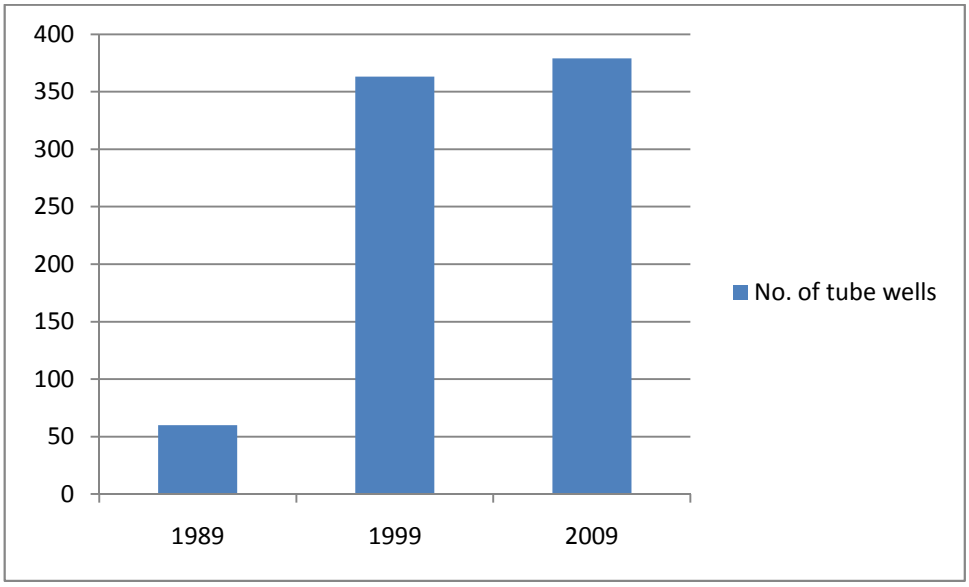

Fig 3.10: Growth of tube wells in the Kathmandu valley

In 1989, the number of the tube wells reported was 60 including 45 private tube wells (GWDB, 2009). Exact number of the tube wells exploiting groundwater resources in the valley is not known. In 2000, Metcalf and eddy reported 218 tube wells in operation including 51 NWSC operated tube wells out of 279 total tube wells (Table 3.12).

Table 3.12: Tube wells in the Kathmandu valley

Groundwater District	Total tube wells		Tube wells in use		Tube wells out of use	
	NSWC	Others	NSWC	Others	NSWC	Others
Northern	57	6	43	43	14	3
Central	12	150	4	114	8	36
Southern	4	10	4	10	0	0
Total	73	206	51	167	22	39

Source: Metcalf and eddy, 2000

In this modeling, we have used 188 pumping wells which are collected from the report (GWDB, 2009) which is included in Appendix B. As some of them have screen data, screen data for other wells were estimated by observing the available screen data which is the limitation of the modeling.

4

GROUNDWATER FLOW MODELING

4.1 Groundwater flow model

A “model” is a representation of a real world system with proper simplifications and assumptions. Models are widely utilized in understanding mechanisms and testing possible responses of real world systems in every branch of science, as well as hydrogeology. Hydrogeologic models, simulating the groundwater flow and transport mechanisms, can serve for a wide range of applications such as evaluation of regional groundwater resources, prediction of the effect of future groundwater withdrawals on groundwater levels, testing of recharge rates, prediction of the possible pattern and migration of contaminants for risk evaluation, design of groundwater monitoring networks.

4.1.1 Governing equations

The Darcy’s law (equation) summarizes much of the physical groundwater flow by relating the velocity vector to the gradient of potential.

$$q = -K \, \mathrm{grad}h \qquad [4.1]$$

where q is the velocity vector and has components qx, qy and qz, K is the hydraulic conductivity, h is the hydraulic head and grad*h* is the gradient vector which has components ∂h/∂x, ∂h/∂y, ∂h/∂z.

Continuity or conservation equation is the second important law. For steady state conditions, continuity requires that the amount of water flowing into a representative elemental volume be equal to the amount flowing out. The existence of steady state conditions implies that the head is independent of time. The continuity equation for steady state conditions can be written as follows (equation [4.2])

$$\frac{\partial q_x}{\partial x} + \frac{\partial q_y}{\partial y} + \frac{\partial q_z}{\partial z} = 0 \qquad [4.2]$$

The left side of the equation [4.2] represents the net change in the volume rate of flow per unit volume, As such, it is called the divergence of q and written as

$$\text{div q} = \frac{\partial \text{qx}}{\partial \text{x}} + \frac{\partial \text{qy}}{\partial \text{y}} + \frac{\partial \text{qz}}{\partial \text{z}} \qquad [4.3]$$

Laplace's equation combines Darcy's equation into a single second order differential equation. The Darcy's law is substituted component by component into equation [4.2] to give:

$$\frac{\partial}{\partial x}\left\{-\frac{K\partial h}{\partial x}\right\} + \frac{\partial}{\partial y}\left\{-\frac{K\partial h}{\partial y}\right\} + \frac{\partial}{\partial z}\left\{-\frac{K\partial h}{\partial z}\right\} = 0 \qquad [4.4]$$

Where K = K(X,Y,Z). If the region is assumed to be homogeneous as well as isotropic, then K is assumed to be independent of X,Y and Z, and the Equation [4.4] becomes:

$$\frac{\partial^2 \text{h}}{\partial \text{x}^2} + \frac{\partial^2 \text{h}}{\partial \text{y}^2} + \frac{\partial^2 \text{h}}{\partial \text{z}^2} = 0 \qquad [4.5]$$

Equation [4.5] is Laplace's equation – governing equation for groundwater flow through an isotropic, homogeneous aquifer under steady state conditions (Wang & Anderson, 1982).

In the derivation of governing equation of transient conditions (the unknown variable is time dependent), the continuity equation is modified such as the volume outflow rate equals the volume inflow plus the rate of release of water from the storage. Therefore, an expression for the rate of release of water from storage must be introduced. This expression involves the use of the storage coefficient S, which represents the volume of water released from the storage per unit area of aquifer per unit decline in head. That is:

$$S = -\frac{\partial V_{\text{w}}}{\Delta x \Delta y \Delta z} \qquad [4.6]$$

Where ΔVw is the volume of water released from the storage within the elemental volume whose area is $\Delta x \Delta y$ and whose thickness is b.

The rate of release from the storage is $\Delta Vw/\Delta t$ and can be written as $-S\Delta x\Delta y(\Delta h/\Delta t)$. As $\Delta t \rightarrow 0$, this expression becomes as $-S\,(\Delta h/\Delta t)(\,\Delta x\Delta y\,)$. Therefore, the form of the continuity equation [4.2] for transient conditions is:

$$\frac{\partial q_x}{\partial x}\Delta x(b\Delta y) + \frac{\partial q_y}{\partial y}\Delta y(b\Delta x) = R(X,Y,Z)(\Delta x\Delta y) - S\frac{\partial h}{\partial t}(\Delta x\Delta y) \qquad [4.7]$$

Where R(X,Y,Z) is the volume of the water added per unit time q_x per unit aquifer area to the infinitesimal volume around the point (X,Y,Z).

Subtracting darcy's law for q_x and q_y and divided through by $-T\Delta x\Delta y$ where T = K.b, yields the transient flow equation:

$$\frac{\partial^2 \mathrm{h}}{\partial \mathrm{x}^2} + \frac{\partial^2 \mathrm{h}}{\partial \mathrm{y}^2} + \frac{\partial^2 \mathrm{h}}{\partial \mathrm{x}^2} = \frac{S}{T}\frac{\partial h}{\partial t} - \frac{R(X,Y,Z)}{T} \qquad [4.8]$$

4.2 Purpose of the model

The purpose of model is to describe the groundwater flow system in Kathmandu valley aquifer using a numerical groundwater flow model. From the conceptual model, a numerical model was developed and integrating all the hydrogeological information gathered and described in the previous chapters. Once the understanding of the system was achieved, the second objective was to investigate the aquifer response to changing stresses such as groundwater abstraction. This was accomplished by examining changes in hydraulic heads.

4.3 Computer code

The code selected to develop the numerical model was MODFLOW ®; a modular, three dimensional finite difference groundwater flow model developed by the USGS (McDonald and Harbaugh, 1988). The version used in this work is Visual MODFLOW 4.2. Selection of this code was justified by its widespread acceptance in groundwater modeling. MODFLOW can be applied as a one dimensional, two-dimensional, quasi- or full three-dimensional model. Furthermore, each simulation feature of MODFLOW has been extensively tested and its theory is well documented; besides it is relatively easy to understand and apply to real conditions (USGS, 1997).

MODFLOW is very effective and widely used model for the development of groundwater modeling because of following reasons:

i) MODFLOW can simulate a wide variety of hydrologic processes in the field condition in three dimensions.

ii) MODFLOW is capable of simulating various geological features such as different hydrological units, heterogeneity, and anisotropy.

iii) Models with MODFLOW help the decision makers and stakeholders to understand about the model so that the models can be used effectively to foster good decision making and wise public policy (Hill *et al*, 2010).

iv) Confined aquifer, unconfined aquifer and aquitard can be simulated under both steady and transient state condition.

v) A variety of hydrological features including rivers, streams, drains, reservoir, and wells as well as hydrological processes including evapotranspiration and recharge can be simulated.

vi) It can be used in the formulation of management plan for groundwater.

vii) It can calculate water budget which is the important aspect of groundwater modeling

This code uses the finite difference method to simulate groundwater flow. In this method, an aquifer system is divided into blocks by a grid. The grid is organized by rows, columns, and layers; each block is called a cell.

4.3.1 Discretization convention

Fig 4.1 shows an hypothetical spatial discretization of an aquifer system with a mesh of blocks called cells, the locations of which are described in terms of rows, columns and layers. An i,j,k indexing system is used. In formulating the equations of the model, an assumption was made that the layers would generally correspond to the horizontal hydrogeologic units. Thus in terms of cartesian coordinates, the k-index denotes changes along the vertical; because the convention followed in this model is to number layers from top to down, an increment in the k- index correspond to the decrease in the elevation. Similarly rows will be parallel to the x-axis, so that increment in the row index-i would correspond to the decrease in y and columns are parallel to y-axis so that increments to the column index j would correspond to increase in x. These conventions were shown in Fig 4.1. The application of the model requires only that the rows and columns fall along the consistent orthogonal directions within the layers and does not require the designation of x,y or z coordinate axes.

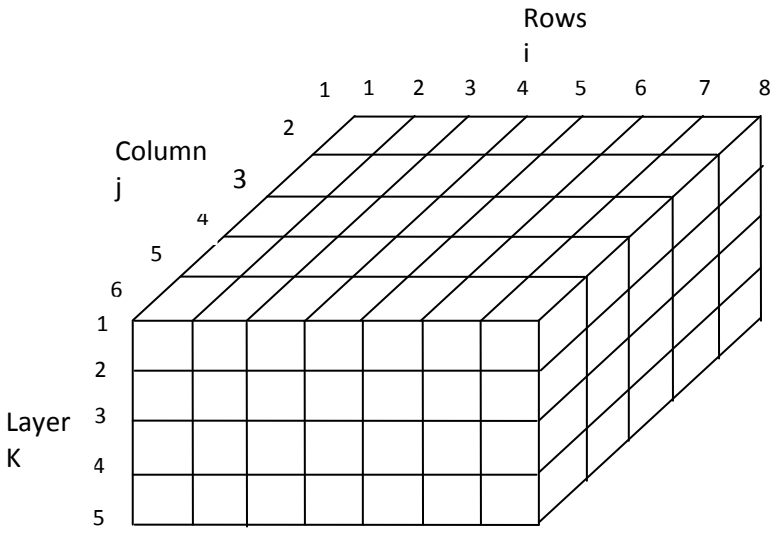

Fig 4.1: Discretized hypothetical aquifer system

4.4 Conceptual model

The first step in the procedure of modeling is the construction of a conceptual model of the problem and the relevant aquifer domain. Development of a conceptual model is one of the critical steps in modeling process. It consists of a set of assumptions that reduce the real problem and the real domain to simplified versions that are acceptable in view of the objective of the modeling. It is critical that the conceptual model is a valid representation of the important hydrogeological conditions. Conceptualization of the system is the basis for the numerical modeling. The nature of the conceptual model determines the dimension of the numerical model and the design of the grid. Failures of numerical models to make accurate predictions can often be attributed to errors in the conceptual model (Kahsay, 2008).

The purpose of developing a conceptual model is to formulate a better understanding of a site condition, to define the groundwater problem, to develop a numerical model and to aid in selecting a suitable computer code. The elements of a conceptual model include defining the extent and characteristic of the aquifer system and developing an understanding of groundwater flow directions, sources and sinks (Kahsay, 2008).

The conceptual model of the Kathmandu valley has been developed by integrating the available data on hydrogeology, well logs, geological map and geologic cross–section from previous studies. A schematic representation of the model of the Kathmandu valley is

shown in Fig 4.2 and includes information on the aquifer system (aquifer layers and limits, recharge area, groundwater flow patterns) and its discritization (grid and principle flow boundaries).

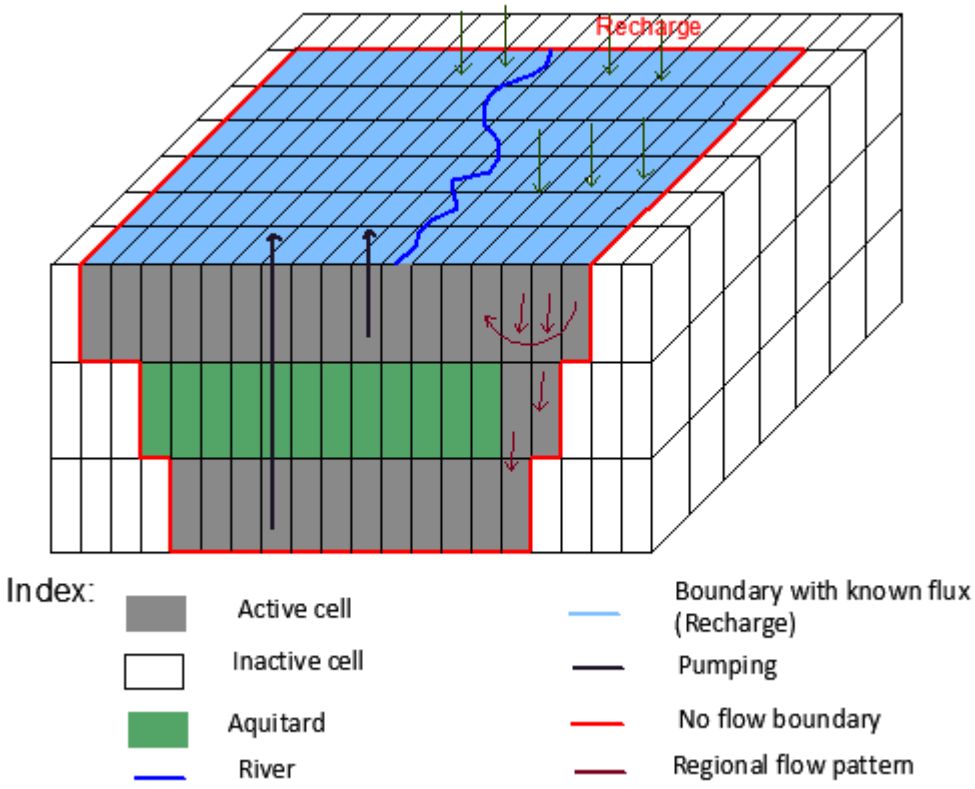

Fig 4.2: Conceptual model of Kathmandu valley showing the aquifer system and boundaries

The construction of the conceptual model is very useful step in constructing a groundwater flow model because it helps to simplify the informations needed for the models. In practice, it is often difficult to obtain site-specific information on hydraulic conductivities and hydrogeology to define hydrogeological units. In a groundwater model it is not possible to include every single detail of the physical system; however, the information used to build the model must contain the essential features of the system and must reproduce the actual conditions of the groundwater flow system.

The development of the aquifer conceptual model included:

1) Definition of the area to be modeled and Identification of the boundaries

The area to be modeled corresponds to the groundwater basin of the Kathmandu valley in Chapter 3, Fig 3.8. Model boundary is the interface between the model calculation domain and surrounding environment. In modeling, we are interested in a specific part from the continuous real world system. Thus, the effect of the real world in terms of hydrological influences at the model boundaries must be described. Correct selection of boundary conditions is a critical step in model design because the boundaries largely determine the flow pattern (Anderson & Woessner, 1992). In other words, flow and mass exchanges across the boundaries are simulated and hence wrong boundary conditions generate wrong water balance of the system under study.

In groundwater flow systems, model boundaries could be physical (impermeable geologic formations and surface water bodies) or hydraulic boundaries (groundwater divides and flow lines). Establishment of the model boundaries is based on the site specific knowledge acquired from the geology topography and flow system prevailing in the area. Kathmandu valley is physically separated by the rock surface in all sides of the basin which are defined as no flow boundaries assuming that the groundwater fluxes across the surface will not occur. In the valley, a river named Bagmati river will flow with its tributaries from North to South which is defined as constant head river boundaries in the model.

2) Definition of the hydrogeological units

Hydrogeological units comprise geological units of similar hydrogeological properties. While formulating the hydrogeological units, several geological formations may combine into a single hydrogeological unit or a geological formation may be subdivided into aquifers and confining units. Understanding the lateral and vertical extent and relationship between the hydrogeological units is crucial for constructing an accurate conceptual groundwater flow model. Geologic information including geological maps (Fig 3.1, Chapter 3) and cross section (Fig 3.2 & Fig 3.3, chapter 3) showing the areal and vertical extent and boundaries of the system.

Based on available borehole data and knowledge gained from the previous studies, the following hydrogeologic units are identified (Table 4.1).

Table 4.1: Correlation of hydrogeologic unit and model layers for the Kathmandu valley

Stage	Lithostratigraphic units	Hydrogeologic unit	Model layer
Holocene	Gravel, sand, silty sand, sandy clay, gravelly clay	Permeable zone 1	1
Pleistocene	Clay, clayey sand, silty clay, lignite	Confining units	2
Late Pleistocene to early Pleistocene	Sand, gravel, sandy gravel, sandy silt, gravely silt	Permeable zone 2	3

3) Flow system: A groundwater flow system is a set of flow paths with common recharge and discharge areas. The conceptualization of how and where water originates in the groundwater flow system and how and where it leaves the system is critical to the development of an accurate model. The local flow system is controlled by the topography and geology. The mechanism of groundwater discharge from the aquifer system is mainly controlled by the discharge to the river and well abstractions. The Bagmati river is well connected to the aquifer system which feeds water to the river as base flow during the dry season. The groundwater discharge from the aquifer due to the springs and seepages along the river banks mainly in the lower reaches of the river and marshy areas in the flat laying parts of the valley. There is one outlet in the study area which drains out water through Bagmati river. Most of the precipitation enters into the river by natural drainage. The water enters into the shallow aquifer through direct infiltration into the deep aquifer through recharge area (Fig 3.5, Chapter 3).

4.5 Model layer elevation data

The development of the conceptual model for the study area established three layers for the model (Fig 4.2). The elevation data of each of the hydrogeologic layer has been determined from the borehole logs. The Kathmandu valley groundwater basin is divided into three hydrogeologic layers; shallow aquifer, aquitard and deep aquifer. The data regarding the bottom of the each aquifer layers are abstracted from analysis of the geological logs in

different parts of the Kathmandu valley. Layers in borehole logs having the same hydrogeological properties will be combined in one layer. Some of the borehole logs with its geological formations are shown in Appendix A. These elevation data for the bottom of the shallow aquifer, aquitard and deep aquifer are less in number. To better represent the real distribution of the each aquifer layer, control points are taken from the DEM prepared by the Pandey & Kazama (2010). The DEM consists of the aerial distribution of the thickness of each hydrologic layers. These control points taken from the DEM (Digital Elevation Model) are included in the Appendix A.

The elevation data for the top of each layer (x, y and z coordinates) was used to produce a grid file using SURFER® 8. Golden software interpolates a Z value at the intersection of each row and column in the grid file, thereby filling holes in the data. The irregularly spaced data points are used to interpolate grid node values. These interpolated values are written to a grid file (Golden Software). The interpolation technique used was kriging. Kriging is a statistical interpolation method that chooses the best linear unbiased estimate and unlike other interpolation methods, it preserves the field value at measurement points (Anderson and Woessner, 1992).

These elevation data collected from the topographic map, DEM data and borehole logs are used to produce .DAT file in Surfer®8. This .DAT file can directly be imported to the MODFLOW software. The origin for the data in the surfer is chosen as (618810.44, 3051036.22). The contour map of the ground elevation, elevation of bottom of shallow aquifer, elevation of bottom of aquitard and elevation of bottom of deep aquifer produced in surfer are shown in Fig 4.3, Fig 4.4, Fig 4.5 & Fig 4.6

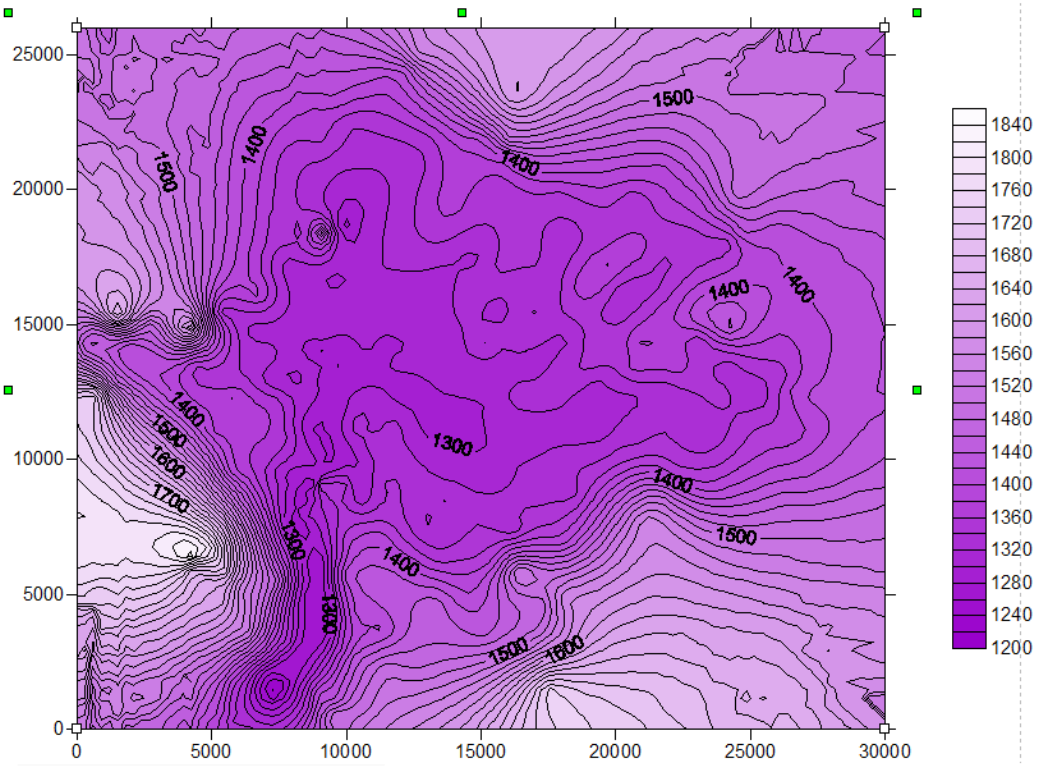

Fig 4.3: Ground elevation contour map

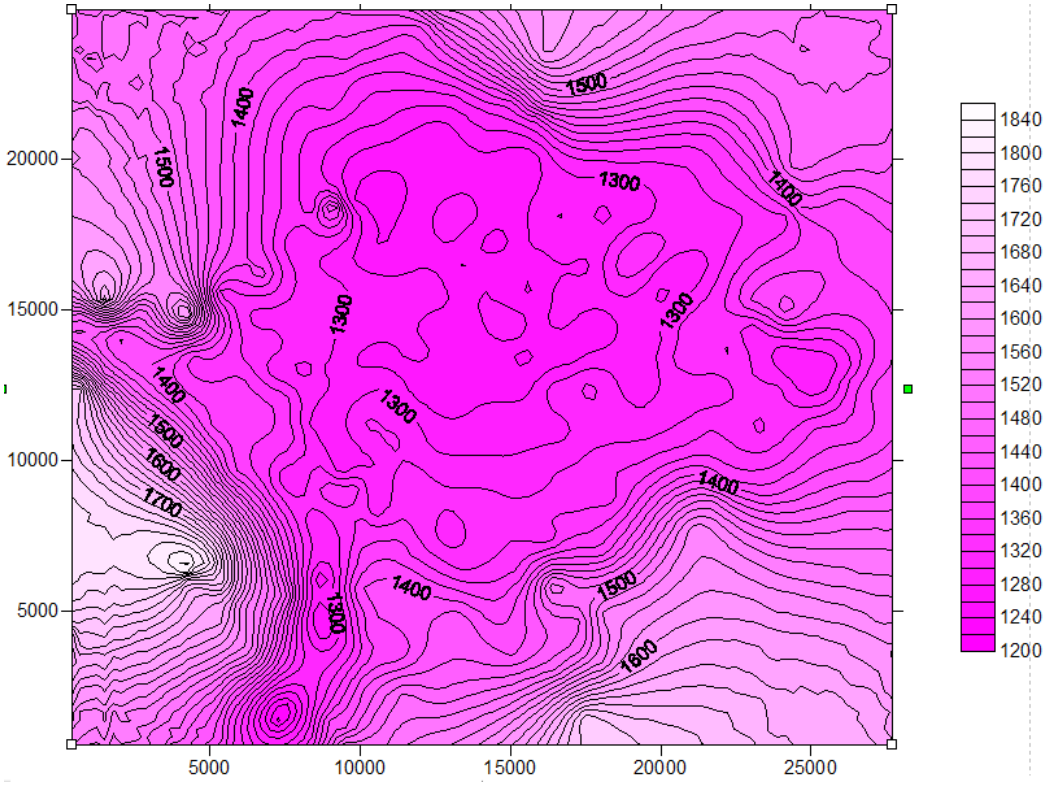

Fig 4.4: Contour map of bottom of shallow aquifer

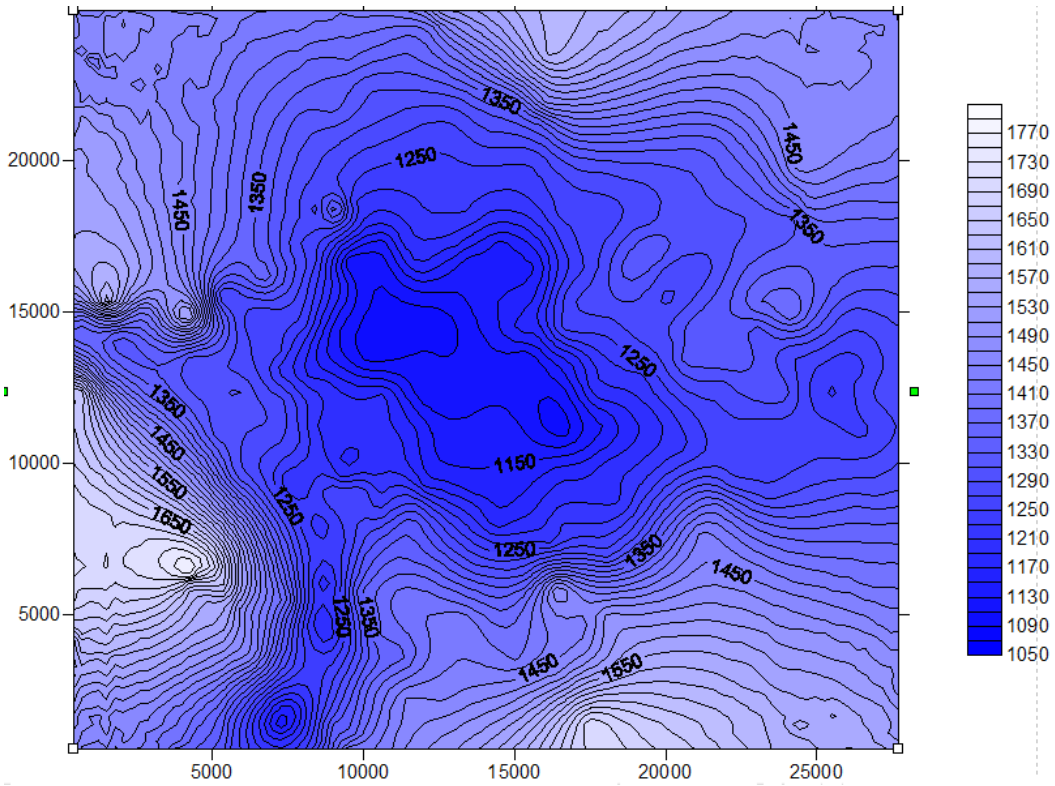

Fig 4.5: Contour map of bottom of aquitard

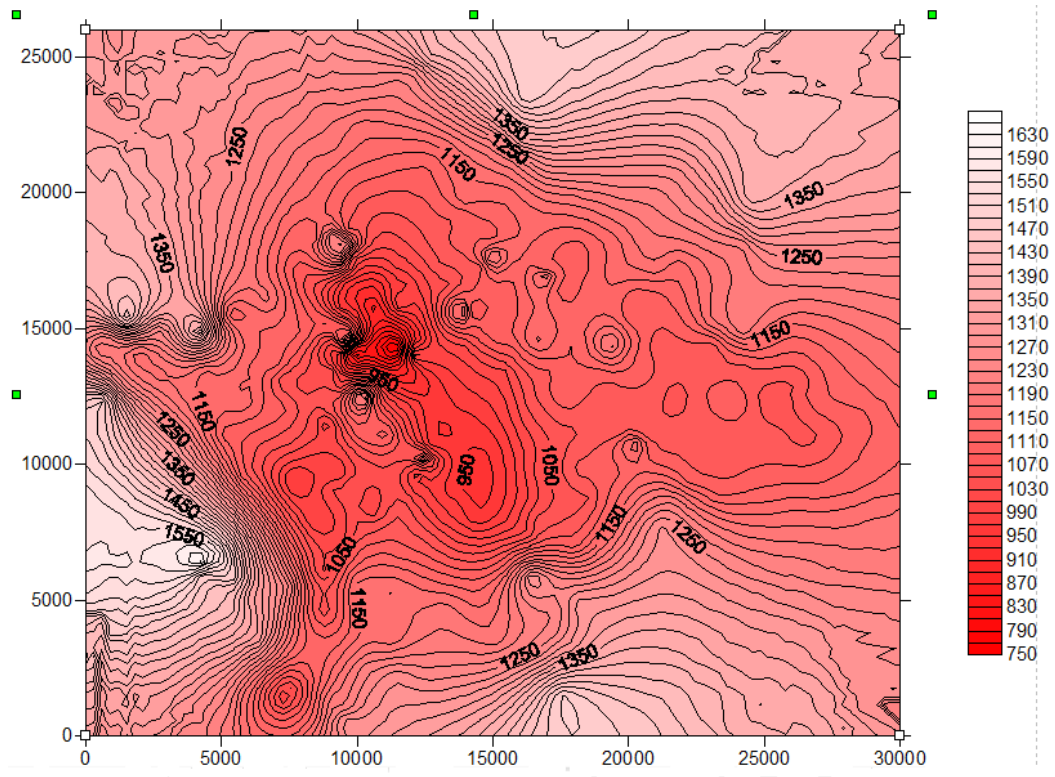

Fig 4.6: contour map of bottom of deep aquifer

4.6 Assumptions

The construction of a model is an attempt to reproduce real conditions as far as possible. But often due to the unavailability of the data, complexity of the field conditions and limitations of the numerical solutions, some assumptions has to be made in the model to make it simple and easily solvable. In this model, following assumptions were made:

i) In the Kathmandu valley, there is complex sediment nature with complex nature. These complex layers have been simplified into three layers. It is assumed that the conductivities of each layer is constant throughout the layer. The conductivities along x and y direction is assumed to be same and that for z direction are assumed to be 10 times lower than the x and y direction.

ii) There may have some flow between the aquifer layers and the adjoining basement rock and surface due to the presence of faults and fractures. It is assumed that there is no flow between them (no flow boundary).

iii) The model for the study area was constructed for the year 2001. The groundwater abstraction for 2001 was interpolated (Table 3.11). The year 2001 was selected because of the availability of groundwater measurement data for year 2001 which is used as initial condition. As there is no proper data of abstraction from the pumping well, it is assumed that the total abstraction is equally distributed to all the wells in the model.

iv) The available pumping well data have well screen location for most of the wells. The screen locations of those wells which do not have such data were estimated by observing the screen of the adjacent wells.

v) The distribution of the recharge is based on basins and distribution of the precipitation. Local attributes such as soil type and topography may control the recharge. Hence it is assumed that the recharge in this study is considered constant in different years and also is equally distributed in different months of the year. It is also assumed that the recharge is equally distributed spatially within the model domain.

4.7 Model design

4.7.1 Grid

The horizontal extent of the model domain is 28.5 by 25.6 km bounded by 618810.44 to 647345.44 m UTM East and 3051036.22 to 3076721.22 m UTM north. The irregular shape of the study area reduces the model domain to an area of about 330 km^2. The digital map of the Kathmandu valley and map of the groundwater basin of the valley was collected from the map prepared by JICA (1990). This map is in the form of shape file which could be inputted directly to the Visual MODFLOW.

The grid in MODFLOW consists of a set of rows and columns that are orthogonal. Cells are formed by the intersection of these lines. A node is located at the center of each cell. It is assumed that the hydrologic and hydraulic properties are uniform all over the extent of the cell area.

For the Kathmandu valley, the grid is taken as a size of 200 column and 200 rows with each cell occupies 0.018 km^2 (18330 m^2). The actual model area of the Kathmandu valley is 28.5 km x 24.5 km. Outside the groundwater basin the boundary of the study area is defined as inactive. In the rest of the area, the active cells (white area in Fig 4.7) covered the modeled area of the valley.

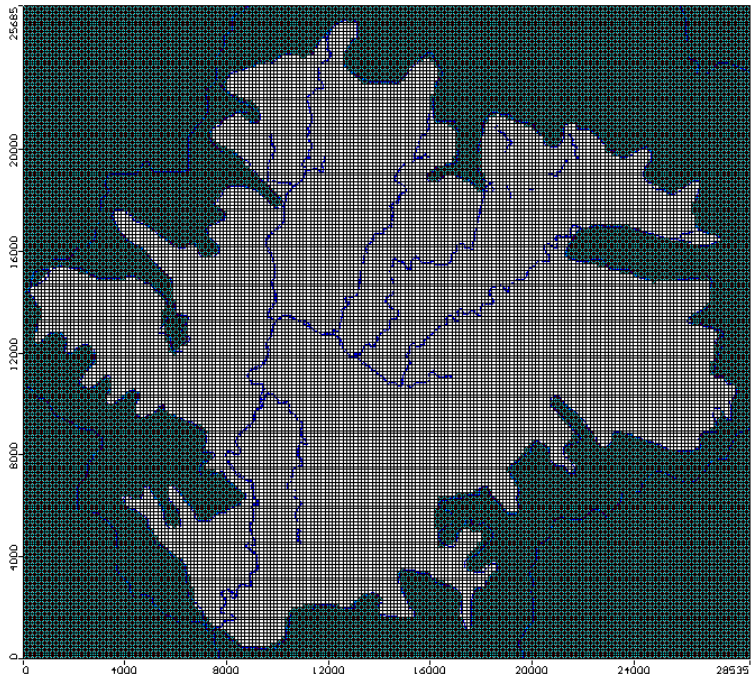

Fig 4.7: x and y grid for the flow model showing white active cells and grey inactive cells

In groundwater modeling, the number of model layers, which are considered in the discretized domain, depends on the hydrogeological stratification of the system. The aquifer system was divided vertically into three layers of cells, each layer representing the modeled aquifers or the confining unit. Bottom elevation of different points of each layer was imported for the design of the model which was created by Surfer 8 as .GRD file. This gives the vertical distribution of each layer.

While importing the bottom elevations of each layer, a minimum thickness of 10m was assigned to each layer to guarantee grid smoothing by preventing discontinuities between cells. Later those cells that have nearly zero thickness were assigned the hydraulic properties of the respective layer so that it will represent real condition. The minimum elevation of the bottom of deep aquifer layer is around 775m elevation as shown in Fig 4.8.

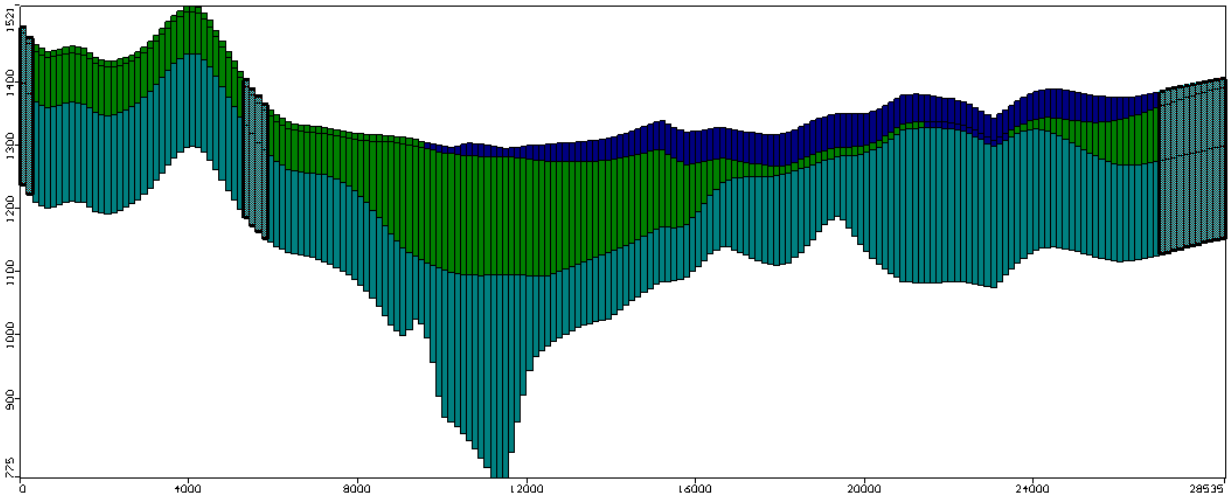

Fig 4.8: Section at row 89 showing minimum elevation of the bed rock and of principle aquifer layers

The top of the model is the shallow aquifer which is assigned as unconfined aquifer. The middle layer is the aquitard which has low conductivity and is assigned as confined /unconfined layer with variable S and T. The lowest layer is the deep aquifer which is assigned as confined aquifer with constant S and T.

4.7.2 Model parameters

a. Assigning hydraulic conductivities and storage parameter

Hydraulic conductivity is in many cases the most critical and sensitive modeling parameter. Attempt is made to design a model with realistic values of K value as far as possible. As pumping test in the field was not found, the conductivity values and storage values for the different layers were collected from published reports.

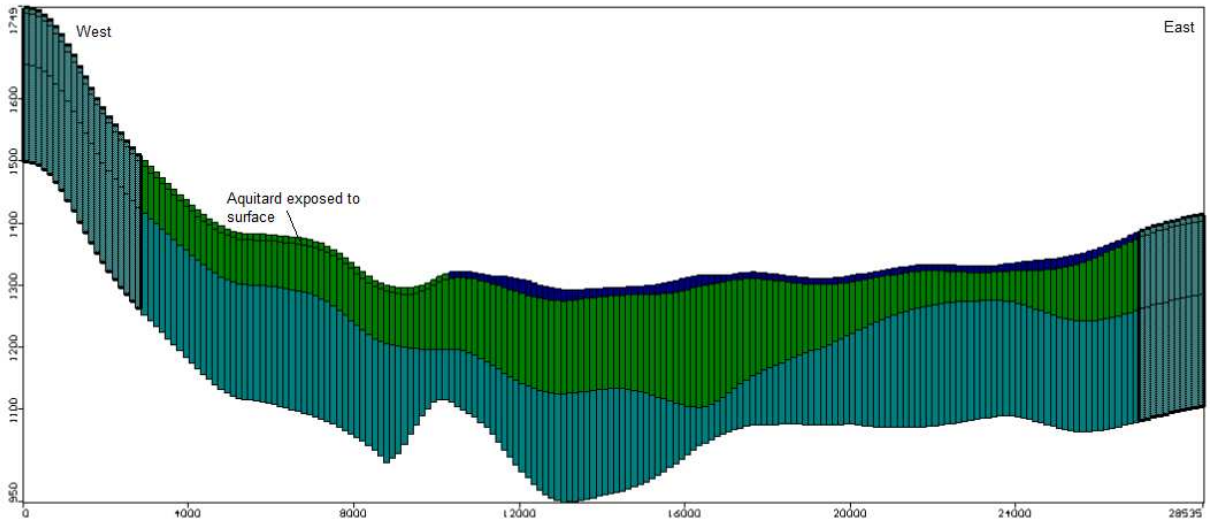

Fig 4.9: Section at row 110 showing the clay layer exposed to the surface

Some northern part and some southeastern part of the valley has no middle aquitard layer and are considered as the recharge zone to the deep aquifer as shown in Fig 4.10.

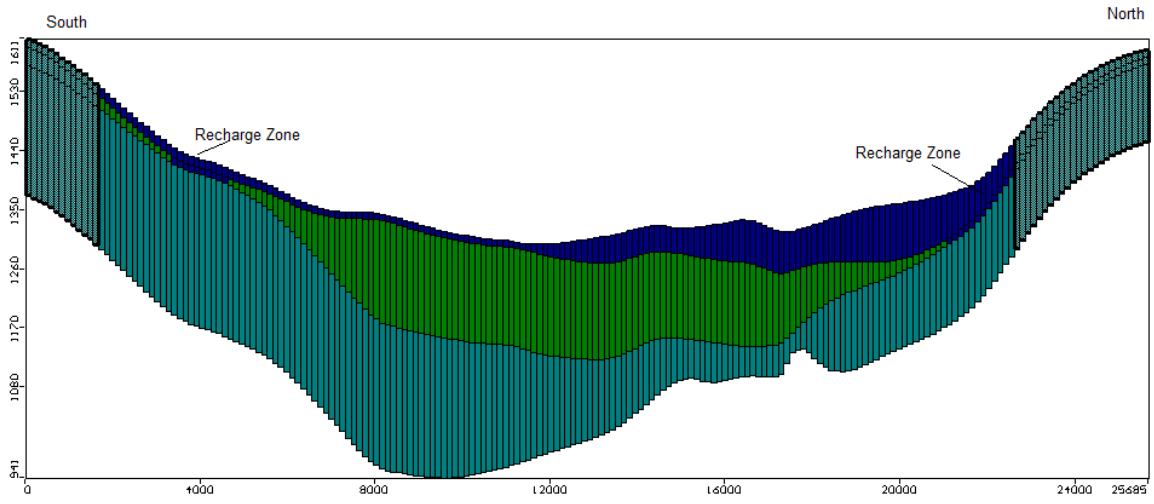

Fig 4.10: Section at column 103 showing the hydrogeological layers with recharge zones

b. Time

Time is an important parameter in the modeling of the groundwater flow. It describes the temporal changes of the model output such as head, drawdown, etc. The time unit selected as day and time period specified 3650 days.

4.7.3 Boundary conditions

The following types of the boundary conditions were assigned in the model.

a. Boundary condition with head-dependent flux

The boundary for which the flow rate is calculated based on the head difference between the boundary cells and the adjacent aquifer cells is called head-dependent flux boundary. The model consists of a river and its tributaries flowing from the north to south which is assigned as the boundary condition for the model (Fig 4.11).

b. No flow boundaries

Boundaries with the flux set to zero are called no-flow boundaries. MODFLOW automatically assumes a no-flow boundary around the perimeter of the grid i.e the boundaries represented by the outline of the inactive cells. The lower part of the deep aquifer which is in contact with the bed rocks is considered as the no flow boundaries. Also the edge of the three layers of the model is in contact with the rock in all sides of the model. Hence these edges are also considered as the no-flow boundary.

c. Boundary with the known flux

Typical boundaries with known flux are inflow/outflow through lateral contacts between different aquifer, seepage from/in from adjacent layers, spring flow and recharge. In this model, Recharge to the model cell is specified as boundary condition. The recharge was assigned to the top layer of the aquifer and only to the active cell. The top layer was designed as the unconfined aquifer. The recharge of 43 mm/year was specified to the entire layer.

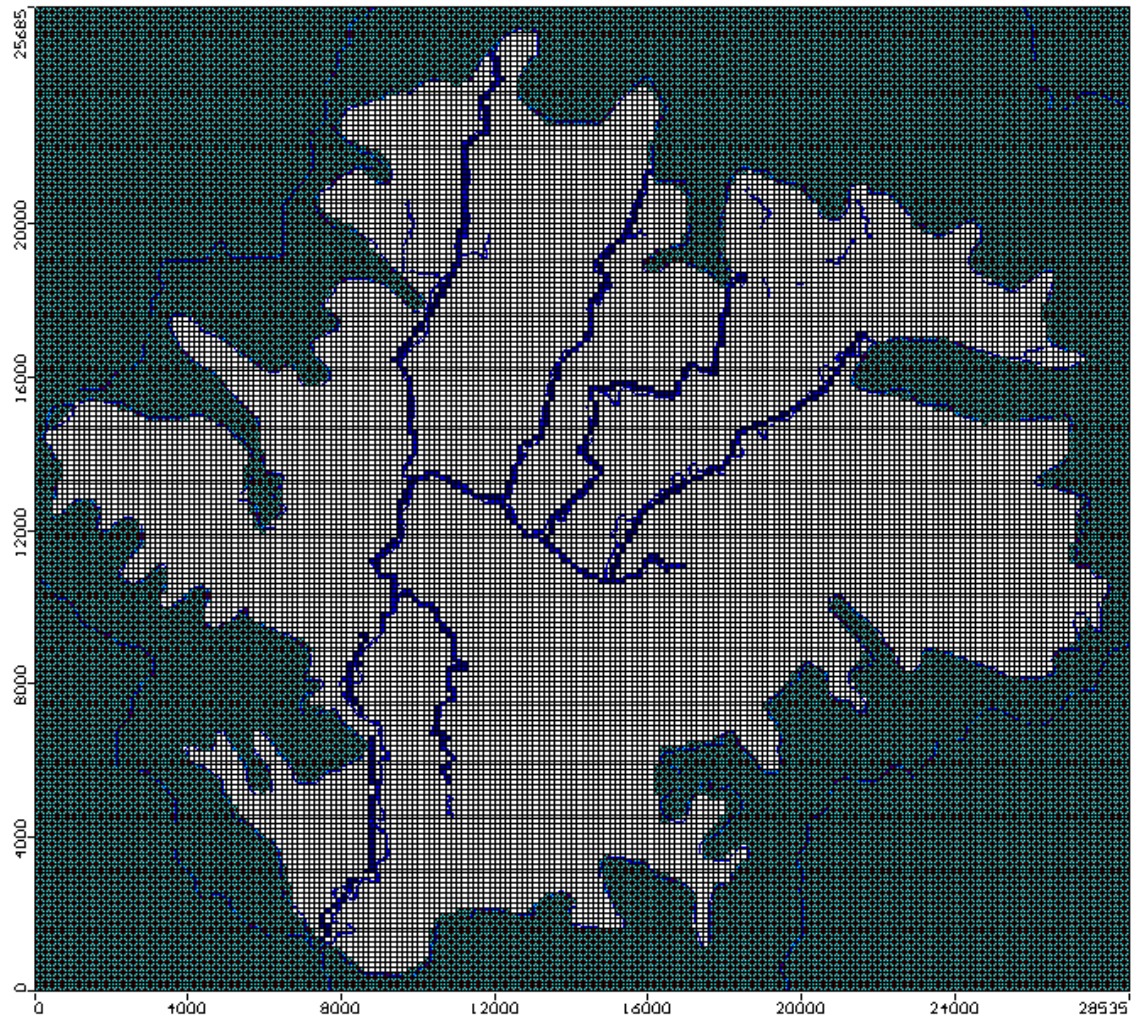

Fig 4.11: Model showing the boundary condition (river)

4.7.4 Initial conditions

Initial conditions refer to the hydraulic head distribution in the system at the beginning of the simulation and thus are boundary condition in time (Anderson & Woessner, 1992). The initial conditions in numerical groundwater models are initial head distributions and have only to be entered to fulfill the convergence criteria of the numerical scheme. If the hydraulic gradient between heads of boundary elements and non boundary elements become too large, many computer codes will fail in their calculations by numeric instabilities. So for steady state models initial heads should be only in the range with the values of the hydraulic head conditions at the boundary element of the model. For the present case, the static water level records of the wells are interpolated within the model to obtain the initial hydraulic heads for the entire model as shown in Fig 4.12.

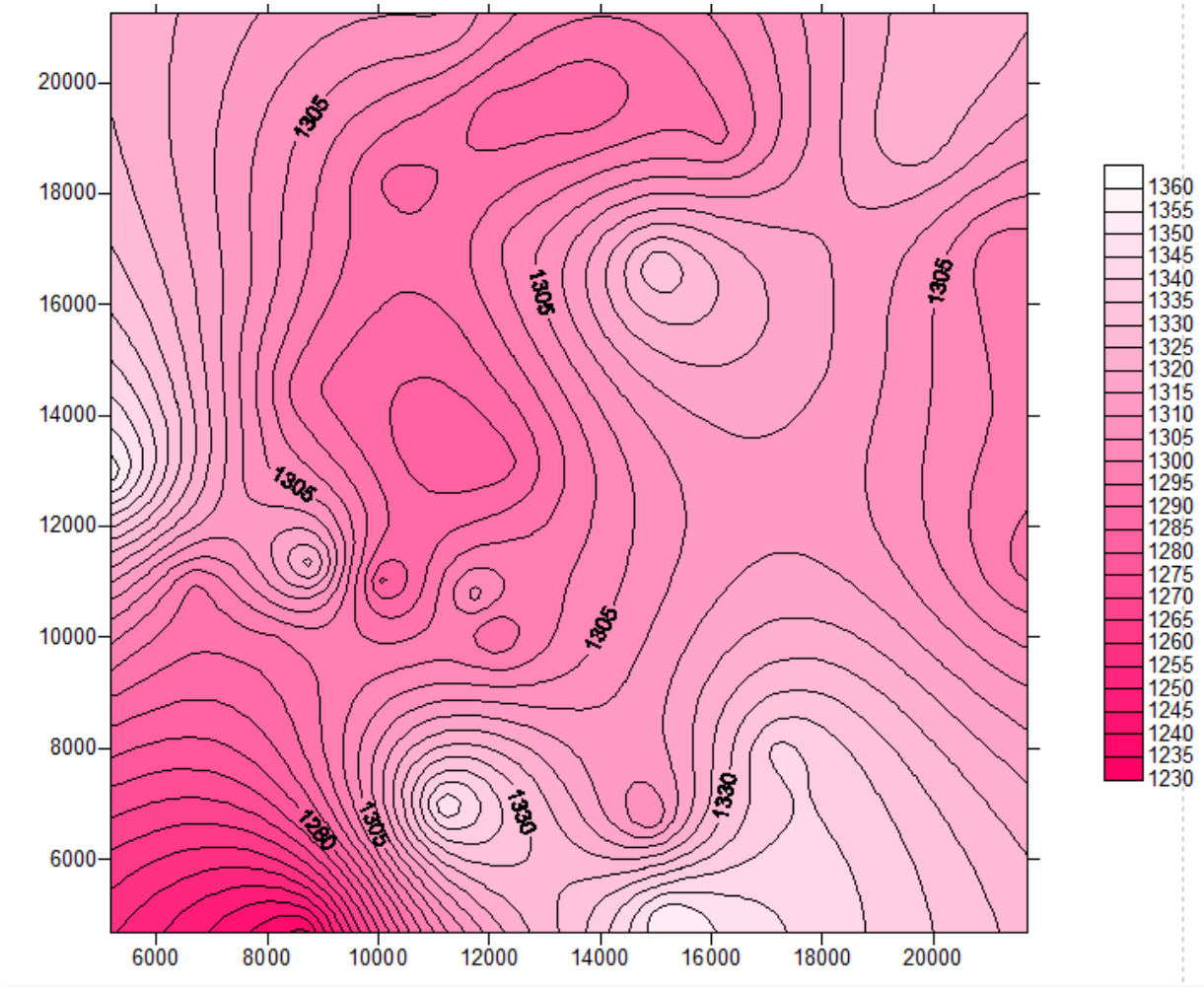

Fig 4.12: Initial groundwater head contour map

4.7.5 Groundwater abstraction

Many pumping wells have been established in the Kathmandu valley. These pumping wells have been input to the model along with its screen location. Pumping wells were simulated using well package and daily pumping rates for 2001. The depth range of screens for wells is shown in Appendix B. A typical well with its screen location is shown in Fig 4.13.

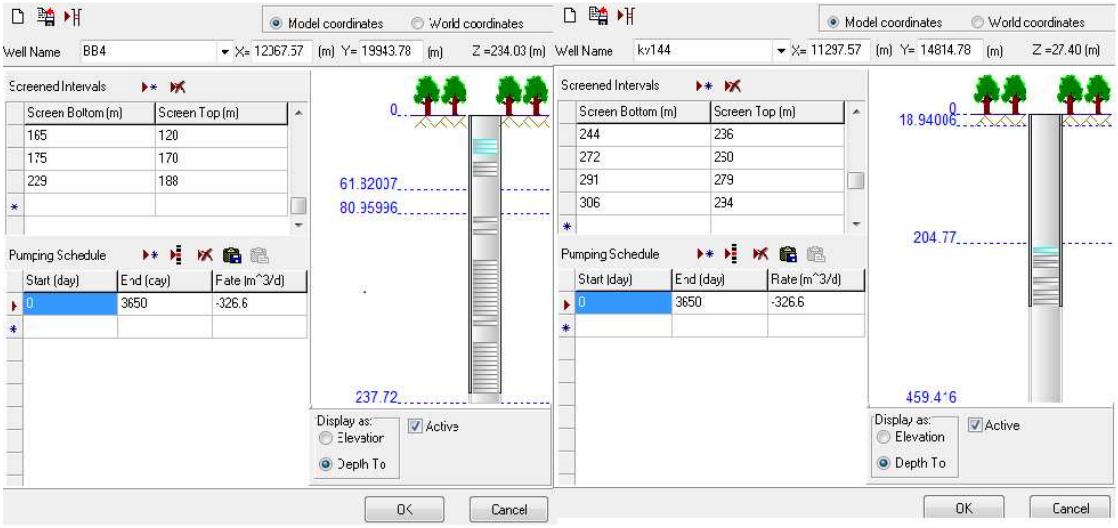

Fig 4.13: Typical wells BB4 and kv144 with details

It has been reported that around 218 pumping wells has been operating in 2001 (GWDB, 2009). But 188 pumping wells with its location can be found in this study which will represent the good indication of the distribution of the pumping wells and also these wells have been assigned in the model with average rate of abstraction as shown in Fig 4.14.

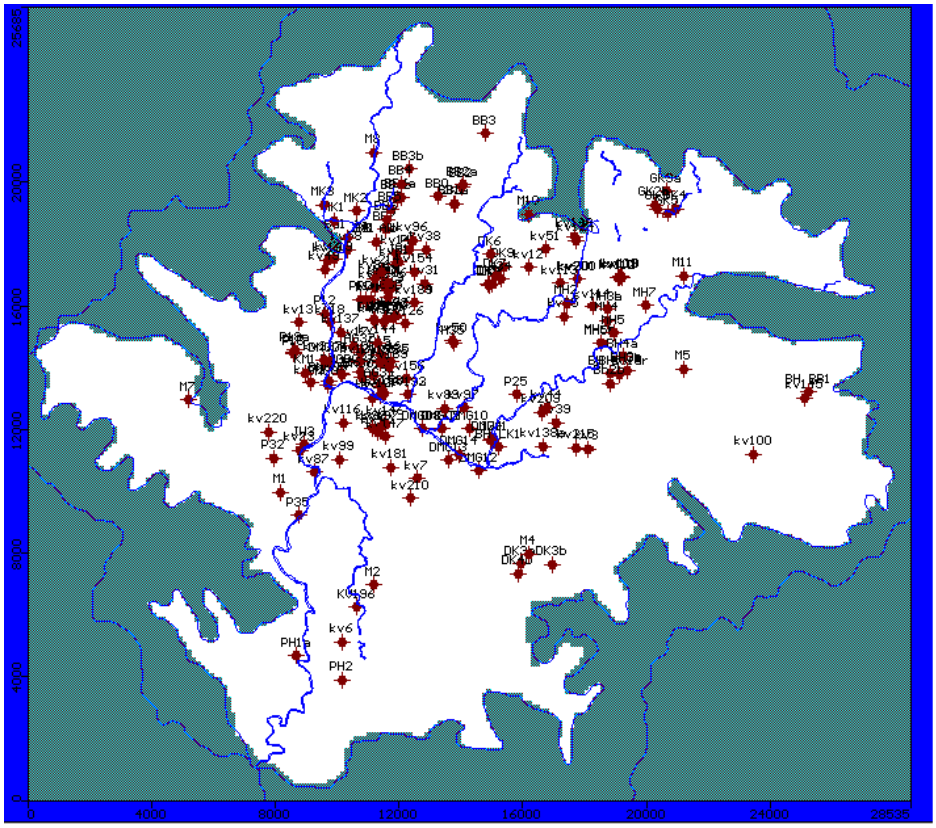

Fig 4.14: Wells locations in the model domain

4.8 Rewetting

Rewetting is a method used in MODFLOW where dry cells can be converted to wet or variable head cell if the head surrounding cells is high enough to trigger rewetting. This method is used MODFLOW is a saturated flow code and consider dry cells as “no-flow” cells since it cannot simulate complicated unsaturated groundwater flow. Cell rewetting was activated for all cells in the model and model must simulate flow with fluctuating water levels in a simulation. Rewetting also presents difficulties with convergence since convergence error used in solving the groundwater flow equation is prone to oscillation, as cells are converted between wet and dry within iterations of each time steps (Toews, 2003). To avoid oscillations in the convergence, rewetting was enabled only on 10 iteration interval. Rewetting was assigned from top and bottom cells. The rewetting threshold was assigned as 0.1 and wetting factor of 1 as in default.

4.9 Solver

The MODFLOW finite difference equation for each model cell expresses the head at the center on the basis of the heads in six adjacent cells i.e. rectangular cells above, below and on the four sides. This requires that the equation for the entire grid is solved simultaneously. The solver used in this model is WHS solver. The maximum number of inner iterations was set at 25 and maximum number of outer iterations at 200. The head change and residual criterion were set as 0.1m for both so that the iteration stop when the maximum absolute values of the head changes and residual from each cell are less than or equal to 0.1m.

4.10 Model run

The next stage of the model after the set up is to run the model. The main objective of the run is to find results that nearly coincide with the actual or real case. Many iteration were done to achieve this objective in steady state condition. This is done by changing the sensitive parameters which affect the results of the model until the suitable results were determined. In order to determine the ground level and the water budget, flow simulation package was run. The output of the model provides most of the results of the model run such as water level, flow direction, particle tracking, velocity, etc. The water budget package is

used to calculate the amount of water that enters and out from the system. Flow path package is used to determine the path lines and velocity vector of the flow.

4.11 Limitations of the model

Numerical models of groundwater flow are limited in their representation of the physical system because they contain simplifications and assumptions that may or may not be valid. Results from groundwater flow models have a degree of uncertainty primarily because of uncertainties in many model input parameters (most importantly hydraulic conductivity and transmissivity) and boundary conditions applied. The various steps in the modeling process may each introduce errors, converting the real world into conceptual model and converting conceptual model into mathematical model. There are some of the limitations of the model which are summarized as follows.

i) Hydrogeological heterogeneity: The hydrogeological heterogeneity caused difficulties in the conceptual simplification of the field conditions due to lack of detailed description of the heterogeneity. The model site is very complex in nature. The borehole logs show sediments distribution in different layers. In building the mathematical model, it is not feasible also is difficult to solve the model considering all the layers. So simplifying the model may add uncertainties to the output of the model.

ii) Input Data: The main constraints in the modeling process were data gaps and poor quality of the available data. The data which have a key role in defining the model geometry (hydraulic conductivities, screen length, abstraction, aquifer thickness) were not found well documented. The available records of the water level measurements were not continuous and only few in number. Furthermore the calibration value is highly associated with the measurements errors and the distributions of measurements within the model domain. Hence these data may lead uncertainties in the model output.

iii) Boundary conditions: Another area of the uncertainties is resulting from the boundary conditions of the model domain. The boundary conditions were defined based on the surface physical features such as impervious beds, rivers etc. The location of the groundwater boundaries may not be certain since they may not exactly coincide with the real surface.

iv) Scale: Accuracy and the applicability of the model vary mainly from the regional to the local scale. This is due to the information in the model and the size of the cell. With the smaller the size of the cell, better will be the accuracy in the output.

4.12 Model calibration

In most cases, the model will not give satisfactory results if the input data to the model do not reflect the real world with enough accuracy mainly due to ambiguity of input data. Thus in order to improve the reliability of the model, adjustments in the model input data are required. In the procedure of parameter value adjustment, the values are adjusted within a pre-determined range of error criterion until the model produces results that approximate the set of field measurements selected as the calibration target.

Prior to the calibration process, setting of calibration target is required. Calibration target is a calibration value and its associated errors. In this study, hydraulic heads obtained from groundwater level measurement data were used as calibration values. And the calibration target was to match hydraulic heads calculated by the model with measured head points. Measured hydraulic heads were obtained from groundwater level monitoring from static water level records measured during time of 2002 by GWDB in 21 wells.

Trial and error calibration is the process of manual adjustment of input parameters until the model produce field measured heads within the range of the error criteria. The model was calibrated for natural steady-state conditions, assuming constant recharge and steady discharge neglecting seasonal fluctuations. Calibration was conducted through trial and error by varying aquifer hydraulic parameters and comparing calculated heads to those measured in wells. During the calibration, hydraulic conductivities of three layers were modified manually and trial runs were carried out. From the output of the each run, different error parameters such as correlation coefficient, residual mean, standard error of estimate and normalized root mean squared error were determined and the error quantifying analysis was done. The main objective of the trial run and error analysis is to minimize the different error parameters and to maximize the correlation coefficient. A scatter plot of measured heads against simulated heads is drawn showing the calibrated fit (Fig 4.15).

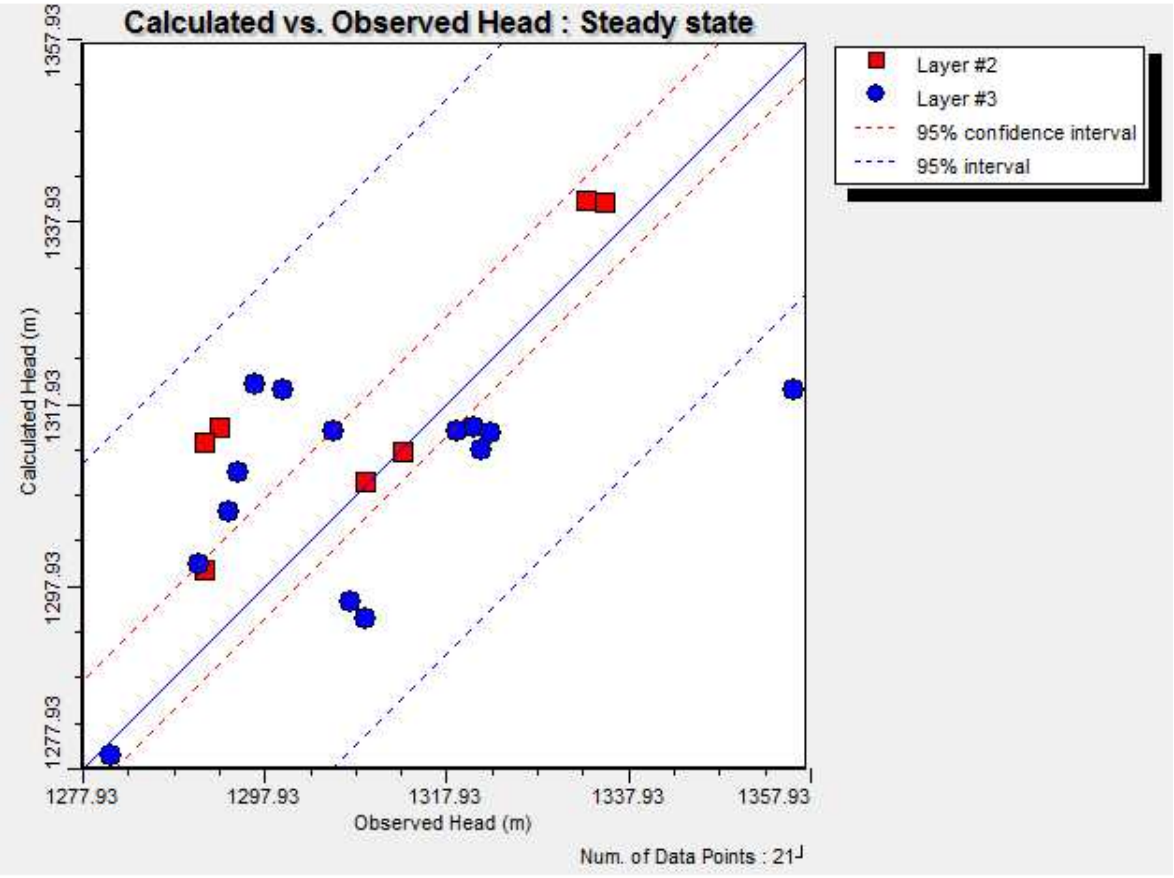

Fig 4.15: Comparison of hydraulic head and measured head for steady state model

The evaluation of the calibrated model result shows that:

i) Most of the simulated heads and the measured heads were fall within the 95% interval which shows that it is calibrated.

ii) Water balance discrepancy was 4% which is small as compared to the extent of the study area.

iii) The overall results of the groundwater model are comparable with the measured well data and in agreement with conceptual model.

iv) The measure of errors evaluated by mean error, mean average error and root mean squared error were evaluated and these errors were found minimum at the calibrated values as shown in Fig 4.27.

v) The measure of the correlation coefficient was evaluated and it was found maximum at the calibrated values as shown in Fig 4.27.

vi) The calibrated values of the hydraulic conductivities for the different layers of the layers are shown in Table 4.2.

Table 4.2: Calibrated hydraulic conductivities values

S.N.	Layers	Kx (m/s)	Ky (m/s)	Kz (m/s)
1	Shallow aquifer	7 E -4	7 E-4	7E-5
2	Aquitard	7 E-8	7 E-8	7 E-9
3	Deep aquifer	1.2E-5	1.2E-5	1.2E-6

vii) It is found the standard error of estimate as 3.19 m; residual mean as 2.81m; normalized RMS as 19.42% and correlation coefficient as 0.619 at the calibrated values.

4.12.1 Discussion on calibration results

The calibration has been performed with the measured heads in the model domain. There may be some reasons that influence the calibration results which are summarized as follows:

i) It is found that the measured heads in the study area are largely varied. For such area, there should be large number of measured points to better represent the real condition. But the number of the wells where static head is measured in the study area is not adequate.

ii) There are no independent monitoring wells, the water level observations are carried out on the pumping wells. This will also influence the calibration result.

iii) There may be some measurement errors related to measuring instrument accuracy and operator errors which will influence the calibration.

iv) Assumptions made during the modeling also influence the calibration of the model.

4.13 Modeling Results

A discussion of these results and their implications to this investigation follows. This discussion includes simulated hydraulic heads, the implications of dry cells, vertical flow, flow direction, and pathlines within the groundwater system.

4.13.1 Simulated heads

The main output from a model such as MODFLOW is hydraulic head values for each cell in the model domain. A water table surface can be interpolated from these hydraulic head

values. The water table is presented as contour lines representing an interpolated surface that indicates the hydraulic head of the model domain. This information is significant because the location of the water table indicates a variety of important observations about the flow system. A reduction in the elevation of the water table can indicate a depletion of groundwater resources. A depletion of groundwater resources could significantly impact the people that rely on groundwater as a primary drinking water source. The location of the water table also dictates the interaction between surface-water and groundwater, which could potentially influence surface water supplies. This information is key to managing groundwater effectively, and assuring a safe and sufficient groundwater supply. The hydraulic head contours from the steady state simulation for each layer are shown in Fig 4.16, Fig 4.17 & Fig 4.18.

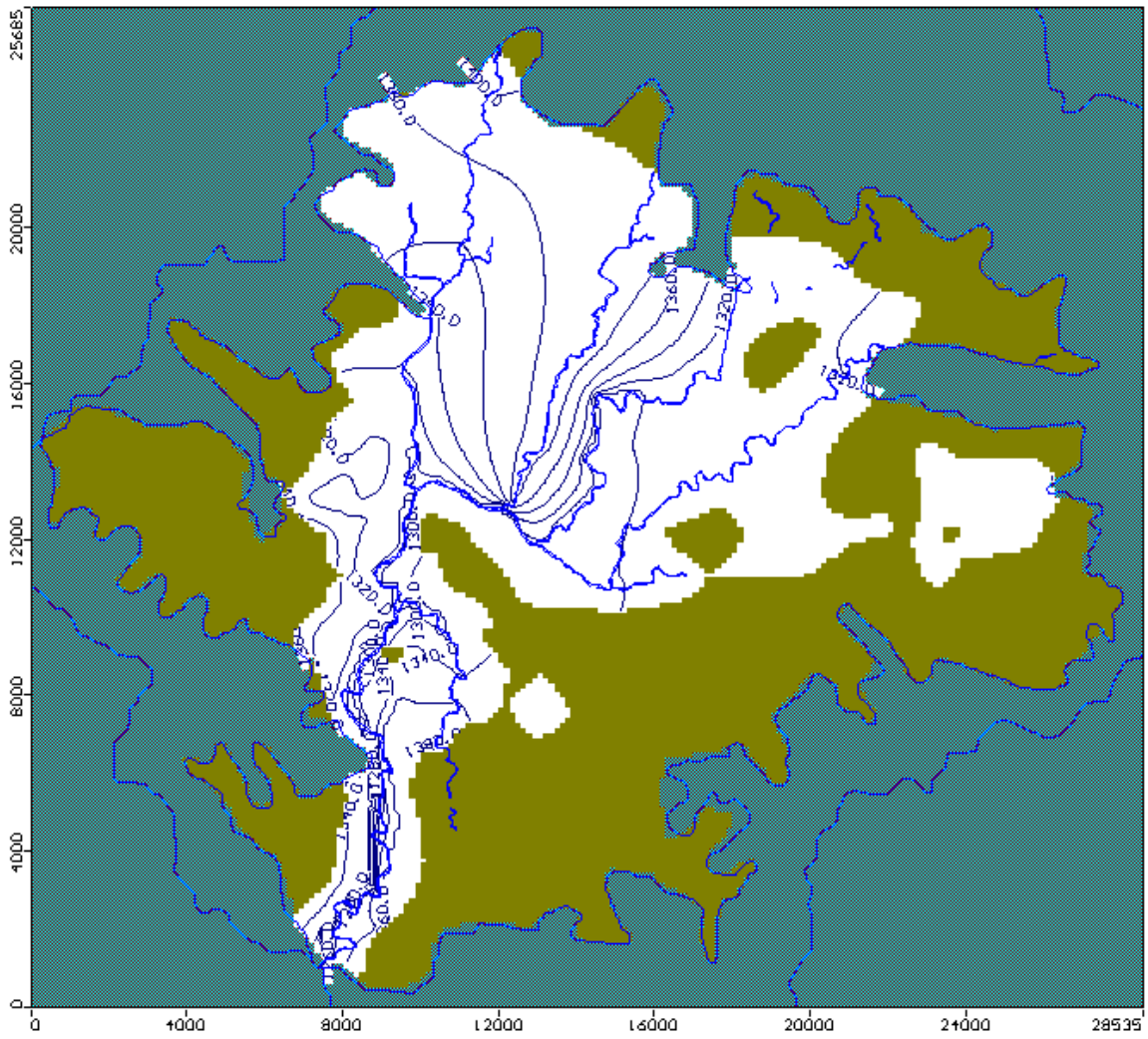

Fig 4.16**:** Shallow aquifer layer showing the dry cells and the hydraulic head

Simulated hydraulic head of shallow aquifer shown in Fig 4.16 shows that the hydraulic head varies from 1400m to 1300 m. In the northern part head decreases towards east and west from the middle of the northern part. This is due to the fact that the northern part consists of four tributaries of Bagmati river. That means there is sub basin formed for these tributaries which shows that there is natural undulation. Simulation has been performed considering the river as boundary condition which results simulated hydraulic head. The thickness of the shallow aquifer is also very small compared to the other layers. The most of the north eastern part and southern part has hydraulic head between 1320 and 1300m which show that it has low hydraulic gradient.

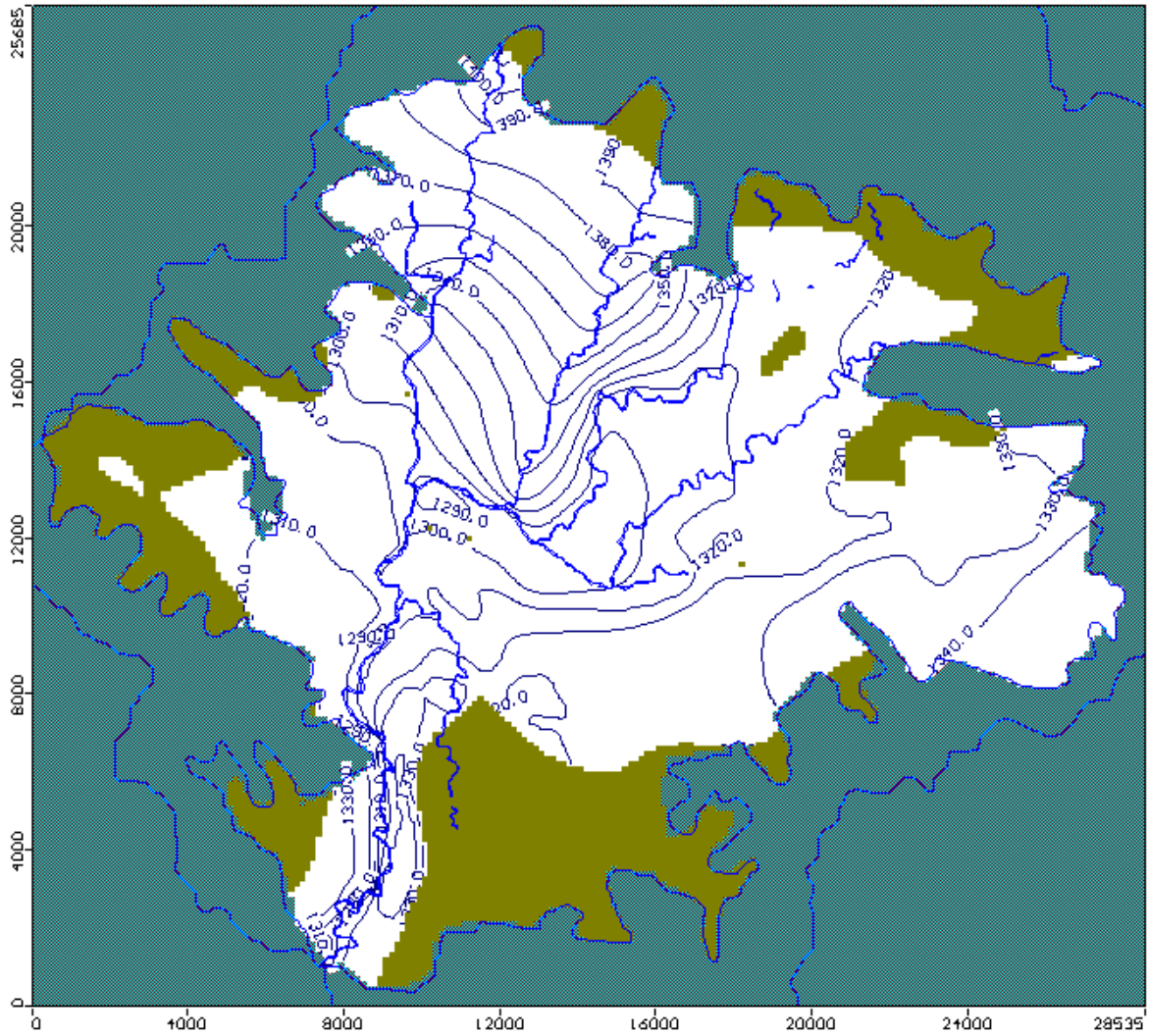

Fig 4.17: Simulated hydraulic head contour in aquitard layer

Simulated hydraulic head of second and third layer shows that the hydraulic head decreases from 1400 to 1300 m from northern part towards the southern part as shown in

Fig 4.17 & Fig 4.18. The most of the north eastern part and south part has hydraulic head ranges from 1320 to 1300 m which is same as in layer 1.

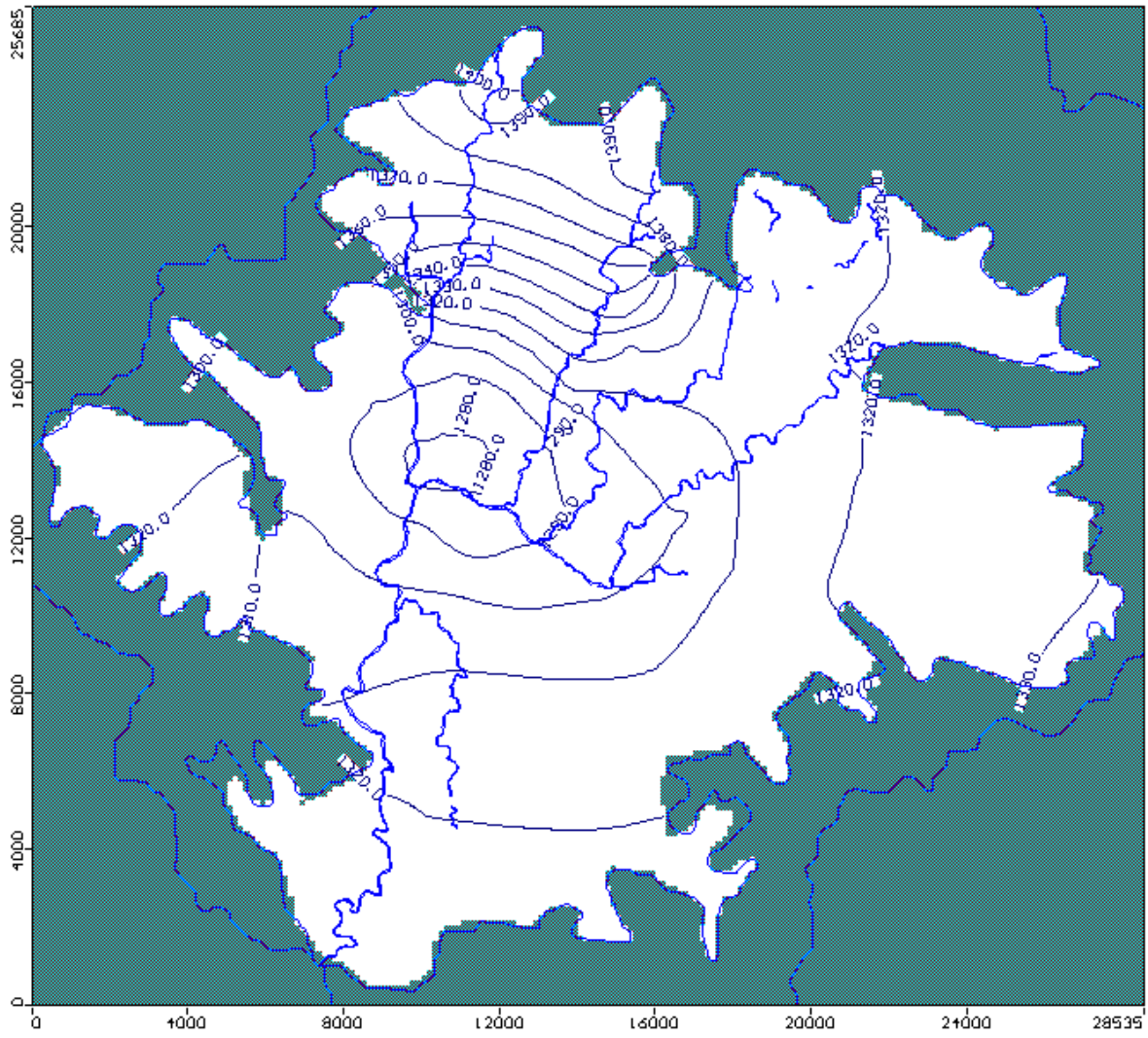

Fig 4.18: Simulated hydraulic head contour in deep aquifer

4.13.2 Dry cell

A majority of layer 1 and some cell of layer 2 “goes dry” (shown in yellow areas Fig 4.16 & Fig 4.17), meaning that the water table resides below the bottom of these cells, and the cells no longer contain any available water. This means that the cells that are “dry” are no longer saturated. Layer 1 conceptually represents the thin layer that lies on top of the aquitard layer system, and it is likely that the hydraulic head resides in layer 2 creating dry cells in layer 1. Fig 4.16 shows that approximately 50% of layer 1 consists of dry cells, which means in these

areas, the hydraulic head resides in layer 2. A majority of these dry cells occur in the east side of the study area where the land surface elevations tend to be higher, steep in slopes and change drastically. In areas such as this, the hydraulic head tends to be deeper than it is in the valleys where the topography changes more gradually and is lower in elevation. Some part of layer 2 also has dry cells. Dry cells in layer 2 occur in those area where the thickness of layer is small with the steep in slopes. These two reason results in the formation of dry cells in the layer 2. The layer 3 does not have any dry cells.

4.13.3 Vertical flow

In a groundwater flow model such as MODFLOW, flow is calculated through the cell faces, and therefore is categorized as predominantly horizontal or vertical flow. Therefore, it is important to identify what type of flow is occurring in order to understand the flow system. Vertical flow represents flow between layers. If vertical flow was occurring, the hydraulic head distributions for each layer would be different (Barone, 2000). In this model, the hydraulic head distribution seems to be different which represent the presence of the vertical flow.

From the flow direction (Fig 4.22) and pathline (Fig 4.25), it can be seen that there is the flow of water between the layers. From the recharge area, it can be seen that water enters from first layer to the third layer. But the flow from first layer to the third layer is small. Only from some part of the area, the flow from first layer to the third layer has taken place. There may have some fractures in the system this is not considered in this model. If deep flow occurs in the natural system, it is not accounted for in the model. The fault system could also promote vertical flow in the system, however, the faults are not represented in the conceptualization of the model for the study area.

The hydraulic conductivity within each cell of model layer was assumed to be isotropic. Therefore, the vertical flow within cells and therefore between layers is simulated. The hydraulic conductivity values estimated using MODFLOW indicate that layer 2 acts as a confining/unconfining unit during the simulations, which permits vertical flow to the other two layers. The second possible explanation for the presence of vertical flow in the simulation could be related to possible recharge issues. One could argue that since recharge is entering the system, vertical flow must occur. Shallow vertical flow driven by recharge could be occurring since some part of the layer 2 has little or null thickness.

4.13.4 Horizontal flow direction

Determining the direction of horizontal flow within the groundwater system can indicate whether the surface-water flow divides for the sub-watersheds within the model. The flow direction can also be used to determine flow paths of possible contaminants in a system. Overall, the flow direction provides a better understanding of flow within the system. Visual MODFLOW gives the user the ability to view the flow direction of each layer in the model. The flow direction is determined by the individual flux values calculated by solving for every node (cell) within the model domain.

The arrows in Fig 4.19 represent the direction of horizontal flow that is occurring within the layer 1. It shows that surface water divide is seemed in the northern part of the valley. In this part, there are four tributaries of bagmati river which itself indicate that there are sub basin formed for these tributaries. The most of the flow direction shows that the water is moving to the natural stream and river which seems to be evident. Local flow tends to flow towards the river/tributaries reaches within the study area, which is expected since the local gradients near the streams induces flow from upland areas towards low areas where reaches reside. All the tributatries will collect water leaking from the ground and flows towards the outlet of the Bagmati river at Chovar. It is in good agreement with the conceptual model.

The flow direction for layers 2 and 3 are identical and shown in Fig 4.20 & Fig 4.21. There is heavy pumping in the central and the northern part and in the southern part there is very low pumping. Due to this, flow direction in fig shows that the most of the water in the layer 2 and layer 3 moves towards the central part of the study area. When water is pumped from the, vacant place should be filled up and water will moves from southern part to the central part. Since there is steep slope of layer 3 in the northern part which slopes towards the central and also major recharge zones to the layer 3 are found in northern part, direction of water is found towards the central part.

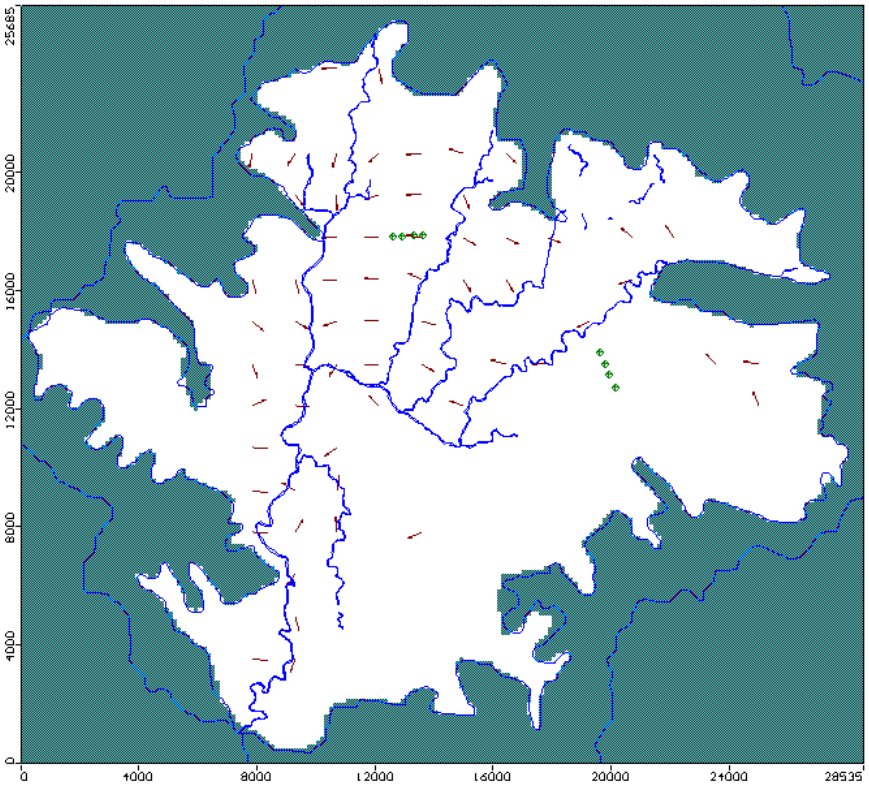

Fig 4.19: Map of the study area showing the flow direction in layer 1

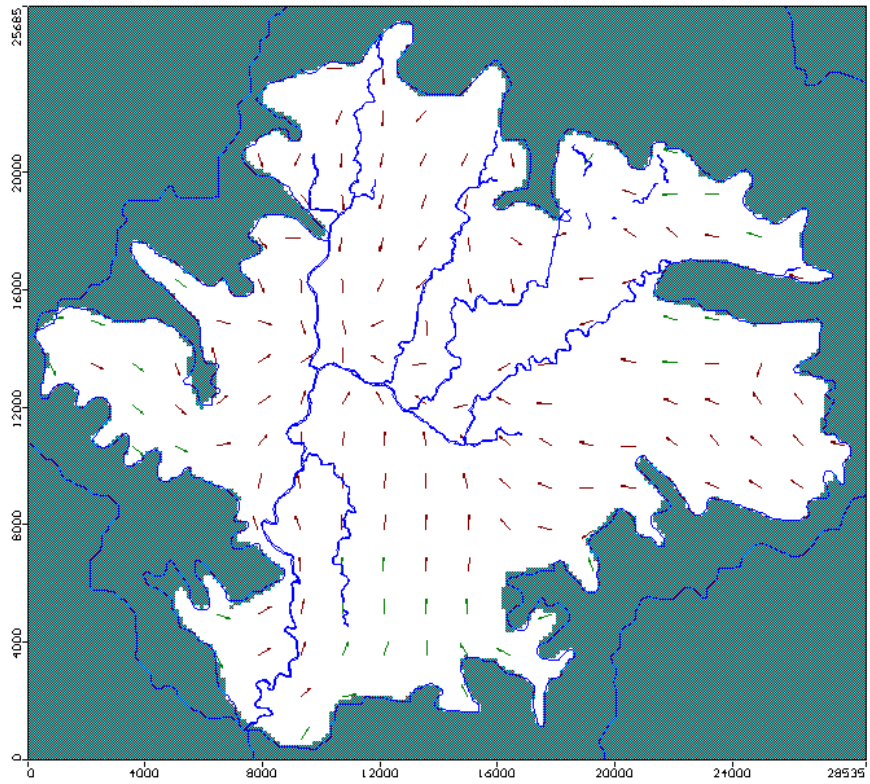

Fig 4.20: Map of the study area showing the flow direction in layer 2

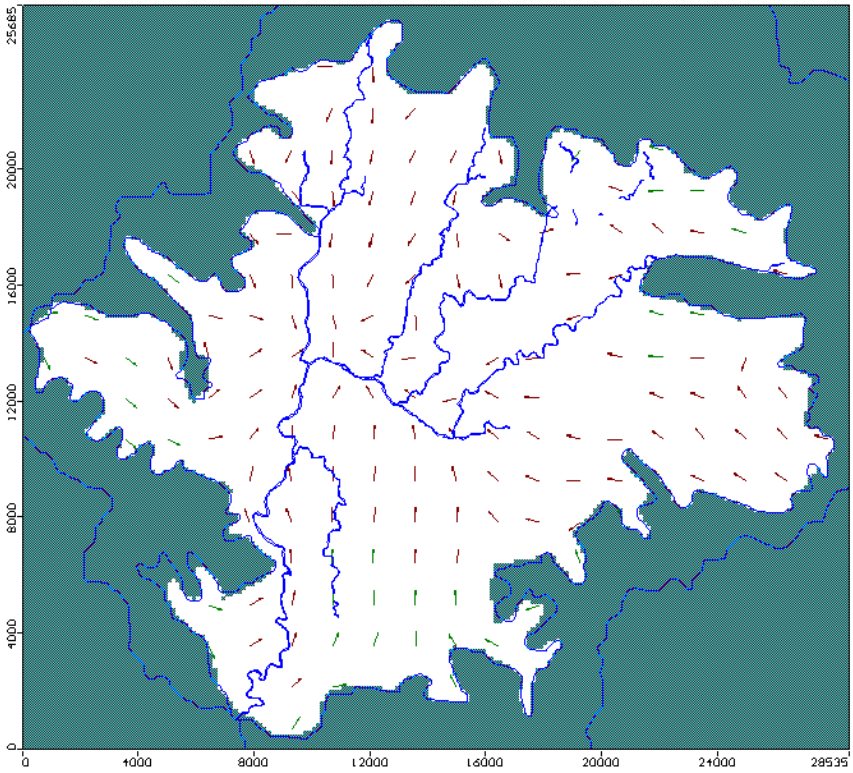

Fig 4.21: Map of the study area showing the flow direction in layer 3

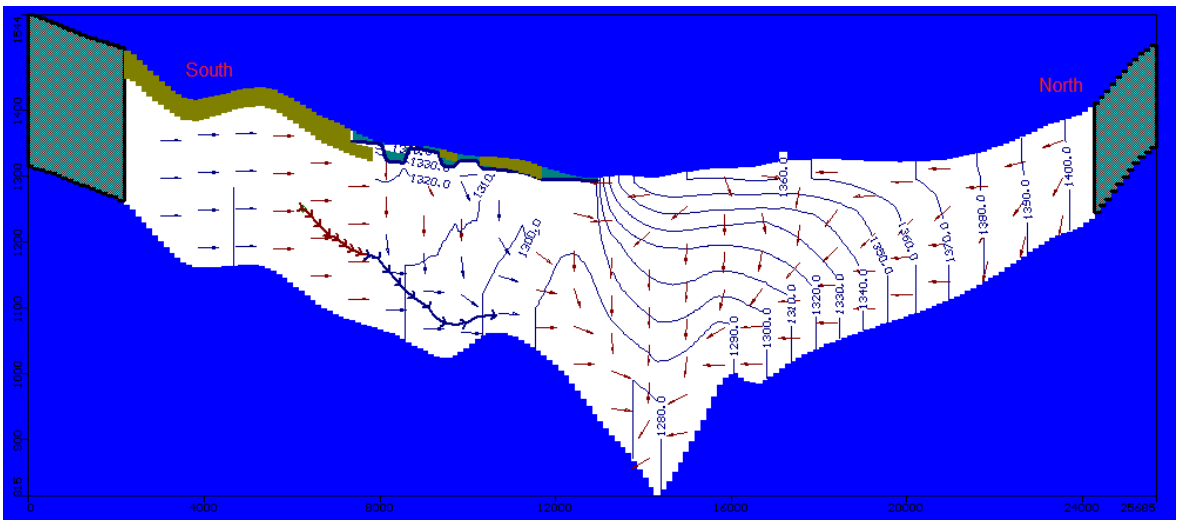

Fig 4.22: Section at column 82 showing the direction of flow within the layer and hydraulic head

4.13.5 Flow velocity

The flow velocity represents the velocity of flow within the layer. In the layer 1, velocity of water seems to be more and appreciable in the northern part (Fig 4.23) where the size of the arrow represents the magnitude of the velocity. This is because there is steep hydraulic gradient in the northern part. The maximum velocity is found in the northern part and some central part and is 0.00069 m/s. The north eastern part and the southern part has low hydraulic gradient which results in the low velocity component.

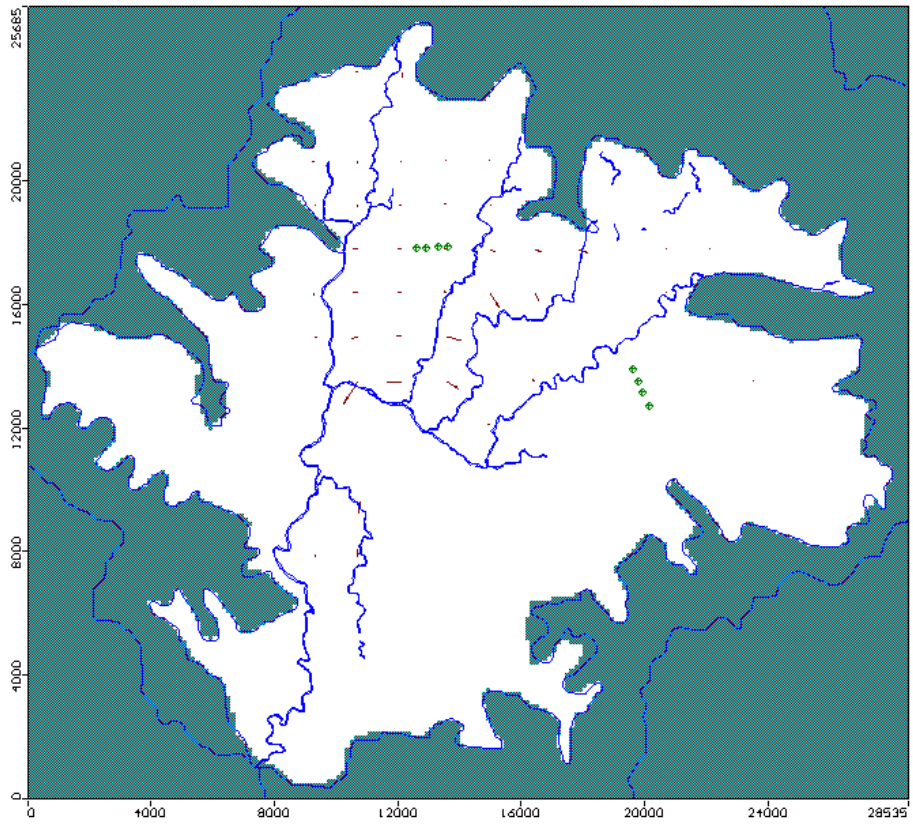

Fig 4.23: showing the velocity in layer 1

The velocity in the second layer is seemed to be small because the conductivity of the layer 2 is very small. The maximum velocity in layer 2 is found to be 0.00012 m/s which is noticed near the recharge area.

4.13.6 Particle tracking

Particle tracking was performed using the MODPATH code (Pollock, 1994) to investigate flow patterns in the aquifer. MODPATH is a particle tracking postprocessing code designed to work with MODFLOW (McDonald and Harbaugh, 1988). The output from MODFLOW is

used in MODPATH to compute paths for imaginary particles of water moving through the groundwater flow system (Pollock, 1994).

Some particles have been added to the first, second and third layer to see the path followed by the particles. In the first layer particles tracking shows that the particles move towards the natural drainage and river. Some of the particles added near the recharge zone shows that the particles move from layer 1 to the layer 3 from the recharge zones (Fig 4.25). This proves that the water will enter into the deep aquifer through the areas where there is minimum thickness of aquitard called recharge zones. This is in good agreement with the conceptual model in this study. In the third layer, particles moves from southern part to the central part of the valley (Fig 4.24)

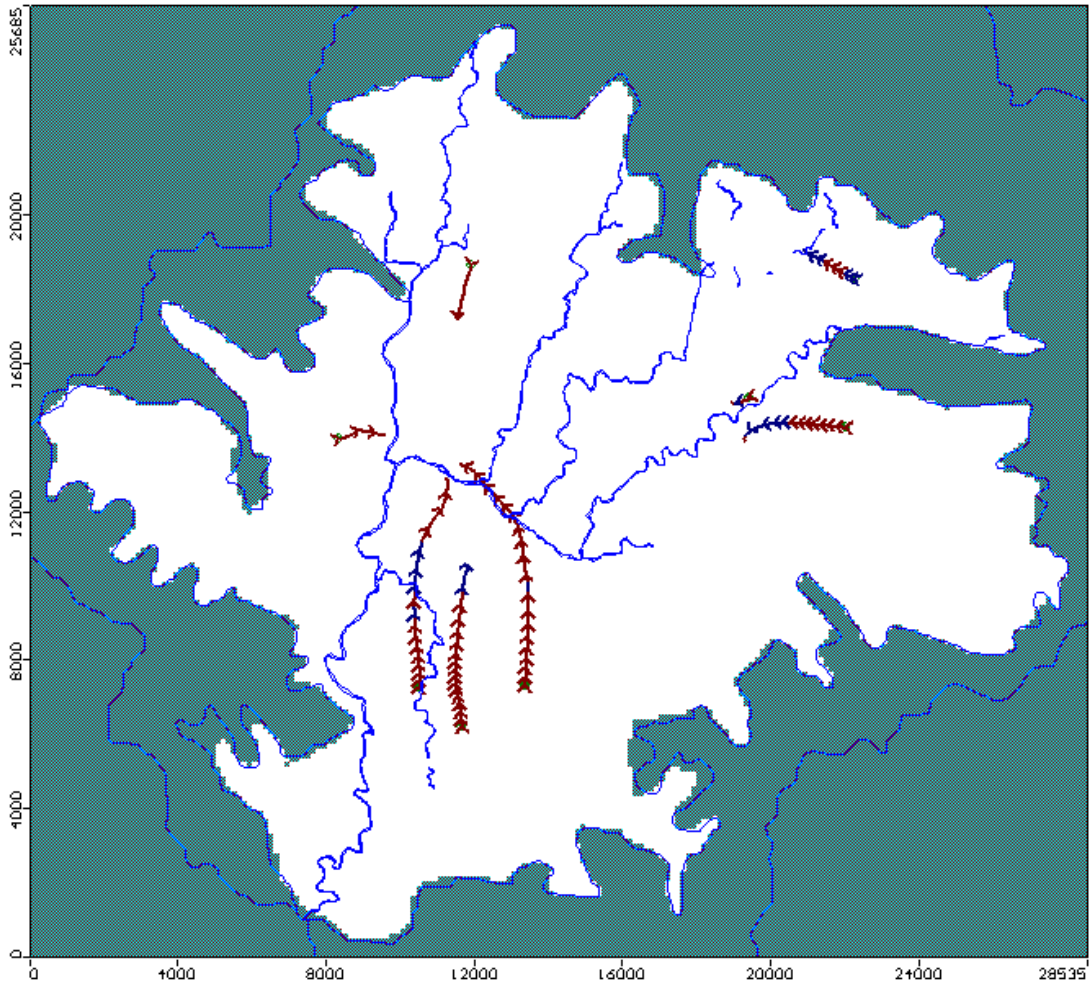

Fig 4.24: Pathlines in layer 3 showing water is moving towards the central part

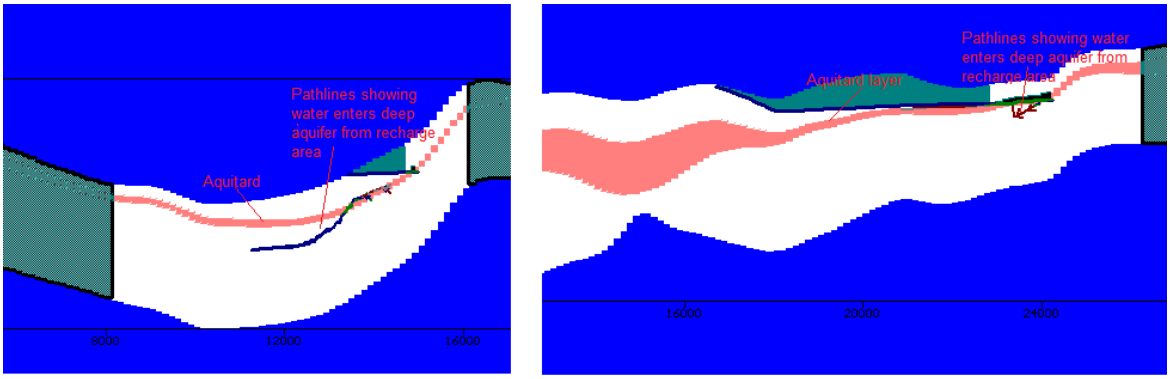

a) b)

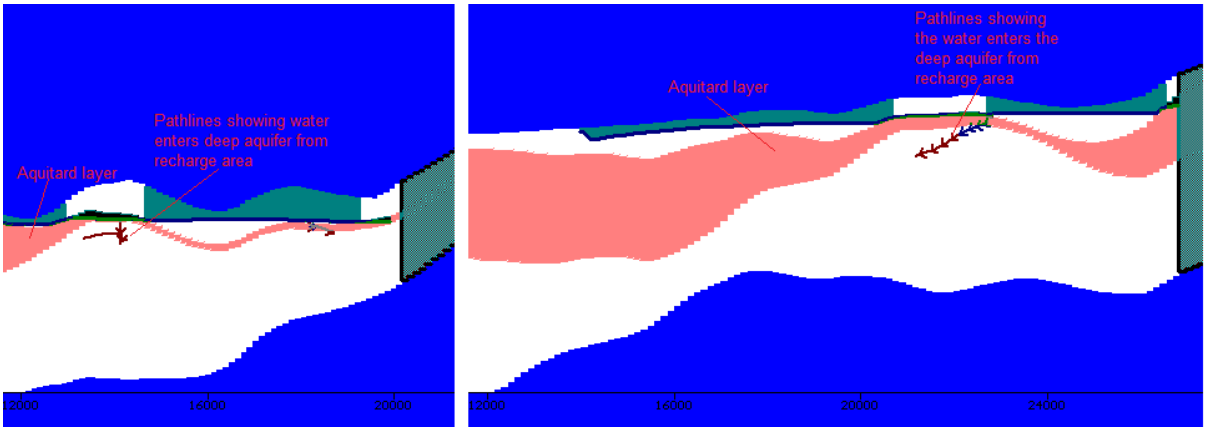

c) d)

Fig 4.25: a), b), c) and d) Pathline showing water enters deep aquifer from recharge area

4.13.7 Water budget

To determine the water availability for the Kathmandu valley, the water balance can be formulated with help of water budget package. This describes the inflow and outflow of the groundwater into and out of the aquifer system.

The groundwater balance can be set up where the groundwater recharge and the discharge mechanism of the groundwater aquifer are known. Precipitation is considered as

the main component of recharge. Discharge component can be divided into water abstraction from well and river leakage.

The balance equation for the groundwater aquifer can be formulated in the following terms:

Inflow – Outflow = Change of storage.

Assuming that the change of storage within the aquifer system over the long time is negligible, the steady state balance equation could be presented in the following forms:

Inflow – Outflw = 0

Calibrated model was used to investigate the volume of water moving from or to the aquifer shown in Table 4.3. In a steady state model, flow into the model equals the flow out of the model. According to the result, total flow through the aquifer system is 3530972 m^3/day. Of this flow, about 3490505 m^3/day discharges to the aquifer from the river leakage whereas 6460838 m^3/day has been discharged to river as outflow from the system. Balance of 23667 m^3/day has been found to discharge into the aquifer system from river leakage. About 62861 m^2/day has been pumped out to meet the water demand. Total recharge to the aquifer system is about 40467 m^3/day as inflow to the aquifer system. As there is no constant head and general boundary head, these values are null. From the water balance result, only 4 % discrepancy is found which is considered as negligible.

Table 4.3:

VOLUMETRIC BUDGET FOR ENTIRE MODEL AT END OF TIME STEP 1 IN STRESS PERIOD 1

CUMULATIVE VOLUMES (m^3)		RATES FOR THIS TIME STEP (m^3/day)	
IN:		IN:	
STORAGE =	0.0000	STORAGE =	0.0000
CONSTANT HEAD =	0.0000	CONSTANT HEAD =	0.0000
WELLS =	0.0000	WELLS =	0.0000
RIVER LEAKAGE =	12740344832.0000	RIVER LEAKAGE =	3490505.5000
RECHARGE =	147705488.0000	RECHARGE =	40467.2578
TOTAL IN =	12888050688.0000	TOTAL IN =	3530972.7500

OUT:	OUT:
STORAGE = 0.0000	STORAGE = 0.0000
CONSTANT HEAD = 0.0000	CONSTANT HEAD = 0.0000
WELLS = 229408928.0000	WELLS = 62851.7617
RIVER LEAKAGE = 12653959168	RIVER LEAKAGE = 3466838
RECHARGE = 0.0000	RECHARGE = 0.0000
TOTAL OUT = 12883367936.0000	TOTAL OUT = 3529690.0000
IN - OUT = 4682752.0000	IN - OUT = 1282.7500
PERCENT DISCREPANCY = 0.04	PERCENT DISCREPANCY= 0.04

4.13.8 Summary of modeling result

There are several indicators that the overall result of the calibrated steady-state groundwater flow model developed for the area is realistic due to following reasons.

i) The deviation of the simulated heads from the observed heads is within the 95% interval
ii) The model calculated inflow and outflow terms are balancing.
iii) Hydraulic head contour in the three layers seems to be reasonable.
iv) Groundwater flow direction simulated by the model is reasonable and in agreement with the flow direction defined in the conceptual model.
v) The velocities of flow within the layer are justifiable.

4.13.9 Uncertainties on modeling result

Groundwater modeling and decision making is beset with uncertainty caused by incomplete knowledge of the underlying system and/or uncertainty due to natural variability in system processes and field conditions. The different sources of uncertainty in the modeling process can be categorized as conceptual uncertainty, parametric uncertainty, and stochastic uncertainty (Singh *et al*, 2010) which may affect the result of the model. Conceptual uncertainty includes the incomplete or imperfect knowledge of the system. Parametric uncertainty may be due the insufficient and erroneous field data. Stochastic uncertainty may be due to the natural variability in the field condition. Different techniques have been

formulated in quantifying such model uncertainties which is not included in the scope of the study.

4.14 Simulation on different conditions

A steady state model was developed to study the flow pattern in the aquifer system and also to assess the impact of the groundwater abstraction in the study area. The steady state model was calibrated with the groundwater abstraction for the year 2001. The year 2001 was chosen because of the availability of the groundwater measurement data on that year which was used as initial head. The pumping rate on year 2001 was 61 MLD. This will give the result of steady state model with pumping on year 2001. Another model was developed with the steady state model with pumping on year 2009. The abstraction rate on year 2009 was 71 MLD.

The purpose of the modeling is to compare the system under two sets of condition; pumping condition on year 2001 and pumping condition on year 2009. The two different sets of hydraulic heads were reproduced using same numerical model and the hydraulic parameters are kept same in two model. Different head observation points were introduced in both model in the same coordinate. After running the models, the hydraulic heads at each observation points were determined. The difference of the hydraulic head in same observation point in two models will give the decline of the hydraulic head in that point due to abstraction. Fig 4.26 a) shows that the hydraulic head decline in less in the northern part and increases towards the central and southern part. Also Fig 4.26 b) shows that the decline in hydraulic head is found to be less in the eastern part and increases towards central and western part.

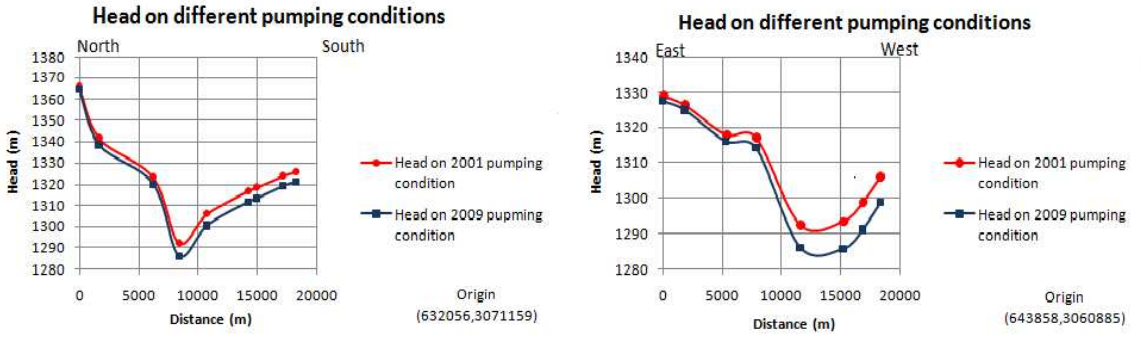

a) b)

Fig 4.26: Sections a) north to south b) east to west; showing hydraulic head due to different pumping conditions.

The study area has been divided into three groundwater district as divided by JICA (1990); northern groundwater district, central groundwater district and southern groundwater district. Hydraulic head at observation points were evaluated according to the location at each district. The calculation tables of hydraulic heads at observation point in each condition were attached in Appendix E which calculates the hydraulic head decline in each district.

From the table in Appendix E, it is found that the average hydraulic head decline is 1.5 m in the northern groundwater district. Although it has appreciable number of pumping wells and abstraction rate, the hydraulic head decline is small as compared to other district because of following reason.

i) Northern groundwater district has thick shallow permeable aquifer which can hold appreciable amount of water which can enter the deep aquifer.
ii) It has more recharge area from where water enters into the deep aquifer. This will fulfill the abstraction.

In the central groundwater district the average hydraulic head decline is 5.9m. This is due to the following reason.

i) The northern groundwater district has more pumping wells and abstraction rate is high.
ii) It has no recharge area and hence recharge to the deep aquifer doesn't occur.

In the southern groundwater district, the average hydraulic head decline is 5.3m. The southern groundwater district has very low abstraction rate, though it has high hydraulic head decline due to the following reason.

i) The slope of the deep aquifer is more in the southern groundwater district which results in the flow of the groundwater from the southern part to the central part as shown in Fig 4.24.
ii) The most of the area of the southern part doesn't have shallow aquifer and hence the aquitard layer is exposed to the surface. Small portion of the area is recharge area. Hence low amount of water will enter the deep aquifer in this part.

4.15 Sensitivity analysis

Sensitivity analysis is an essential step in all modeling applications. As discussed by Anderson & Woessner (1992), the purpose of a sensitivity analysis is to quantify the sensitivity of the model simulations in the calibrated model caused by uncertainty in the estimates of aquifer parameters, stress and boundary conditions. Sensitivity analysis

provides information on which model parameters are most important to the simulated system. Sensitivity analysis is also inherently part of model calibration. The most sensitive parameters will be the most important parameters for matching the model result with the observed values. It also identifies which parameters have most influence to the model result and can identify the parameters that require additional study.

To assess the sensitivity of the simulations in the calibrated model, a sensitivity analysis was performed. The sensitivity analysis was performed by systematically changing one calibrated parameter at a time and other kept constant while noting the observed changes in error parameters. A number of sensitivity analyses were conducted to test the effects on model results due to changes in input parameters or boundary conditions. After changing the input parameters by a certain factor, the model was run and different error parameters such as standard error of estimate, coefficient of correlation, residual mean error and root mean squared % were noted. A graph of fraction of calibrated value of the input parameters against the value of different error parameters was plotted in Fig 4.27.

From this plot it is found that the hydraulic conductivity for the shallow aquifer is the most sensitive because it can be seen that the value of error parameters is oscillating with the change of the value of the input parameters. It is also found that hydraulic conductivity of deep aquifer is sensitive to the model results. Among the three hydraulic conductivities, less sensitive input parameters is that for aquitard.

It is also found from the plot that the error parameters (residual mean, standard error and RMS %) is found to be minimum when the value is equal to the calibrated value. The value of coefficient of correlation is found to be maximum at the calibrated value.

Sensitivity analysis was also conducted on the recharge. The value of recharge was varied systematically keeping the all other input parameters constant with the calibrated values. The values of different errors were noted and were plotted against the recharge value shown in Fig 4.28. The recharge is seemed to be less sensitive to the model result. It is found that the error parameters such as standard error and RMS % are found to be minimum at recharge of 43 mm/year. The value of correlation coefficient is maximum at the value of 43mm/year. With the value of recharge less than 37 mm/year and more than 47 mm/year, the model was not converged to the solution.

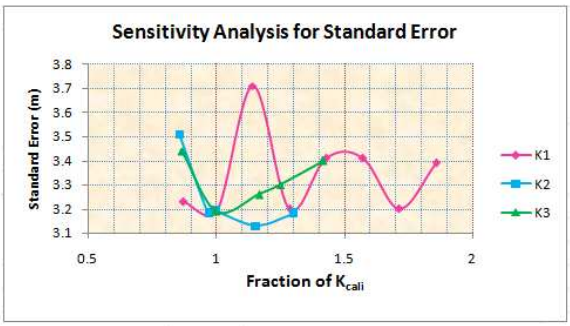

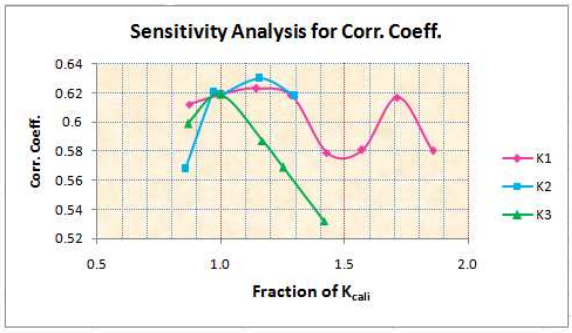

a) b)

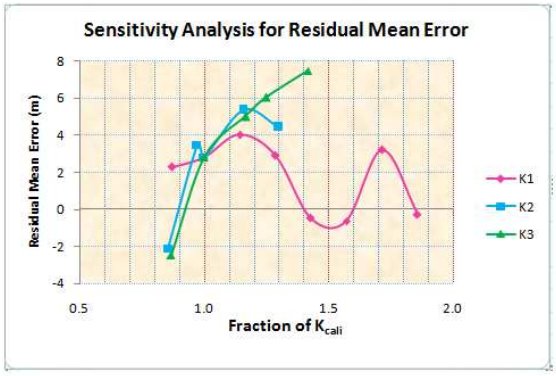

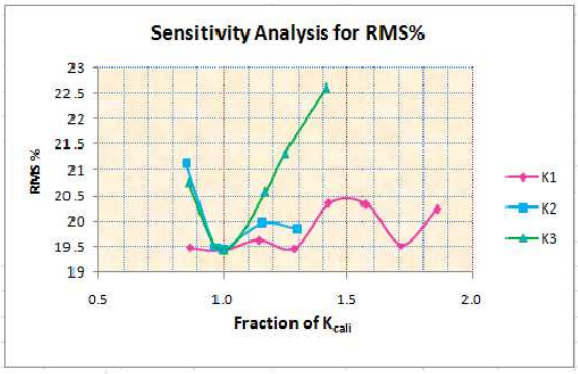

c) d)

Fig 4.27: a), b), c) and d) Calibration plots with respect to hydraulic conductivity

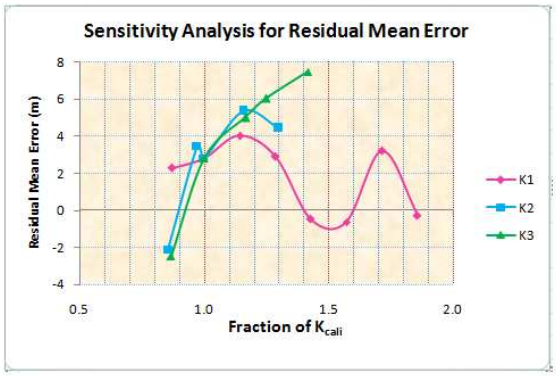

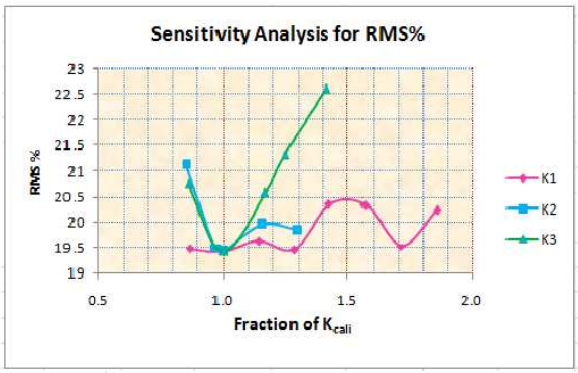

a) b)

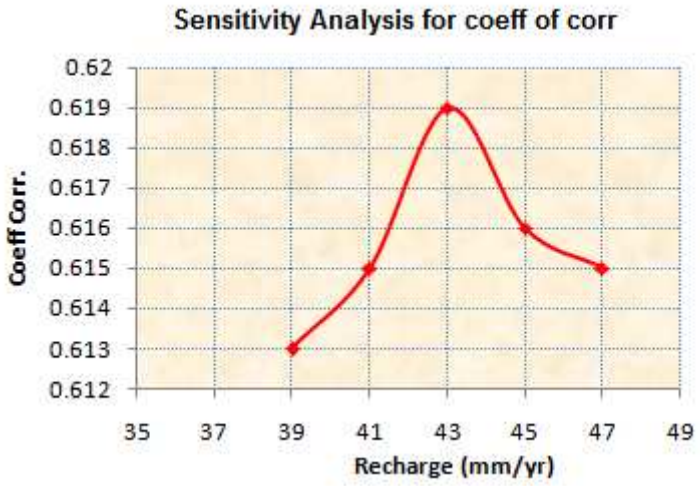

c)

Fig 4.28: a), b) and c) Sensitivity plots with respect to recharge

By changing the value of the storage parameters in the model, it is found that the storage parameters did not affect the result of the model in the steady state condition. From equation [4.5] storage parameters will not involve in the equation.

4.16 Result comparison

In order to determine if the estimated parameters accurately represent the system, a data set of current observed hydraulic heads contour would have to be compiled to validate the model for other years. For all practical purposes, the parameter set calculated by the model represents a steady-state simulation during the study year. If this model were to be used as an actual management tool for future development scenarios, a parameter set that was validated with at least one more year of data would have to be estimated. A great deal of data is necessary to accurately represent the system. Ideally, a model could not be properly validated for the Kathmadu valley aquifer system, due to a lack of data. However, to meet the objectives of this investigation, it is assumed that the input parameter set developed during the calibration procedure accurately represents the natural system. For this, it is tried to compare the result of the model in following terms.

4.16.1 Conductivities value

After model calibration, the horizontal conductivities for the different layers are estimated and are summarized in Table 4.2. The horizontal conductivity for shallow aquifer is estimated as 7 E-4 m/s. Pandey & kazama (2010) has reported that the average horizontal conductivity for the shallow aquifer is 3.3 E-4 m/s which is close to the value estimated in this model. Similarly the conductivity for the deep aquifer is estimated as 1.2E-5 m/s. Pandey & Kazama (2010) has reported that the average horizontal conductivities for the deep aquifer is 5E-5. Hence the estimate of hydraulic conductivity in deep aquifer is in good agreement with values reported in Pandey & Kazama (2010) for shallow and deep aquifer.

4.16.2 Distribution of thickness of layer

The shallow aquifer is unconfined aquifer consisting sand and silt whose thickness varies from 0 to 85 m. The thickness of shallow aquifer is minimum in the southern part whereas it is maximum northern part. It is found that southern part doesn't have shallow aquifer and aquitard layer has been exposed to the surface in the southern part of the Kathmandu valley Fig 4.29 a) which is closely comparable to the map prepared by JICA (1990) (Fig 4.29 b).

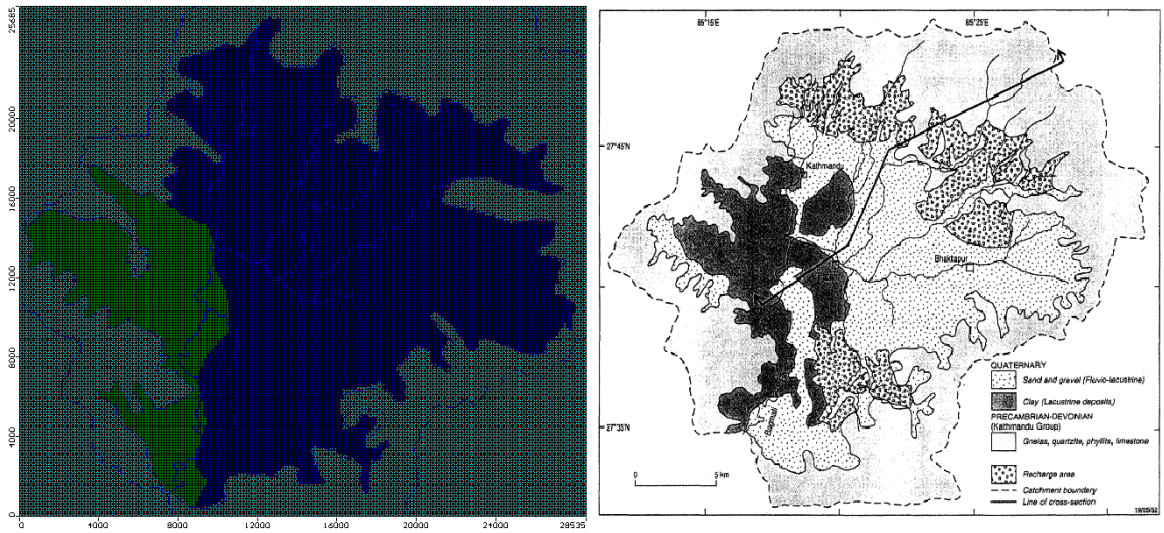

a) b)

Fig 4.29: Comparison of aquitard exposed to the surface a) hydraulic conductivity distribution in layer 1 showing the aquitard exposed to the surface (green) b) Clay layer exposed to the surface delineated by JICA (1990) (black part)

In the second layer some part of the study area is missing the aquitard layer. Some northern part and some south eastern part of the valley doesn't contain the aquitard layer which is the recharge area to the deep aquifer (Fig 4.30 a). It is compared to the map for the recharge area prepared by the JICA (1990) (Fig 4.30 b). It seems that the recharge area to the deep aquifer is closely matched with the map prepared by the JICA .

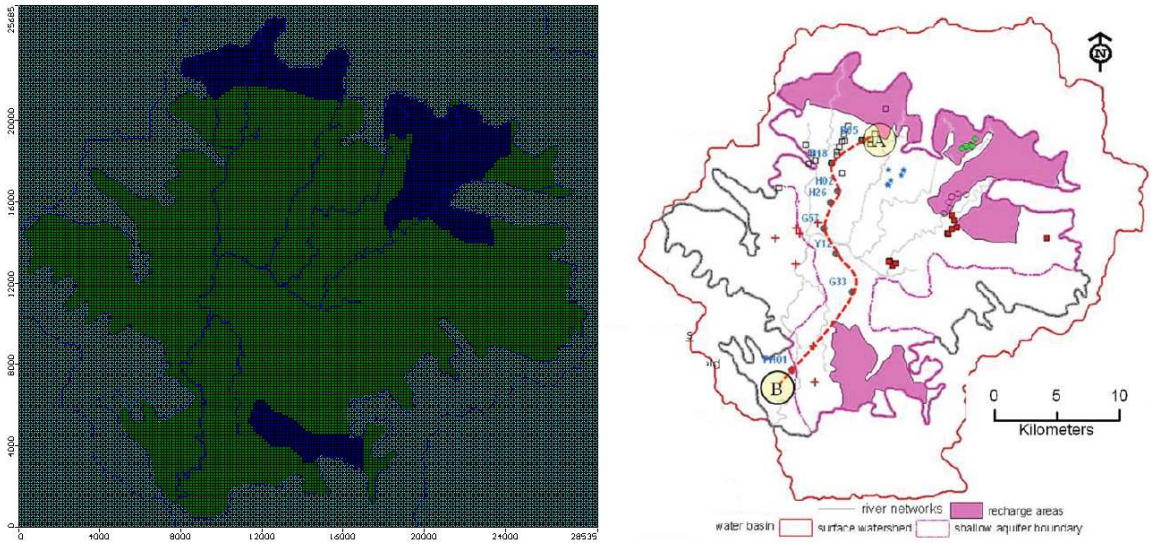

a) b)

Fig 4.30: Comparison of the recharge area in the model a) hydraulic conductivity distribution in layer 2 showing recharge area (blue) b) delineation of recharge area by JICA (1990) (red part)

The section of the layer from North to South has been shown in Fig 4.31 a). The distribution of the shallow aquifer, aquitard and deep aquifer is irregular with some discontinuities occuring horizontally and vertically. In this section, a deep depression can be seen in the central part of the Kathmandu valley. The thickness of the shallow aquifer is more in the northern part whereas is thinner in the central and southern part. The thickness of the aquitard is more in the central part of the valley. It is in good agreement with the section generated from the simplified model by Piya (2004) (Fig 4.31 b).

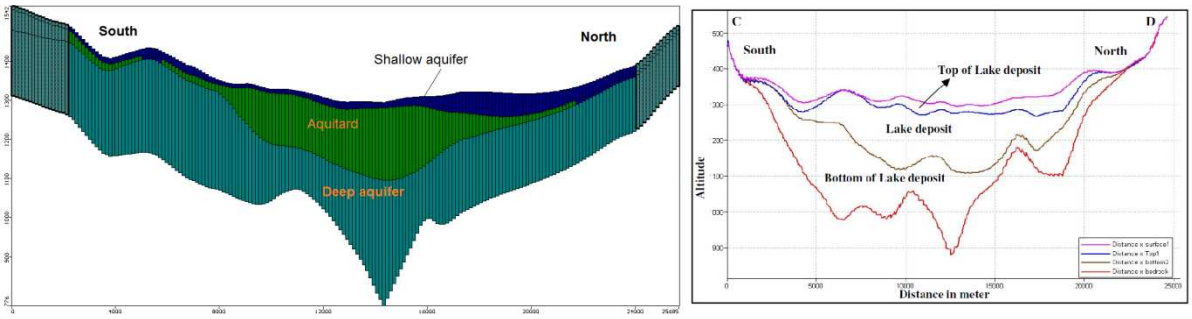

a) b)

Fig 4.31: Comparison of the section from north to south of the study area a) section at column 80 showing the vertical distribution of layers b) section showing the vertical distribution of layer by Piya (2004)

4.16.3 Hydraulic head decline

In this study the model has been simulated in two conditions, 2001 pumping condition and 2009 pumping condition. The hydraulic head at different points in both condition shows that the average hydraulic head has been declined by 1.5m in the northern part, 5.9m in central part and 5.3m in the southern part (Appendix E). In an average hydraulic head is declined by 4m from 2001 to 2009 due to the effect of abstraction.

Table 4.4: Calculation of decline from measured water level in northern groundwater district

Well ID	Static level at 2000 (mbgl)	Static level at 2005 (mbgl)	Decline (m)
BB6a	20.99	29.27	8.28
Dk1	29.83	31.85	2.02
Dk2	0.11	0	-0.11
Dk8	2.53	3.35	0.82
BB1	78.66	82.5	3.84
MH6a	0.97	0.97	0.43
Gk2a	19.3	23.73	4.43
GK5	24.95	24.95	20.33
Gk4	18.98	16.57	-2.41
BHK1	38.07	45.27	7.2
M5	92.5	95.23	2.73
M6	12.7	14.7	2.0
		Average	2.0

Table 4.5: Calculation of decline from measured water level in southern groundwater district

Well ID	Static level at 2000 (mbgl)	Static level At 2005 (mbgl)	Decline (m)
M1	7.97	7.94	-0.03
M2	19.7	28.11	8.41
M3	41.82	42.8	1.78
M4	30.11	30.05	-0.06
		Average	2.5

.

Table 4.5 shows that the static water level declines by 2.5 m in the southern groundwater district from 2000 to 2005. The water level measured data is very few in number in this district. Hence it might not represent the actual condition.

Table 4.6: Calculation of decline from measured water level in central groundwater district

Well ID	Static level at 2000 (mbgl)	Static level At 2005 (mbgl)	Decline (m)
Bal 1a	0.98	8.33	7.35
G17	10.78	10.66	0.38
G16	0.63	1.79	1.16
G13	22.81	31.39	8.58
H26	19.36	24.34	4.88
I26	7.26	8.26	1.0
P22	13.08	19.11	6.03
P15	1.8	3.98	2.18
Do137	33.16	37.58	4.42
		Average	4.0

Some of the water level monitoring data at Kathmandu valley has been performed by the Melamchi Development Board and these data are included in the report (GWDB, 2009). Although the data are few in number and discontinuous, it is tried to determine the measured decline of static water level. Table 4.4 shows that the static water level has been declined in the northern groundwater district by 2m from 2000 to 2005. .

Table 4.5 shows that the static water level declines by 2.5 m in the southern groundwater district from 2000 to 2005. The water level measured data is very few in number in this district. Hence it might not represent the actual condition.

Table 4.**6** shows that the static water level has been declined in the central groundwater district by 4m from 2000 to 2005. This shows that the decline calculated by the model closely matches with the measured decline

Also some of the researches have shown the decline in the groundwater. Dhakal (2010) has reported that from 2000 to 2008 there is drawdown of 0 to 5 m in northern groundwater district; 1 to 5m in the central groundwater district and 0 to 0.4m in the southern groundwater district which nearly resemble the output of the model.

5

CONCLUSIONS AND RECOMMENDATIONS

5.1 Conclusions

The aim of this study was to develop a model for the groundwater system for Kathmandu valley aquifer system where groundwater is the main source of fresh water. All the available data regarding physiography, meteorology, geology and hydrogeology of the system have been collected, evaluated and utilized to develop a conceptual model for the system. However, due to lack of data, all of the components of the groundwater budget could not be precisely determined. Consequently, a mathematical groundwater flow model based on the conceptual model has been utilized to determine the groundwater budget and also to determine the effect of the groundwater abstraction.

By analysis the results of the model, following conclusions have been drawn.

i) The hydrogeology of the Kathmandu valley aquifer system is complex. The thickness of the each layers vary horizontally as well as vertically. Hence it should be handled carefully when modeling to get the accurate results

ii) The model was designed with three aquifer system with aquitard at the middle. The hydraulic conductivity for the shallow aquifer was found to be high with respect to other layer. The hydraulic conductivity of the aquitard is found to be very low which will block the entry of flow towards the deep aquifer.

iii) The recharge calculated by the water balance method is found to be 43mm/year which is only 2.5% of the total rainfall.

iv) The pathlines of the model shows that the water enters the deep aquifer from the recharge area which is mainly located in the northern and the northeastern part of the valley.

v) The hydraulic heads is more in the northern part and is decreases towards the southern part. There is steep hydraulic gradient found in the northern and some

part of the central and there is low hydraulic gradient found in the northeastern and southern part of Kathmandu valley that ranges from 1300 m to 1330m.

vi) The direction profile of the model shows that water moves into the natural drainage in the shallow aquifer whereas it moves towards the central of the valley in the deep aquifer.

vii) As it is the steady state model, the inflow to the system equals the outflow from the system. Water budget shows that the abstraction which is found to be 61 MLD exceeds the recharge (40.4 MLD) and hence illustrates that the groundwater in the Kathmandu valley is overstressed.

viii) The velocity of water is found to be maximum at the shallow aquifer in the northern part where there is steep hydraulic gradient. In the second layer near the recharge area, velocity of water is found to be appreciable whereas the velocity in the deep aquifer is found to be very small.

ix) The sensitivity analysis shows that the hydraulic conductivity of the first layer is more sensitive to the model output whereas that for aquitard and deep aquifer is also sensitive to the model output.

x) It is found that abstraction of groundwater adversely impact the groundwater system. The decline in the hydrailuc head is found to be more in the central and southern part of the valley due to the effect of the abstraction from 2001 to 2009. Decline in the hydraulic head is small in the northern port and is increases towards central part and reaches maximum and again decreases slightly towards southern part. The decline in the hydraulic head is small in the eastern part and increases towards the western part.

5.2 Recommendations

Based on the data available and analysis of the results, following recommendations will be made.

i) With additional data, further refinement of the model is possible, which is expected to improve the accuracy of the model. Further extensive field-based observations combined with geophysical well logging and hydraulic testing techniques, detailed delineation of fractures and other secondary porosity is required to compile the hydrogeological framework for each geological sequence. Prior to detail groundwater modeling, detail structural mapping is required which

will have a great importance in aquifer characterization and definition of boundary conditions.

ii) This model offers the conceptualization of flow within the aquifer system. If it were to be used as a management tools to support decisions with regards of the flow pattern and the effect of the abstraction, the model would have better validate with the field data because adequate data were not available to validate the results. This validation will greatly improve the models predictive capability and would minimize the uncertainty in the model results.

iii) The groundwater model was greatly simplified since the geological formations such as faults system in this study were not simulated. Data need to be collected as to how geologic formations would affect the groundwater flow system. These geologic formations could then be modeled changing the model to more accurately represent the natural system.

iv) The model is a steady state model which does not includes the temporal variation of output and input. Hence transient state simulation should be carried out to better represent the field condition for the prediction of flow pattern and the pumping effect.

v) The model was set up and calibrated on the basis of available data which are not distributed uniformly throughout the area comprising the aquifer system, especially in the southern part of Kathmandu valley. In order to understand the better characterize the system and improve the model, new monitoring wells distributed evenly and monitor regularly from these wells are recommended.

vi) The river survey should be performed to obtain the data for streambed conductance and thickness estimation. This would be useful to improve the model results.

vii) Many of the pumping wells in Kathmandu valley were not properly documented and the locations of the screens in each well were not properly identified. Hence the number of the wells should be properly documented and the exact location of the screen in each wells should be indentified which will enhance the result of the model.

viii) Pumping tests in the aquifer system should be performed to obtain the more realistic conductivity estimates to better represent the real condition which will help to improve the uncertainty of the model results.

ix) The numerical model developed can be used to build the a model to address the contamination problem and to delineate the wellhead protection areas for the

water supply wells because most of the pumping wells in the Kathmandu valley are used for water supply.

x) Impact of climate change in the groundwater system can be assessed which will help in the planning and management of groundwater.

xi) The development of this groundwater model was a part of the larger investigation which includes other sub groups. An effort to integrate all the components of the model developed in the investigation needs to be continued.

REFERENCES

1. Anderson, M.P. & Woessner, W.W. (1992). Applied groundwater modeling: simulation of flow and advective transport.

2. Arita, K., Ohta, Y., Akiba, C., and Maruo, Y. (1973). Kathmandu Region, in geology of the Nepal Himalayas, pp. 99-145.

3. Barone, V.A. (2000). Modeling the Impacts of Land Use Activities on the Subsurface Flow Regime of the Upper Roanoke River Watershed, MSc Thesis, Virginia Polytechnic Institute and State University, Virginia, pp. 113.

4. Binnie & partner (1973). Master Plan for the water Supply and Sewarage of Greater Kathmandu and Bhaktapur, World Health Organization Programme, Nepal

5. Brassington, R. (1998). Field hydrogeology (Second edition ed.). Chichester etc.: Wiley & Sons.

6. Central Bureau of Statistics (2002). National report published by Department of Statistics, Nepal, year 2002.

7. Central Bureau of Statistics (2003). National report published by Department of Statistics, Nepal, year 2001.

8. D.M.G./BGR/DOI (1998). Hydrogeological Conditions and Potential Barrier Sediments in the Kathmandu valley. Technical Cooperation project-Envoronmental Geology. Final report pp. 17-59, Appendix 3.

9. Dhakal, H.P. (2010). Groundwater Depletion in Kathmandu valley need for management, International Forum for Sustainable Asia and Pacific (ISAP 2010) Yokohama, Japan, Sharing Groundwater issues in Asian countries, pp.9.

10. Dixit, A. & Upadhya, M. (2005). Initiative for Augmenting groundwater resources by Artificial Recharge (AGRAR); Augmenting Groundwater in Kathmandu valley: Challenges and Possibilities, Report

11. DMG (1988). Engineering and Geology map of the Kathmandu Valley, Department of Mines and Geology, Kathmandu, Nepal

12. Dongol, G.M.S. (1985). Geology of the Kathmandu fluvial lacustrine sediments in the light of new vertebrate fossil occurrences. Jour. Nepal Geol. Soc. V.3, pp. 43-57.

13. Dongol, G.M.S. (1987). The stratigraphic significance of vertebrate fossils from the Quaternary deposits of the Kathmandu basin, Nepal. Newsl. Stratigr., v.18, pp.21-29.

14. FAO (1997). FAO Publication on Irrigation Potential in Africa, website: http://www.fao.org/nr/water/aquastat/watresafrica/index4.stm Date of access 14 Dec 2010

15. Fetter, C. W. (2001). Applied hydrogeology + Visual Modflow, Flownet and Aqtesolv student version software on CD - ROM (Fourth edition ed.). Upper Saddle River: Prentice Hall.

16. Fort, M. & Gupta, V.J. (1981). Plio-Pleistocene Midland Himalayan basins of Kathmandu, Pokhara and Kashmir. Neogene/Quaternary Boundary \Field Conference, India. 1979, proceedings, geological Survey of India, pp. 37-43.

17. Gautam, R. & Rao, G.K. (1991). Groundwater Resources Evaluation of the Kathmandu valley. Jour. Nepal Geol. Soc., v.7, pp.39-48

18. Golden Software, 1999. Surfer® 7.0 Help.

19. Grad, A. (2009). Palynological Investigation on Plio-Pleistocene Sediments of the Lukundol formation, Kathmandu Basin, Nepal, M.Sc. Thesis, Universitat Wien.

20. Gupta, A.G., Poudyal, G.N. and Shrestha, M.N. (1990). Assessing Safe Yield for Groundwater Basin in Kathmandu Valley. AIT Research Report, November.

21. Gurung, J.K., Ishiga, H., Khadka, M.S. & Shrestha, N.R. (2007). Report on Characterization of groundwater in the reference of arsenic and nitrate mobilization, Kathmandu Basin, Nepal, pp. 13-14.

22. GWRDB (2009). Study on Status of Groundwater extraction in the Kathmandu Valley and its potential impacts, Final report, Groundwater Resources Development Board, Department of Irrigation, Nepal, pp. 1– 88.

23. Hagen, T. (1969). Report on the geological survey of Nepal. V.1. Preliminary reconnaissance, Denkschriften der Schweizerischen naturforschenden Gesellschaft, 86, pp. 185.

24. Harbaugh, A.W. and McDonald, M.G. (1996). User's documentation for MODFLOW-96, an update to the U.S. Geological Survey modular finite difference groundwater flow model.

25. Hill, M.C., Poeter, E. & Zheng, C. (2010). Forward: Groundwater Modeling and Public Policy, Vol. 48, Ground Water, September-October 2010, pp. 625-625.

26. HMG (1994). Bagmati Basin Water Management Strategy & Investment Program, His Majesty's Government of Nepal, Ministry of Housing & Planning, Kathmandu

27. ICIMOD (2007). Kathmandu Valley Environment Outlook, report, pp. 1 – 127.

28. Japan International Coorporation Agency (JICA) (1990). Groundwater management Project in the Kathmandu valley, Final Report, main report

29. Kahsay, H.G.(2008). Groundwater resources assessment through distributed steady state flow modeling, Anylam Wellfield (mekele, Ethiopia) M.Sc Thesis , International Institute for Geo-Information and Earth Observation, Enschede Netherllands, pp. 45-50.

30. Le Fort, P. (1975). Himalaya: the collided range: Present Knowledge of the continental arc. American Journal of Science 275A, pp. 1-44.

31. McDonald, M. G., & Harbaugh, A. W. (1988). A modular three-dimentional finite difference groundwater flow model,U.S.Geological.Survey.tech.Water resources Investigation.

32. Metcalf & Eddy (2000). Urban water supply reforms in the Kathmandu valley, completion report, v. I and v. II, main report.

33. Nakata, T., Iwata, S., Yamanaka, H., Yagi., and maemoku, H. (1984). Tectonic landforms of several active faults in the Nepal Himalayas. Nepal geologic society V. 4 (Special issue), pp. 177-199.

34. Pandey, V. & Kazama, F. (2010). Hydrogeologic characteristics of groundwater aquifers in Kathmandu valley, Nepal. Jour. Environ Earth sci.

35. Pandey, V.P., Chapagain, S.K. & Kazama, F. (2009). Evalaution of groundwater environment of Kathmandu valley, Jour. Environ Earth Sci., v.60, pp. 1329-1342.

36. Pant, P.R. & Dongol, D. (2009). Kathmandu valley profile, a briefing paper, Workshop, Kathmandu Metropolitan City, pp. 1-13

37. Piya, B.K. (2004). Generation of a geological database for the Liquefaction hazard assessment in Kathmandu valley, MSc Thesis, International Institute for Geo-Information Science and Earth Observation, Enschede, Netherlands, pp. 18-141

38. Pollock, D.W. (1994). User's Guide for MODPATH/MODPATH-PLOT, version 3: A particle tracking post processing package for MODFLOW, U.S. Geological Survey finite difference groundwater flow model.

39. Saiju, K., Kimora, K.. Dangol, G., Komatsubara, T., and Yagi, H. (1995). Active Faults in South western Kathmandu basin, Central Nepal, Journal Nepal Geologic Society v 11 (sp. Issue), pp. 217 – 224

40. Sakai H. (2001). The Kathmandu Basin as archive of Himalayan uplift and past monsoon climate, Journal Nepal Geologic Society, v 25 (sp. Issue), pp. 1-7.

41. Sakai, H., Fujii, R., Kunwahara, Y., Upreti, B.N. & Shrestha, S.D. (2001). Core drilling of the basin-fill sediments in the Kathmandu valley for paleo climatic study, preliminary results Jour geol. Soc. v.25, pp. 19-32.

42. Scanlon, B. R., Mace, R. E., Barrett, M. E., & Smith, B. (2003). Can we simulate regional groundwater flow in a karst system using equivalent porous media models? Case study, Barton Springs Edwards aquifer, USA. Journal of Hydrology, 276(1-4), 137-158.

43. Sharma, P.N. & Singh, O.R. (1966). Report of groundwater exploration program, HMG and Geological Survey of India.

44. Shrestha, M.N. (2002). Assessment of Effect of landuse change in Groundwater storage in Kathmandu valley, pp. 1-13

45. Shrestha, O.M., Koirala, A., Karmacharya, S.L., Pradhananga, U.B., Pradhan, R., and Karmacharya, R. (1998). Engineering and environmental geological map of Kathmandu valley, Department of Mines and Geology, Nepal.

46. Shrestha, P. (2010). Climate Change Impact on River Dynamics of the Bagmati Basin, Kathmandu, Nepal, Final report, pp.5 - 30

47. Singh, A., Mishra, S. & Ruskauff, G. (2010). Model Averaging Techniques for Quantifying Conceptual Model Uncertainty, Vol. 48, Ground Water, September-October 2010, pp. 701-715.

48. SMEC (1992). Greater Kathmandu Water Supply Project, Final report, volume 3, Hydrology, November.

49. Stocklin, J. & Bhattarai, K.D. (1977). Geology of Kathmandu area and central Mahabharat Range, Nepal Himalaya, HMG/UNDP Mineral Exploration Project, Kathmandu.

50. Stocklin, J.,(1980). Geology of Nepal and its regional frame. Journal of the Geological Society London, Vol. 137, pp. 1-34.

51. Toews, M.W. (2003). Modeling Climate Change Impacts on Groundwater Recharge in a Semi-Arid Region, Southern Okanagan, British Columbia, M.Sc. Thesis, University of Calgary, pp. 128-130

52. U.S. Geological Survey (1997). MODFLOW fact sheet FS – 121-97. United States Geological Survey.

53. Upreti, B.N. & Le Fort, P. (1997). In Lesser Himalayan Crystalline Nappes of Nepal; problem of their origin. Geological society of American bulletin.

54. Wang, H.F. & Anderson, M.P. Introduction to groundwater modeling; finite difference and finite element method.

55. World Weather Information service Kathmandu Website. http://www.worldweather.org/031/c00114.htm, access on 04 January 2011.

56. Yagi, H., Maemiku, H., Ohtsuki, Y., Saiju, K.and Nakata, T. (2000). Recent activities faults distributed in and around Kathmandu valley, Lower Himalayan zone, Active faults research for the new millennium proceedings of the Hokundan Intl. Symposium and School on Active faulting. pp. 557-560.

57. Yamanaka, H. (1982). Classification of geomorphic surfaces in the Kathmandu valley and its concerning problems. Reprint congress Assoc. Japanese Geogr., pp. 58-59.

58. Yoshida, M. & Gautam, P. (1988). Magnetostratigraphy of Plio-Pleistocene lacustrine deposits in the Kathmandu valley, central Nepal, Proc. Indian. Nat. Sci. Acad,. v.54A, pp. 410-417.

59. Yoshida, M. & Igarashi, Y. (1984). Neogene to Quaternary lacustrine sediments in the Kathmandu valley, Nepal, Jour. Nepal Geol. Soc., v4, pp. 73-100.

APPENDIX

A

BOREHOLE LOG INFORMATIONS

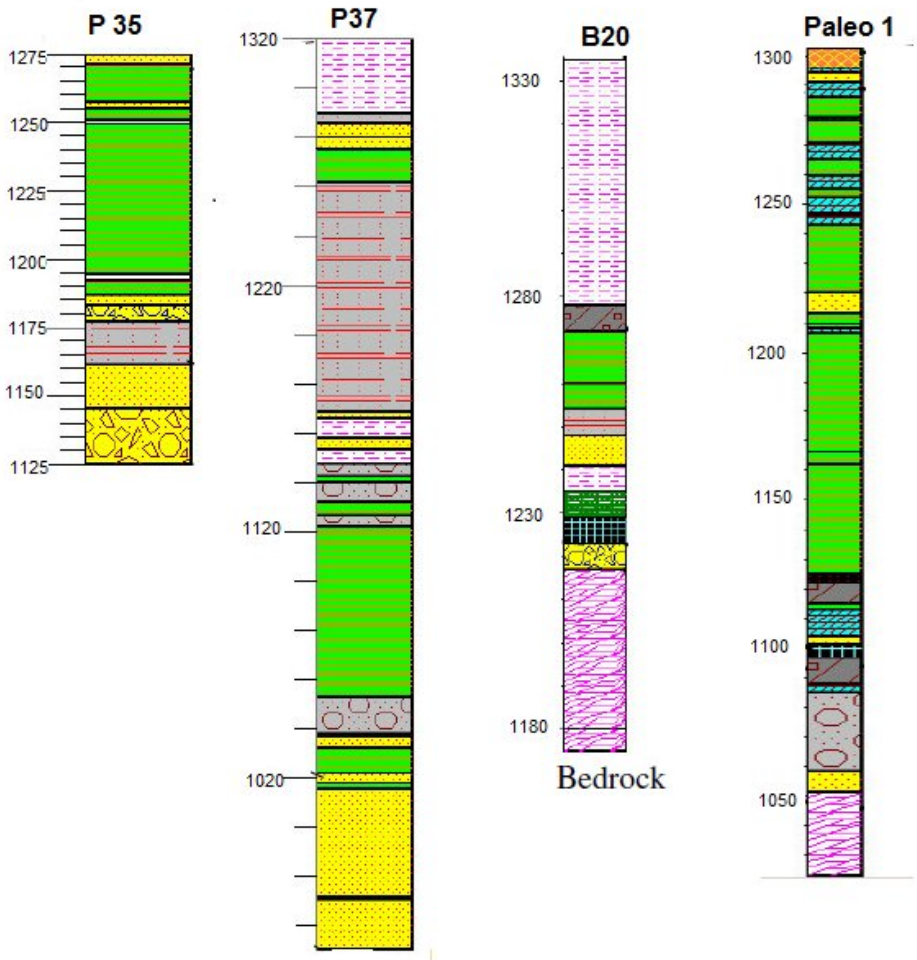
P 35
1275
1250
1225
1200
1175
1150
1125
P37
1320
1220
1120
1020
B20
1330
1280
1230
1180
Bedrock
Paleo 1
1300
1250
1200
1150
1100
1050

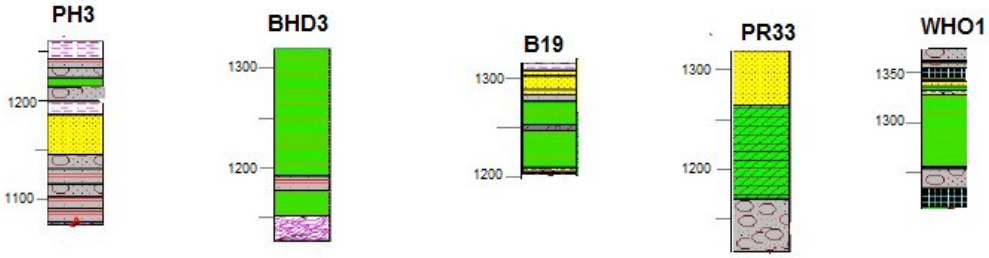
PH3
1200
1100
BHD3
1300
1200
B19
1300
1200
PR33
1300
1200
WHO1
1350
1300

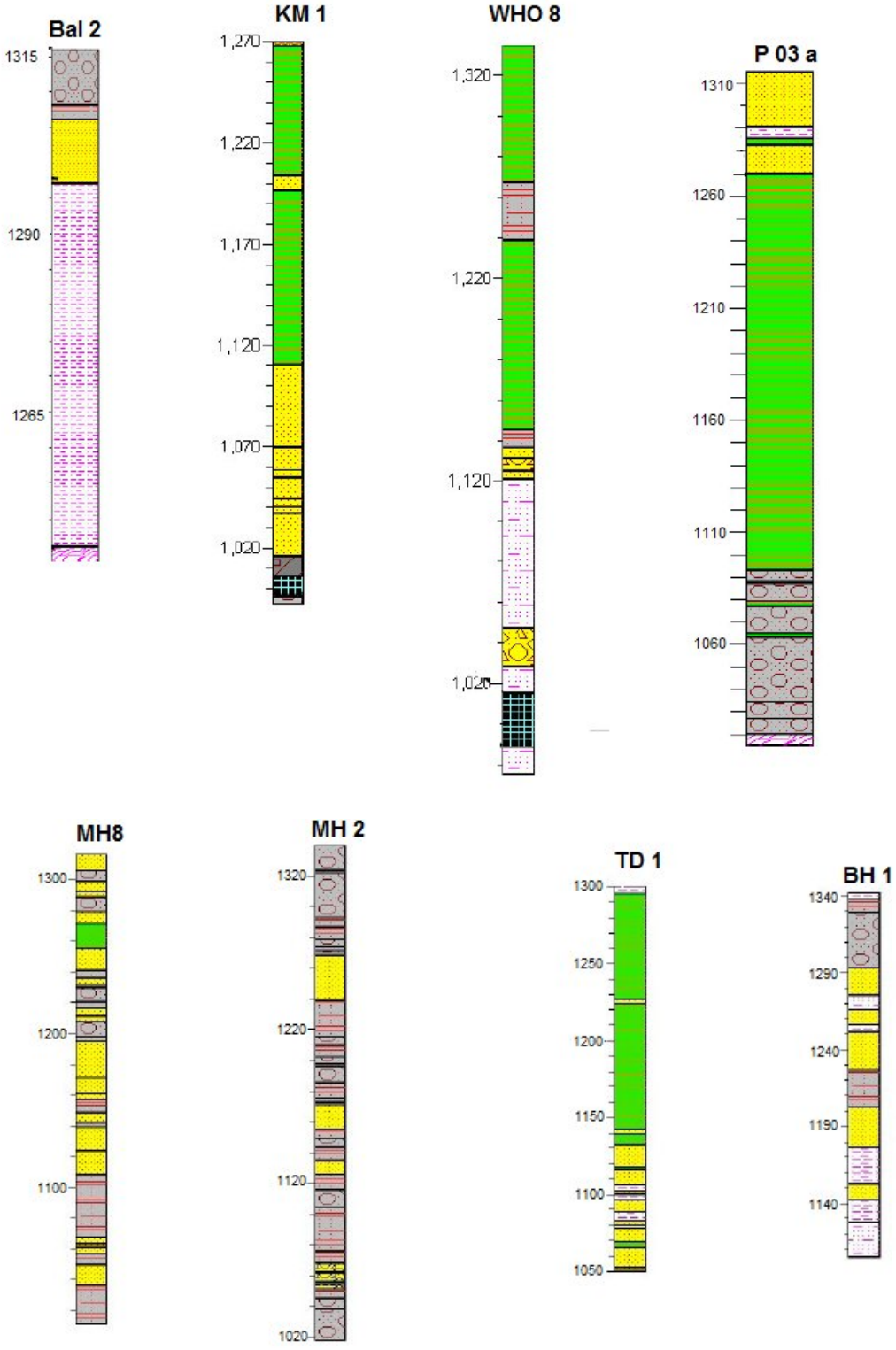
Bal 2
1315
1290
1265
KM 1
1,270
1,220
1,170
1,120
1,070
1,020
WHO 8
1,320
1,220
1,120
1,020
P 03 a
1310
1260
1210
1160
1110
1060
MH8
1300
1200
1100
MH 2
1320
1220
1120
1020
TD 1
1300
1250
1200
1150
1100
1050
BH 1
1340
1290
1240
1190
1140

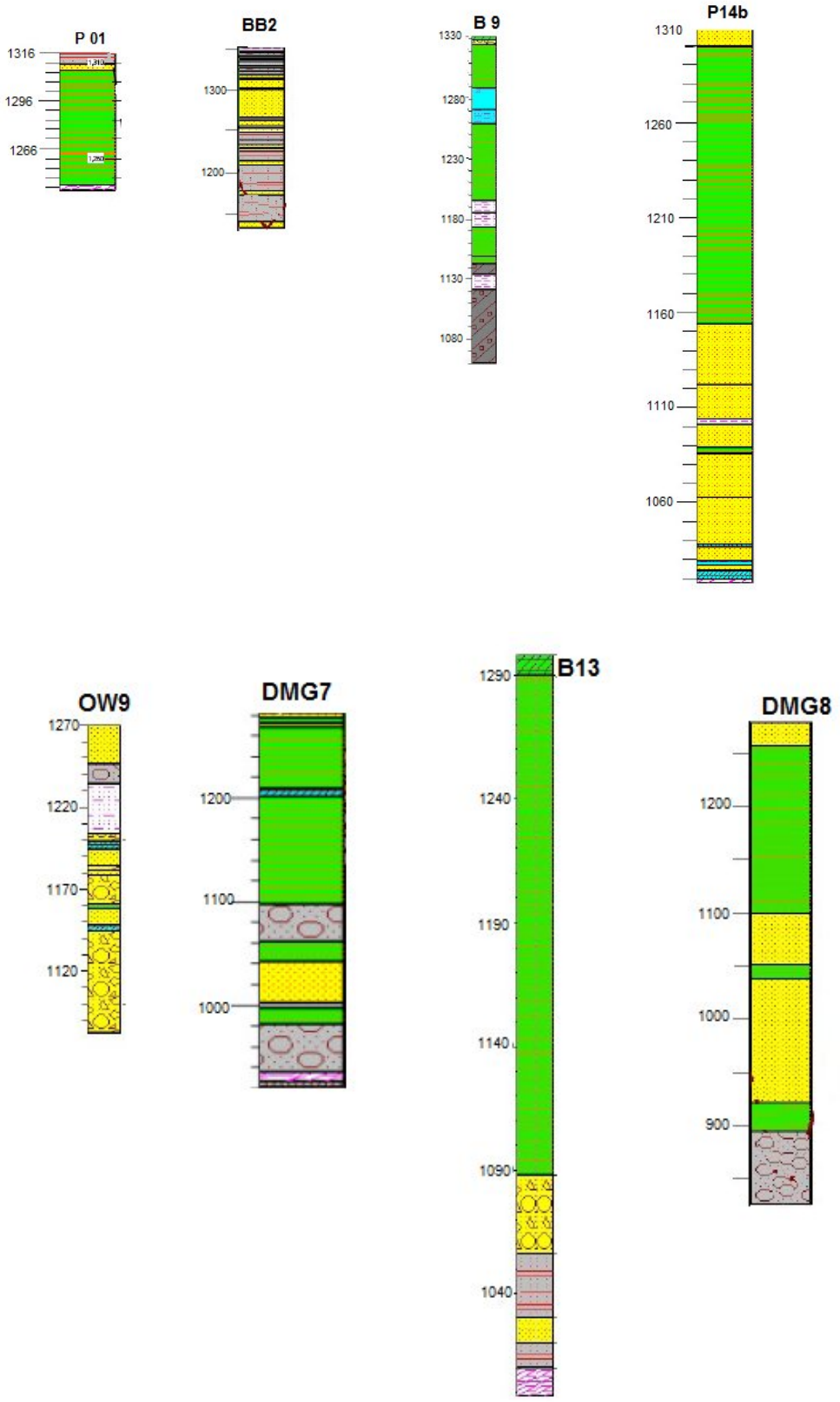
P 01
1316
1296
1266
BB2
1300
1200
B 9
1330
1280
1230
1180
1130
1080
P14b
1310
1260
1210
1160
1110
1060
OW9
1270
1220
1170
1120
DMG7
1200
1100
1000
B13
1290
1240
1190
1140
1090
1040
DMG8
1200
1100
1000
900

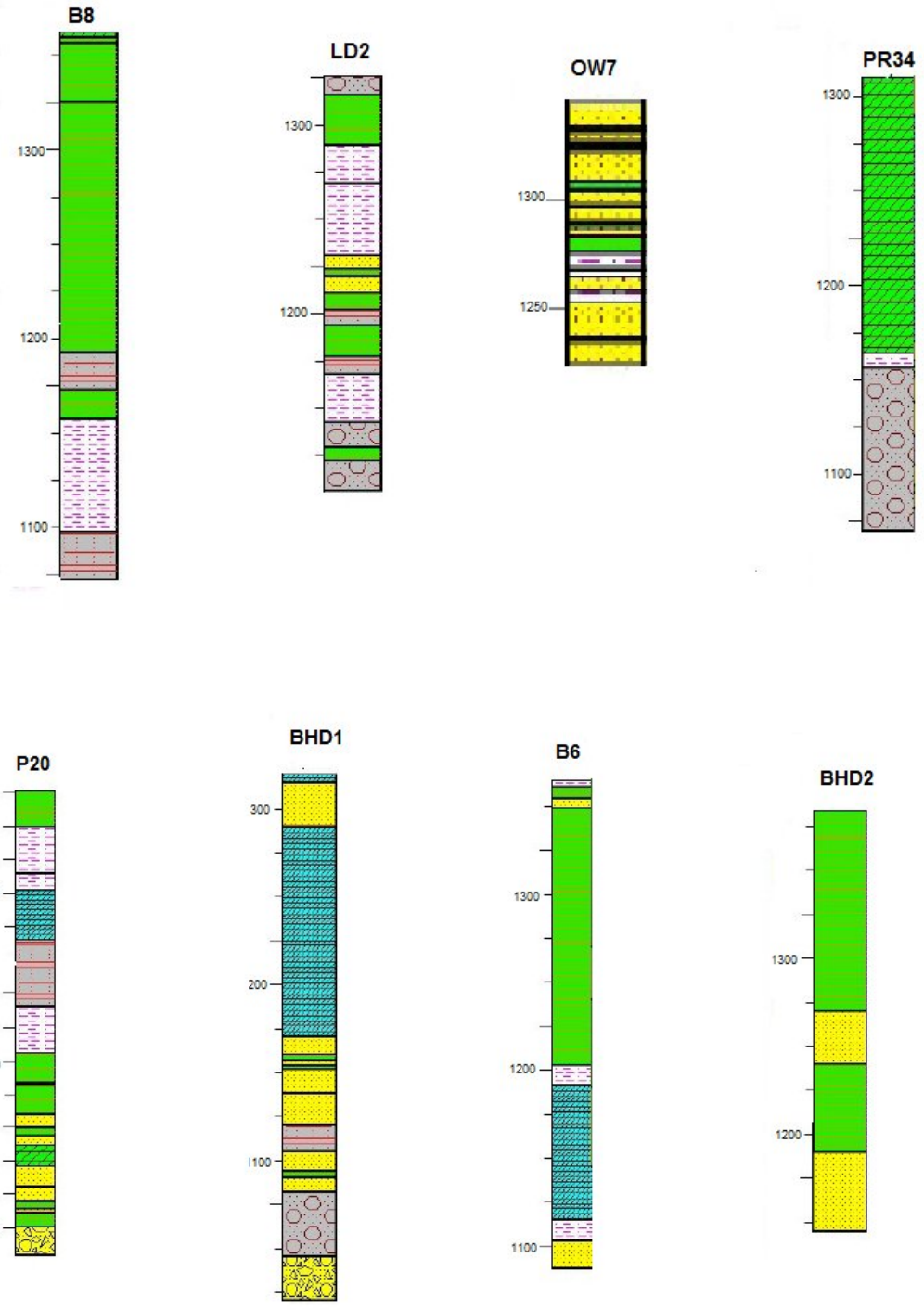
B8
1300
1200
1100
LD2
1300
1200
OW7
1300
1250
PR34
1300
1200
1100
P20
1300
1200
1100
BHD1
300
200
100
B6
1300
1200
1100
BHD2
1300
1200

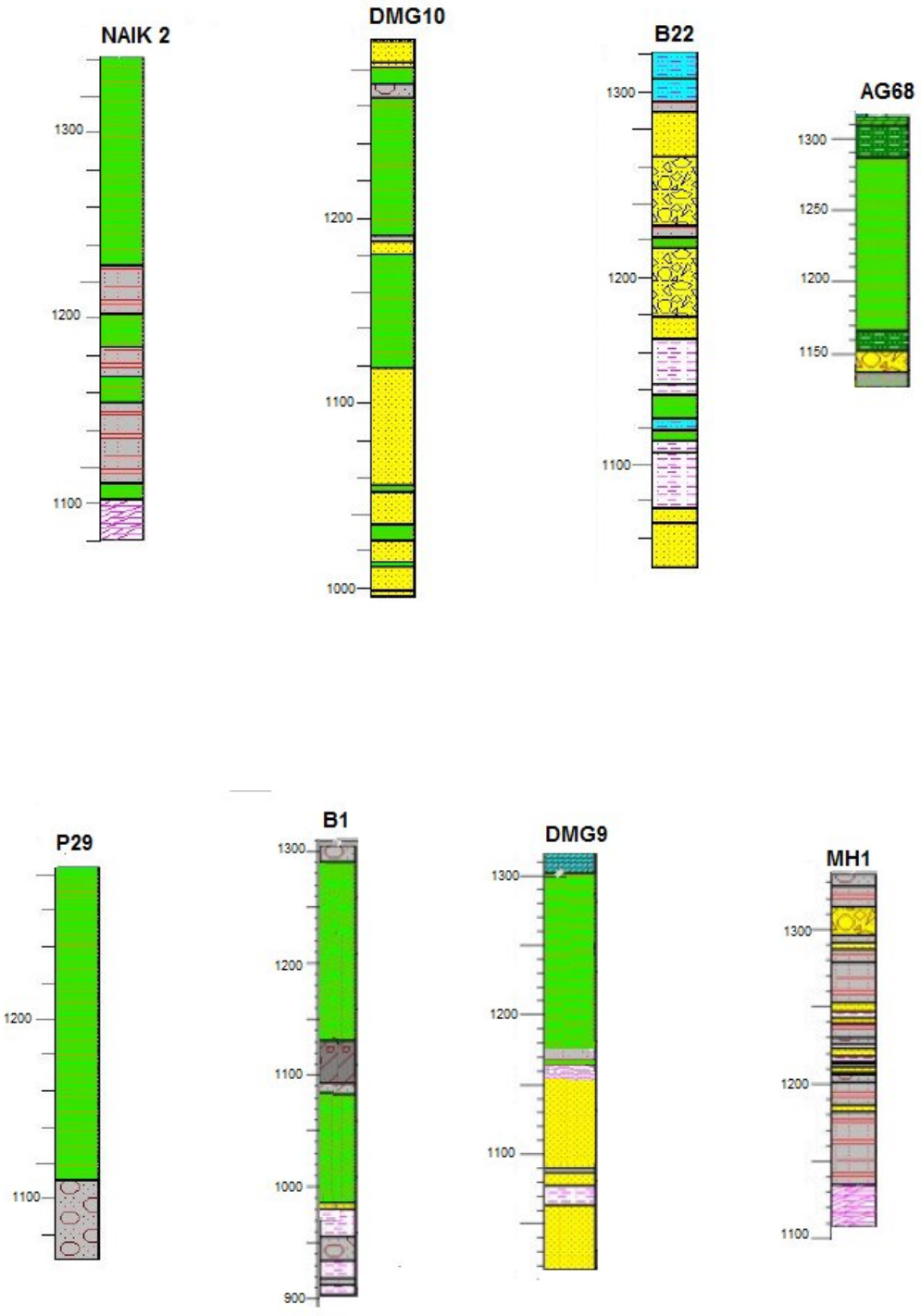
NAIK 2
1300
1200
1100
DMG10
1200
1100
1000
B22
1300
1200
1100
AG68
1300
1250
1200
1150
P29
1200
1100
B1
1300
1200
1100
1000
900
DMG9
1300
1200
1100
MH1
1300
1200
1100

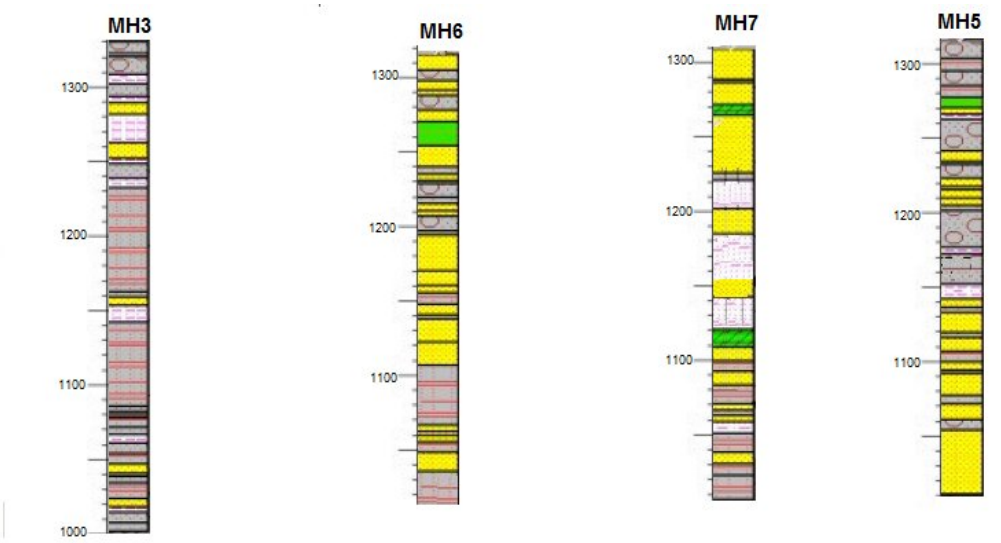
MH3
1300
1200
1100
1000
MH6
1300
1200
1100
MH7
1300
1200
1100
MH5
1300
1200
1100

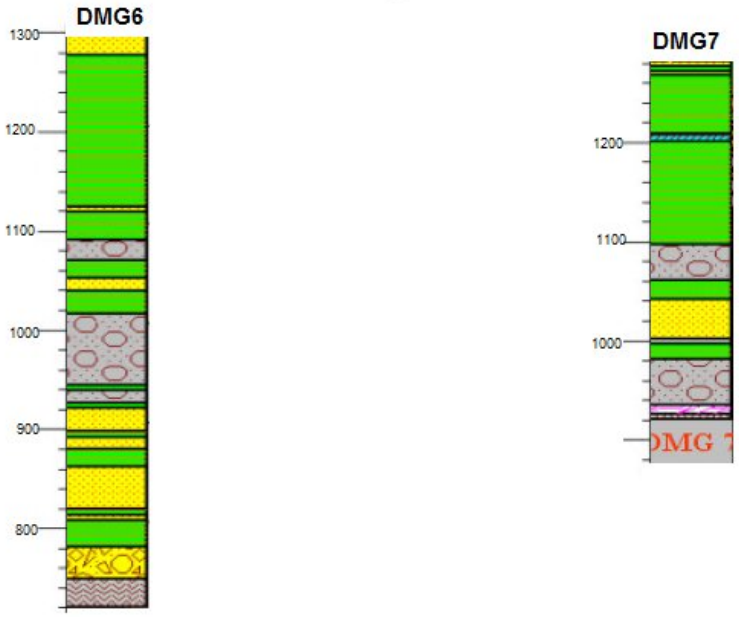
DMG6
1300
1200
1100
1000
900
800
DMG7
1200
1100
1000

LEGEND


Silt
Sand
Gravel
Clay
Silty clay
Silty sand
Silty gravel
Sandy silt
sandy clay
sandy gravel
clayey silt
clayey gravel
clayey sand
gravelly clay
gravelly sand
gravelly silt
weathered rock
Boulder & Gravel
Lignite
phyllite

Elevation data for Hydrogeological units Source: Piya, 2004

Bore ID	Locations	X	Y	elev_GL	elev_b_sa	elev_b_aqt	elev_b_da
B10/P21	Rabibhawan	627776	3064610	1304			1032
B13	Tahachal	628474	3065547	1298	1290	1090	1210
B15	Swambhunath	627793	3066279	1310	1305	1140	1098
B17	singh Durbar	630955	3065101	1300	1290	1165	1032
B19	Gaushala	632728	3066677	1315	1275	1210	1204
BB2	Bansbari	632688	3070725	1370	1325	1325	1140
B20	Katunje	639011	3061774	1335	1275	1220	1180
B24	Shanta Bhawan	628982	3063517	1295			1235
B25	Surendra Bhawan	628970	3063211	1310			1176
BAL2	Balaju	628460	3069017	1316	1297	1247	1247
BB1	Bansbari	632581	3070260	1366			1092
DK6	Mahankal chaur	633791	3068653	1320			1217
DMG6	Bhrikuti mandap	630250	3065300	1294	1284	1020	745
DMG 7	Teku kathmandu	628518	3064492	1279	1274	1099	933
DMG 5	Hyumat tole	628649	3065258	1285			800
GK5	Gokarna	639546	3070712	1345			1213
JP1	Jorpati	635688	3068070	1330			1200
MH1	Bramhakhel	640586	3068310	1335	1280	1280	1134
MK1	Mahadev Khola	628683	3069764	1270			1087
NAIK 1	Naikap	624638	3063901	1350			1138
NAIK 2	Naikap	624541	3063799	1340	1340	1230	1102
P 14b	Hotek Yak & yeti	630347	3066956	1310	1300	1154	1020
P 31b	Hortic Dev proj.	627686	3062524	1282	1278	1198	987
P4	Kathmandu, hatch	628423	3068644	1316			1179
P 01	Balaju Ind Dis.	628460	3069017	1315	1306	1245	1245
P 03a	Bottlers Nepal	628517	3068689	1315	1270	1093	1020
Paleo 1	Rabibhawan	627811	3064569	1303	1288	1095	1051
PH 3	Pharping	627575	3055700	1260	1225	1215	1058
PR 14	Rabibhawan	627808	3064561	1304			1052
PR 19	Bhakt. Woolen ind.	639249	3062254	1330			1075
PR 16	Nursing campus Sane	629043	3063538	1295			1247
NA 14	Airport Gulf Course	633715	3066092	1320			1105
KM 1	Kalimati, Soaltee	627766	3064886	1270	1270	1120	990
BHD 3	B & B hospital	631282	3061316	1319	1319	1150	1150
AG68	Patan Hospital	629879	3062149	1315	1315	1150	1126
OW 9	Gokarna	639546	3070712	1370	1345	1354	1180
WHO8	Bungmati	629250	3057850	1335	1335	1145	1075
DMG8	Shankhamul	631300	3063800	1280	1262	1100	835
WHO1	Mahankal Chaur	633475	3070150	1370	1320	1260	1220
OW7	Budanilkantha	632250	3072650	1335	1275	1270	1215
PR 34	Bhaktapur	639450	3062150	1310	1310	1180	1065
B8	Sunakothi	629875	3058240	1362	1358	1155	1070
BHD2	Sipadol, BKT	643620	3064300	1384	1384	1190	
B6	Bhaktapur	642850	3063950	1360	1355	1202	1085
LD2	Lubhoo	635075	3059475	1327	1315	1290	1110

Appendix A: Borehole and Hydrogeological information

Elevation data for Hydrogeological units Source: Piya, 2004

Bore ID	Locations	X	Y	elev_GL	elev_b_sa	elev_b_aqt	elev_b_da
P20	Naikap	623075	3064000	1362	1362	1340	1080
MH5	Manohara	637700	3066420	1315	1275	1270	1000
P35		627580	3060261	1275	1270	1187	1125
P37		631700	3060650	1320	1290	1055	950
B9		635075	3060675	1330	1330	1145	1060
TD1		636025	3062650	1300	1295	1030	
BH1		637652	3054512	1341	1290	1290	
PR33		632800	3068000	1320	1260	1165	
BHD1		640500	3062150	1320	1285	1170	
P29		630400	3064050	1285	1285	1112	
DMG9		632194	3063054	1315	1315	1175	
MH6		637361	3065830	1318	1270	1255	
MH7		638803	3067042	1310	1270	1265	
MH2		635250	2067116	1340	1295	1295	
MH3		637845	3066923	1330	1295	1295	

Control Points extracted from DEM

X	Y	elev_GL	t_sa	t_aqt	t_da	elev_b_sa	elev_b_aqt	elev_b_da
626100	3052320	1213.0	0.0	80.7	121.4	1213.0	1132.3	1010.9
625870	3053080	1274.0	0.0	79.1	119.6	1274.0	1194.9	1075.3
625339	3053719	1398.0	0.0	83.0	111.8	1398.0	1315.0	1203.2
625170	3054655	1526.0	0.0	82.4	114.2	1526.0	1443.6	1329.3
624470	3055356	1584.0	0.0	82.0	119.4	1584.0	1502.0	1382.6
624180	3055760	1629.0	0.0	81.5	124.5	1629.0	1547.5	1423.0
623711	3056465	1644.0	0.0	79.0	129.7	1644.0	1565.0	1435.3
623130	3056990	1689.0	0.0	76.1	135.9	1689.0	1612.9	1477.0
623010	3057400	1854.0	0.0	74.6	139.5	1854.0	1779.4	1639.8
623537	3057282	1755.0	0.0	78.1	141.9	1755.0	1676.9	1535.0
623770	3057632	1798.0	0.0	79.9	155.8	1798.0	1718.1	1562.2
624237	3056932	1708.0	0.0	79.2	137.6	1708.0	1628.8	1491.1
624879	3056173	1546.0	0.0	82.0	128.2	1546.0	1464.0	1335.8
624645	3057340	1635.0	0.0	80.6	151.2	1635.0	1554.4	1403.2
626279	3056523	1458.0	0.0	81.4	138.3	1458.0	1376.6	1238.3
627505	3057107	1266.0	3.1	70.0	170.9	1262.9	1192.9	1022.0
624587	3060668	1384.0	0.0	81.2	203.7	1384.0	1302.8	1099.1
623420	3060668	1530.0	0.0	81.5	191.4	1530.0	1448.5	1257.1
623362	3061368	1472.0	0.0	81.4	189.6	1472.0	1390.6	1201.0
622253	3062010	1517.0	0.0	77.6	169.4	1517.0	1439.4	1270.0
621611	3063120	1458.0	0.0	73.1	161.1	1458.0	1384.9	1223.8
620619	3063120	1547.0	0.0	78.3	161.1	1547.0	1468.7	1307.6
620210	3063878	1492.0	0.0	79.9	159.3	1492.0	1412.1	1252.8
619452	3063411	1734.0	0.0	81.7	159.6	1734.0	1652.3	1492.7
619218	3065221	1435.0	0.0	80.6	160.0	1435.0	1354.4	1194.3
619627	3065805	1463.0	0.0	75.2	156.1	1463.0	1387.8	1231.6
620327	3066389	1689.0	0.0	65.7	150.4	1689.0	1623.3	1472.9
621553	3066038	1467.0	0.0	67.1	149.0	1467.0	1399.9	1250.9
623011	3065922	1644.0	0.0	67.7	144.4	1644.0	1576.3	1432.0
624179	3065338	1392.0	0.0	60.9	147.6	1392.0	1331.1	1183.5
624295	3063820	1353.0	0.0	61.9	151.9	1353.0	1291.1	1139.2
624587	3063470	1383.0	0.0	66.0	161.9	1383.0	1317.0	1155.2
624937	3064637	1336.0	0.0	63.5	147.2	1336.0	1272.5	1125.3
624704	3065571	1345.0	0.0	63.8	134.3	1345.0	1281.2	1146.9
624120	3066564	1330.0	0.0	66.9	153.5	1330.0	1263.1	1109.7
625521	3067206	1390.0	0.0	21.6	186.5	1390.0	1368.4	1181.9
626046	3068023	1337.0	3.6	22.5	193.1	1333.4	1310.8	1117.7
626688	3068257	1310.0	8.6	32.2	192.8	1301.4	1269.3	1076.5
626688	3069307	1348.0	18.1	36.8	175.6	1329.9	1293.2	1117.5
627213	3069483	1330.0	24.5	46.2	151.4	1305.5	1259.2	1107.8
627913	3069424	1451.0	35.5	58.0	123.5	1415.5	1357.5	1234.0
628438	3069658	1312.0	46.5	31.5	147.8	1265.5	1234.0	1086.2
627855	3070241	1331.0	36.2	22.4	148.0	1294.8	1272.4	1124.4
627271	3070825	1335.0	27.6	16.9	145.2	1307.4	1290.5	1145.3
626513	3071993	1352.0	19.7	10.1	141.8	1332.3	1322.2	1180.4

Control Points extracted from DEM

X	Y	elev_GL	t_sa	t_aqt	t_da	elev_b_sa	elev_b_aqt	elev_b_da
626980	3072401	1347.0	19.6	8.6	145.4	1327.4	1318.8	1173.4
627855	3072810	1363.0	16.8	8.8	156.5	1346.2	1337.4	1180.9
626863	3073627	1378.0	16.0	7.9	144.6	1362.0	1354.0	1209.5
627622	3074153	1382.0	14.4	10.9	156.3	1367.6	1356.7	1200.4
628322	3074445	1400.0	14.8	11.1	154.3	1385.2	1374.1	1219.8
629489	3074736	1392.0	16.6	10.8	142.4	1375.4	1364.6	1222.2
630306	3075028	1389.0	19.1	9.9	139.0	1369.9	1360.0	1221.0
631415	3076021	1538.0	18.1	8.5	126.8	1519.9	1511.4	1384.5
634974	3074503	1623.0	19.1	7.5	113.0	1603.9	1596.4	1483.4
634858	3072868	1492.0	40.4	5.0	113.7	1451.6	1446.6	1332.9
635733	3071934	1413.0	36.2	9.7	106.7	1376.8	1367.1	1260.4
636725	3070884	1357.0	44.0	13.5	113.4	1313.0	1299.4	1186.0
637250	3072518	1444.0	20.9	11.9	104.2	1423.1	1411.2	1307.0
639818	3071117	1373.0	46.3	8.3	91.8	1326.7	1318.3	1226.5
640576	3071818	1395.0	33.9	8.6	91.3	1361.1	1352.5	1261.1
641860	3070815	1400.0	27.1	8.5	88.8	1372.9	1364.4	1275.6
643261	3070825	1490.0	19.8	8.2	78.3	1470.2	1462.0	1383.7
643436	3069599	1431.0	17.2	10.3	99.9	1413.8	1403.5	1303.6
644778	3069483	1405.0	17.2	8.4	93.8	1387.8	1379.4	1285.5
641860	3066330	1418.0	33.3	14.1	199.3	1384.7	1370.6	1171.3
642969	3065980	1449.0	38.1	20.1	183.9	1410.9	1390.8	1206.8
644836	3065863	1382.0	22.4	80.6	147.0	1359.6	1279.0	1132.0
644953	3064112	1348.0	41.0	75.2	163.8	1307.0	1231.8	1067.9
646003	3063353	1404.0	14.2	108.9	172.8	1389.8	1280.9	1108.1
646178	3062069	1385.0	0.0	121.8	187.5	1385.0	1263.2	1075.7
646528	3061368	1408.0	0.0	123.0	188.0	1408.0	1285.0	1097.0
645711	3060201	1424.0	0.0	124.3	186.9	1424.0	1299.7	1112.8
645070	3059442	1458.0	0.0	120.3	190.2	1458.0	1337.7	1147.5
643319	3069675	1414.0	17.5	10.1	93.5	1396.5	1386.4	1292.9
642210	3059967	1389.0	0.0	108.4	177.4	1389.0	1280.6	1103.2
641043	3060376	1377.0	0.0	101.2	171.4	1377.0	1275.8	1104.4
639584	3061485	1341.0	0.0	110.3	136.2	1341.0	1230.7	1094.4
640109	3060084	1444.0	0.0	110.3	160.0	1444.0	1333.7	1173.7
640518	3059617	1488.0	0.0	110.2	168.6	1488.0	1377.8	1209.2
639993	3058741	1555.0	0.0	120.1	159.8	1555.0	1434.9	1275.1
637838	3058625	1415.0	0.0	126.3	156.8	1415.0	1288.7	1131.9
636842	3057982	1388.0	0.0	108.2	174.6	1388.0	1279.8	1105.3
635733	3057457	1436.0	6.6	65.1	187.0	1429.4	1364.4	1177.4
635266	3056873	1533.0	10.9	25.7	199.0	1522.1	1496.4	1297.4
636083	3055647	1467.0	13.7	15.1	210.7	1453.3	1438.1	1227.4
636958	3055881	1561.0	10.1	46.0	203.2	1550.9	1504.8	1301.7
636083	3054772	1487.0	15.6	7.1	218.4	1471.4	1464.3	1246.0
636900	3054305	1557.0	14.5	19.0	216.0	1542.5	1523.5	1307.5
636316	3052495	1748.0	14.0	27.9	210.9	1734.0	1706.1	1495.1
635266	3054013	1499.0	15.8	9.5	222.5	1483.2	1473.7	1251.2
633865	3054597	1432.0	15.5	10.6	229.4	1416.5	1406.0	1176.6
633749	3052904	1535.0	14.4	17.6	214.7	1520.6	1503.0	1288.3

Control Points extracted from DEM

X	Y	elev_GL	t_sa	t_aqt	t_da	elev_b_sa	elev_b_aqt	elev_b_da
631415	3053254	1479.0	14.9	17.8	205.9	1464.1	1446.3	1240.4
630247	3053254	1495.0	11.4	30.5	188.1	1483.6	1453.1	1264.9
629197	3052845	1453.0	6.3	48.5	158.0	1446.7	1398.1	1240.1
628322	3051561	1496.0	0.0	73.1	140.7	1496.0	1422.9	1282.2
627271	3051795	1346.0	0.0	77.1	130.4	1346.0	1268.9	1138.4
627797	3052320	1407.0	0.0	71.0	135.1	1407.0	1336.0	1201.0
628380	3052145	1416.0	0.0	66.4	142.1	1416.0	1349.6	1207.5
626338	3052845	1228.0	0.0	78.6	121.8	1228.0	1149.4	1027.6
625871	3053721	1347.0	0.0	80.8	118.2	1347.0	1266.2	1148.0
626629	3054246	1333.0	0.0	75.8	118.4	1333.0	1257.2	1138.8
625988	3054597	1410.0	0.0	80.0	117.4	1410.0	1330.0	1212.6
625637	3055589	1485.0	0.0	81.7	119.5	1485.0	1403.3	1283.8
626863	3055589	1318.0	0.0	77.8	115.6	1318.0	1240.2	1124.6
627680	3055356	1264.0	0.0	68.2	121.0	1264.0	1195.8	1074.8
628618	3054772	1348.0	6.8	46.6	158.9	1341.2	1294.6	1135.7
629080	3053604	1430.0	7.4	43.3	162.3	1422.6	1379.3	1217.0
630072	3054671	1394.0	13.7	20.5	211.5	1380.3	1359.8	1148.3
629255	3055356	1412.0	11.5	30.4	197.6	1400.5	1370.1	1172.5
628614	3055998	1365.0	8.6	46.8	169.9	1356.4	1309.6	1139.7
627388	3055998	1267.0	0.0	74.1	121.9	1267.0	1192.9	1071.0
628688	3056873	1397.0	10.8	47.3	201.8	1386.2	1338.9	1137.1
628789	3056698	1410.0	11.3	43.9	201.2	1398.7	1354.8	1153.6
629956	3056523	1432.0	17.8	16.8	233.5	1414.2	1397.4	1163.9
630773	3056173	1431.0	18.1	5.0	247.2	1412.9	1407.9	1160.7
632056	3055706	1454.0	16.4	5.0	248.9	1437.6	1432.6	1183.7
633457	3055998	1400.0	14.0	12.7	231.3	1386.0	1373.4	1142.1
634157	3057224	1379.0	9.4	50.0	206.1	1369.6	1319.6	1113.5
632232	3057515	1344.0	12.0	23.7	233.8	1332.0	1308.3	1074.5
630423	3057807	1384.0	21.9	15.7	249.5	1362.1	1346.3	1096.8
628789	3058041	1371.0	10.5	55.4	226.4	1360.5	1305.2	1078.8
627388	3058975	1306.0	0.0	86.4	232.4	1306.0	1219.6	987.2
626396	3060609	1298.0	0.0	91.1	245.3	1298.0	1206.9	961.6
628147	3060668	1291.0	0.0	94.7	203.1	1291.0	1196.3	993.2
629489	3060493	1312.0	0.0	88.3	182.0	1312.0	1223.7	1041.6
630831	3060318	1339.0	10.9	142.8	189.2	1328.1	1185.4	996.2
632465	3059500	1341.0	2.7	137.7	219.9	1338.3	1200.6	980.7
633749	3058916	1340.0	0.0	141.8	223.6	1340.0	1198.3	974.6
635033	3058508	1322.0	0.0	105.1	193.1	1322.0	1216.9	1023.8
635324	3058975	1347.0	0.0	114.6	177.2	1347.0	1232.4	1055.2
633224	3059092	1334.0	0.0	159.0	223.2	1334.0	1175.0	951.9
631940	3059033	1318.0	5.8	73.0	237.1	1312.2	1239.2	1002.1
630364	3059033	1354.0	11.0	18.0	249.0	1343.0	1325.0	1076.1
628905	3059033	1349.0	4.9	63.5	227.9	1344.1	1280.6	1052.8
627330	3059033	1305.0	0.0	86.1	233.1	1305.0	1218.9	985.8
626513	3060084	1310.0	0.0	89.6	241.3	1310.0	1220.4	979.0
627797	3060084	1359.0	0.0	87.8	240.2	1359.0	1271.2	1031.0
629314	3060084	1300.0	0.0	75.4	205.7	1300.0	1224.6	1018.9

Control Points extracted from DEM

X	Y	elev_GL	t_sa	t_aqt	t_da	elev_b_sa	elev_b_aqt	elev_b_da
630656	3060142	1341.0	9.4	117.8	194.9	1331.6	1213.9	1018.9
632348	3060084	1324.0	4.3	152.2	213.1	1319.7	1167.5	954.4
633807	3059967	1316.0	0.0	149.7	215.7	1316.0	1166.3	950.5
635208	3059792	1325.0	0.0	119.9	189.5	1325.0	1205.1	1015.6
637250	3059734	1335.0	0.0	128.6	140.6	1335.0	1206.4	1065.8
638592	3060843	1351.0	0.0	117.9	124.4	1351.0	1233.1	1108.7
636958	3060843	1340.0	0.0	134.9	107.3	1340.0	1205.1	1097.8
635324	3060726	1323.0	3.4	136.7	150.6	1319.6	1182.9	1032.4
633515	3060726	1305.0	0.0	150.7	214.3	1305.0	1154.3	940.0
631064	3060843	1327.0	13.1	156.1	178.0	1313.9	1157.7	979.7
629255	3060843	1296.0	0.0	99.5	159.0	1296.0	1196.5	1037.5
627563	3060843	1321.0	0.0	95.4	227.0	1321.0	1225.6	998.6
626338	3060785	1324.0	0.0	91.1	243.3	1324.0	1232.9	989.7
623945	3062127	1375.0	0.0	78.6	198.2	1375.0	1296.4	1098.2
625696	3062361	1368.0	0.0	78.1	205.9	1368.0	1289.9	1083.9
627330	3062302	1288.0	0.0	81.7	167.2	1288.0	1206.3	1039.1
629022	3062244	1325.0	0.0	124.6	85.5	1325.0	1200.4	1115.0
630656	3062244	1327.0	24.0	137.8	138.2	1303.0	1165.2	1027.0
631881	3062244	1295.0	12.0	146.8	188.8	1283.0	1136.2	947.3
633399	3062186	1298.0	4.2	148.4	184.5	1293.8	1145.4	960.9
635208	3062361	1314.0	19.4	195.9	59.8	1294.6	1098.7	1038.9
636842	3062302	1305.0	0.0	153.2	84.5	1305.0	1151.8	1067.3
638417	3062244	1308.0	0.0	108.3	126.1	1308.0	1199.7	1073.6
640576	3062127	1340.0	0.0	76.3	182.1	1340.0	1263.7	1081.6
642152	3062010	1319.0	2.1	64.8	178.4	1316.9	1252.1	1073.7
644078	3062010	1367.0	0.0	105.3	181.1	1367.0	1261.7	1080.6
645303	3062010	1369.0	0.0	123.9	183.3	1369.0	1245.1	1061.8
645128	3063587	1376.0	28.2	91.2	170.0	1347.8	1256.6	1086.6
643786	3063528	1328.0	43.3	46.5	176.3	1284.7	1238.2	1061.9
642035	3063528	1342.0	19.0	18.9	205.0	1323.0	1304.0	1099.0
640635	3063528	1322.0	14.8	30.8	220.9	1307.2	1276.4	1055.5
639351	3063470	1318.0	12.7	39.1	183.1	1305.3	1266.2	1083.1
638009	3063295	1310.0	16.0	79.4	135.7	1294.0	1214.6	1078.9
636550	3063295	1331.0	5.1	127.2	99.0	1325.9	1198.7	1099.8
635441	3063236	1324.0	14.6	192.0	52.4	1309.4	1117.4	1065.0
634157	3063355	1300.0	27.9	153.7	114.9	1272.1	1118.4	1003.5
632582	3063353	1299.0	23.6	151.0	144.7	1275.4	1124.4	979.7
630831	3063353	1294.0	24.1	158.4	127.2	1269.9	1111.5	984.3
629489	3063295	1315.0	11.0	108.1	131.9	1304.0	1195.9	1064.0
627913	3063003	1290.0	0.0	86.9	136.6	1290.0	1203.1	1066.5
626221	3063120	1352.0	0.0	79.9	178.6	1352.0	1272.1	1093.6
626046	3064112	1299.0	0.0	74.8	167.1	1299.0	1224.2	1057.2
626980	3063995	1294.0	0.0	109.5	150.1	1294.0	1184.5	1034.4
628263	3063878	1283.0	0.0	121.1	141.3	1283.0	1161.9	1020.5
629781	3063820	1298.0	16.0	139.8	148.3	1282.0	1142.2	994.0
631123	3063820	1296.0	21.2	155.7	187.1	1274.8	1119.1	931.9
632407	3063820	1304.0	37.8	153.6	130.4	1266.2	1112.7	982.3

Control Points extracted from DEM

X	Y	elev_GL	t_sa	t_aqt	t_da	elev_b_sa	elev_b_aqt	elev_b_da
633865	3063762	1307.0	35.9	146.5	120.2	1271.1	1124.6	1004.4
634974	3063387	1324.0	25.8	185.9	61.1	1298.2	1112.3	1051.3
636608	3063411	1328.0	7.2	119.0	104.1	1320.8	1201.8	1097.7
638359	3063411	1315.0	17.9	67.7	145.6	1297.1	1229.4	1083.8
639759	3063470	1324.0	12.3	33.7	198.0	1311.7	1278.0	1080.0
641101	3063470	1335.0	15.2	28.2	214.7	1319.8	1291.6	1076.9
642677	3063353	1349.0	21.8	24.6	189.4	1327.2	1302.6	1113.2
644311	3063295	1333.0	32.3	74.4	174.3	1300.7	1226.3	1052.0
644369	3064637	1358.0	58.9	45.6	161.8	1299.1	1253.5	1091.8
642969	3064637	1333.0	48.6	13.0	188.2	1284.4	1271.4	1083.2
641160	3064579	1373.0	29.4	14.1	246.1	1343.6	1329.6	1083.5
639468	3064462	1368.0	33.8	15.0	220.6	1334.2	1319.2	1098.6
637717	3064462	1347.0	54.0	47.2	143.1	1293.0	1245.8	1102.7
635791	3064462	1308.0	39.5	89.8	92.1	1268.5	1178.6	1086.6
634216	3064462	1312.0	60.4	140.4	85.9	1251.6	1111.2	1025.3
632757	3064462	1305.0	32.9	151.3	121.0	1272.1	1120.9	999.9
630831	3064579	1306.0	21.6	168.0	199.1	1284.4	1116.4	917.3
629255	3064637	1295.0	18.2	181.4	178.1	1276.8	1095.5	917.3
627505	3064637	1310.0	0.0	157.0	113.8	1310.0	1153.0	1039.2
625871	3064812	1337.0	0.0	69.3	147.3	1337.0	1267.7	1120.4
625404	3065805	1309.0	0.0	64.3	119.3	1309.0	1244.7	1125.4
626829	3065746	1306.0	0.0	59.4	141.4	1306.0	1246.6	1105.2
627908	3065524	1306.0	2.4	167.4	140.2	1303.6	1136.2	996.0
629465	3065413	1306.0	22.1	188.7	260.9	1283.9	1095.2	834.3
631189	3065524	1302.0	27.6	185.5	138.1	1274.4	1088.9	950.8
632690	3065469	1311.0	34.5	145.2	103.6	1276.5	1131.2	1027.6
633969	3065413	1343.0	43.8	122.6	87.1	1299.2	1176.7	1089.6
635415	3065524	1335.0	48.4	28.9	100.3	1286.6	1257.7	1157.4
636861	3065469	1314.0	50.7	7.6	148.8	1263.3	1255.7	1106.9
638140	3065469	1352.0	53.5	12.6	79.2	1298.5	1285.9	1206.8
639752	3065413	1383.0	46.8	10.0	242.7	1336.2	1326.2	1083.4
641865	3065413	1341.0	38.1	7.3	221.4	1302.9	1295.6	1074.2
640364	3066247	1370.0	43.4	10.1	221.3	1326.6	1316.5	1095.2
638807	3066469	1324.0	50.3	10.6	165.4	1273.7	1263.1	1097.7
637250	3066580	1348.0	47.0	7.5	174.8	1301.0	1293.5	1118.7
635637	3066580	1343.0	50.1	27.2	128.7	1292.9	1265.7	1137.0
634470	3066580	1309.0	52.1	91.6	67.4	1256.9	1165.4	1098.0
632913	3066691	1330.0	49.4	132.3	75.4	1280.6	1148.3	1072.9
631022	3066802	1315.0	22.4	157.5	154.2	1292.6	1135.1	980.9
629410	3066802	1318.0	26.3	183.7	225.8	1291.7	1108.1	882.2
628131	3066802	1309.0	4.8	136.9	200.8	1304.2	1167.3	966.4
627130	3067692	1304.0	3.2	38.9	209.7	1300.8	1261.9	1052.2
628353	3067692	1295.0	13.4	169.3	147.4	1281.6	1112.3	964.9
629465	3067636	1306.0	40.5	144.7	190.7	1265.5	1120.8	930.1
630633	3067581	1313.0	37.2	85.5	205.0	1275.8	1190.3	985.3
632245	3067581	1305.0	48.6	120.4	87.9	1256.4	1136.0	1048.1
633524	3067581	1341.0	68.5	128.4	41.7	1272.5	1144.0	1102.4

Control Points extracted from DEM

X	Y	elev_GL	t_sa	t_aqt	t_da	elev_b_sa	elev_b_aqt	elev_b_da
634492	3067469	1326.0	66.3	112.1	45.9	1259.7	1147.6	1101.7
636249	3067469	1321.0	48.4	19.4	154.2	1272.6	1253.3	1099.0
637639	3067469	1378.0	41.2	11.6	195.9	1336.8	1325.2	1129.4
639085	3067358	1328.0	46.3	10.3	171.0	1281.7	1271.4	1100.4
639863	3068192	1353.0	46.7	8.2	136.7	1306.3	1298.1	1161.4
638418	3068136	1387.0	41.8	10.9	187.4	1345.2	1334.3	1146.9
637027	3068081	1341.0	42.8	15.0	180.9	1298.2	1283.1	1102.3
635693	3068192	1344.0	49.5	49.9	132.7	1294.5	1244.7	1111.9
634525	3068190	1346.0	63.3	108.3	63.0	1282.7	1174.4	1111.5
633358	3068303	1314.0	65.7	105.1	62.6	1248.3	1143.2	1080.6
631850	3068359	1327.0	45.2	83.3	129.7	1281.8	1198.5	1068.8
630244	3068303	1323.0	53.8	68.7	188.1	1269.2	1200.5	1012.4
629465	3068303	1305.0	46.9	117.3	156.0	1258.1	1140.8	984.8
629632	3069248	1309.0	56.3	48.2	164.0	1252.7	1204.6	1040.6
630911	3069248	1333.0	56.5	47.5	169.6	1276.5	1228.9	1059.4
632301	3069192	1344.0	52.0	64.9	133.6	1292.0	1227.1	1093.5
633802	3069303	1331.0	61.2	61.5	105.8	1269.8	1208.3	1102.5
635359	3069248	1354.0	50.9	46.7	125.3	1303.1	1256.4	1131.1
636861	3068970	1326.0	48.1	19.4	158.9	1277.9	1258.5	1099.7
638251	3069081	1351.0	57.3	11.4	145.5	1293.7	1282.2	1136.7
639641	3068914	1369.0	52.3	8.5	125.8	1316.7	1308.2	1182.3
641420	3069192	1347.0	29.1	9.1	112.1	1317.9	1308.9	1196.7
642977	3069081	1351.0	18.2	12.2	113.1	1332.8	1320.6	1207.5
640975	3070471	1378.0	35.8	8.2	93.1	1342.2	1334.0	1240.9
638366	3070860	1375.0	60.0	9.2	95.7	1315.0	1305.7	1210.1
634470	3071137	1346.0	78.3	11.7	109.8	1267.7	1256.1	1146.2
632913	3071860	1374.0	77.4	10.5	130.8	1296.6	1286.1	1155.3
631467	3072027	1331.0	60.7	12.7	147.0	1270.3	1257.6	1110.6
629576	3072249	1327.0	26.1	14.2	156.2	1300.9	1286.7	1130.6
628965	3073527	1342.0	16.1	12.0	154.1	1325.9	1314.0	1159.9
630633	3074305	1381.0	22.2	10.1	137.8	1358.8	1348.8	1211.0
631967	3072971	1359.0	48.4	9.2	136.9	1310.6	1301.4	1164.4
633858	3072916	1402.0	49.4	7.1	116.6	1352.6	1345.5	1228.9
627519	3063579	1311.0	0.0	108.1	139.7	1311.0	1202.9	1063.2
620735	3065191	1397.0	0.0	78.7	157.0	1397.0	1318.3	1161.3
621514	3064302	1401.0	0.0	75.2	162.2	1401.0	1325.8	1163.6
623182	3064524	1356.0	0.0	58.9	149.1	1356.0	1297.1	1148.1
622737	3063079	1400.0	0.0	66.2	169.2	1400.0	1333.8	1164.7
624294	3062301	1374.0	0.0	76.3	195.6	1374.0	1297.7	1102.1
630355	3060189	1344.0	6.9	101.7	193.5	1337.1	1235.4	1041.8
630466	3058966	1350.0	11.8	17.6	251.4	1338.2	1320.6	1069.2
629298	3059355	1312.0	4.8	55.7	242.2	1307.2	1251.5	1009.3
628687	3060135	1351.0	0.0	82.7	210.0	1351.0	1268.3	1058.3
628353	3058299	1331.0	5.4	69.2	231.5	1325.6	1256.5	1025.0
630133	3058077	1394.0	23.1	22.9	250.0	1370.9	1348.0	1098.0
630522	3059578	1343.0	8.4	53.5	223.0	1334.6	1281.2	1058.2
629910	3061634	1333.0	9.1	125.8	120.0	1323.9	1198.1	1078.1

Control Points extracted from DEM

X	Y	elev_GL	t_sa	t_aqt	t_da	elev_b_sa	elev_b_aqt	elev_b_da
629243	3062412	1325.0	5.3	122.0	103.0	1319.7	1197.8	1094.7
631411	3061634	1306.0	13.7	149.9	176.2	1292.3	1142.4	966.2
630021	3056465	1438.0	17.8	15.3	234.3	1420.2	1404.8	1170.5
630577	3057410	1399.0	20.7	11.4	249.8	1378.3	1366.9	1117.1
626240	3052130	1259.0	0.0	80.6	122.5	1259.0	1178.4	1055.8
628186	3061078	1284.0	0.0	100.1	180.7	1284.0	1183.9	1003.2
629688	3055576	1411.0	14.3	19.6	216.1	1396.7	1377.2	1161.0
628798	3064357	1287.0	9.5	163.2	146.9	1277.5	1114.3	967.4
629521	3069581	1310.0	62.3	31.6	163.3	1247.7	1216.1	1052.8
628520	3071638	1320.0	29.1	10.8	157.6	1290.9	1280.0	1122.5
630967	3075472	1422.0	18.8	9.0	136.9	1403.2	1394.2	1257.3
630855	3063801	1291.0	19.7	157.2	177.0	1271.3	1114.1	937.1
634748	3072305	1397.0	52.5	5.7	111.6	1344.5	1338.8	1227.2
631745	3062912	1292.0	21.7	152.8	166.4	1270.3	1117.5	951.1
636910	3069192	1325.0	50.0	18.1	150.5	1275.0	1256.9	1106.4
633524	3061912	1298.0	3.8	149.0	187.8	1294.2	1145.2	957.4
640030	3067581	1328.0	43.1	8.7	158.9	1284.9	1276.1	1117.2
635471	3062023	1308.0	15.6	189.5	66.4	1292.4	1102.9	1036.5
626463	3061745	1350.0	0.0	85.5	217.5	1350.0	1264.5	1047.1
631634	3058466	1321.0	9.8	31.6	229.8	1311.2	1279.5	1049.8
632245	3059911	1330.0	4.7	143.3	216.4	1325.3	1182.0	965.7
633802	3061622	1298.0	2.6	151.4	188.8	1295.4	1144.0	955.2
635359	3063301	1329.0	16.0	193.0	51.9	1313.0	1120.0	1068.1
634525	3065302	1320.0	52.7	98.7	82.6	1267.3	1168.6	1086.0
635804	3065246	1320.0	47.9	28.8	116.1	1272.1	1243.4	1127.3
636416	3063690	1337.0	16.0	117.1	96.9	1321.0	1203.9	1107.0
638084	3063912	1316.0	32.9	55.6	144.6	1283.1	1227.5	1082.9
639029	3064913	1347.0	45.2	15.5	178.1	1301.8	1286.3	1108.1
638251	3062579	1306.0	4.0	100.1	127.3	1302.0	1201.9	1074.6
630299	3056465	1437.0	18.4	10.5	240.5	1418.6	1408.0	1167.6

Notes:
t_sa: thickness of shallow aquifer
elev_GL: Elevation of Ground Level
t_aqt : thickness of aquitard
t_da: thickness of deep aquifer
elev_b_sa: Elevation of bottom of shallow aquifer
elev_b_aqt: Elevation of bottom of aquitard
elev_b_da: Elevation of bottom of deep aquifer

APPENDIX

B

PUMPING WELLS DETAILS

Appendix B: Pumping wells details

Northern Groundwater District

ID	Location	X	Y	Depth (m)	screen (mbgl)								
KV3	Katunje	636637	3062405	150	60-70	77-82	102-127	139-148					
kv12	Jorpati	635024	3068288	61									
kv14	Maharajhunj	630706	3068735	215	113-119	128-132	137-185	210-213					
kv16	maharajgunj	630704	3066730	205									
kv25	Jorpati	636169	3066688	73									
kv31	Baljuwatar	631643	3067749	275	194-205	212-221	231-234	244-247	253-259	265-272			
kv38	lazimpat	631712	3068852	260	209-234	235-240	242-254						
kv51	Gothatar	635538	3068885	186									
kv52	Panipokhari	630701	3068384	200	125-143	149-155	164-176						
kv58	gangabu	629146	3068849	200									
p7	maharajgunj	631162	3068839	250	160-172	178-196							
kv95	Bkt	640509	3062409	290									
kv96	Maharajgunj	631270	3069162	140									
kv100	Libali, bkt	642285	3062229	238									
kv109	Gokarna	637934	3067975	80	23-29	35-42	72-79						
kv110	Gokarna	638017	3067963	81	23-35	72-78							
kv111	Gokarna	637983	3067991	81	60-78								
kv112	Gokarna	637903	3067945	80	33-43	61-67	73-77						
kv113	Gokarna	636011	3067771	74	31-37	41-47	62-68						
kv114	Gokarna	637067	3067003	82	35-47	74-79							
kv124	Jorpati	636554	3069151	85									
M5	Duwakot	640000	3065000	200									
M8	Phutung	630000	3072000	103									
M10	Kapan	635000	3070000	104									
M11	Danchhi	64000	3068000	125									
kv138	Jorpati	636481	3069283	76									
kv140	Jorpati	636481	3069283	79									
kv145	NEA TC	643923	3064050	280	112-118	124-130	181-187	211-217	223-235	241-259	271-277		
kv154	Baluwatar	631298	3068131	250	117-135	215-218	226-234	241-244					
Bal 1a	Balaju	629052	3069237	219	79-86	100-139							
Bal 1b	Balaju	630077	3069112	158	84-87	104-107	110-137	142-157					
BB2	Bansbari	632856	3070894	190	86-92	98-100	106-118	129-143	170-179	184-190			
BB1a	bansbari	632603	3070341	239	63-84.5	118-123	129-134	151-156	167-178	184-189	222-233		
BB1b	Bansbari	632607	3070334	242	81-87	123-123	127-157	169-182	186-193	209-227	236-242		
JW2	Bansbari	632613	3070340	230	122-140	170-176	182-192	221-224					
BH solar	Bhaktapur	637923	3064835		94-100	109-121							
BH1	Bode	637652	3064835	175	41-57	75-86	92-110	139-169					
BH3a	Bode	638206	3064948	151	53-92	96-102	115-146						
BH4a	Bode	638051	3065402	161	45-51	52-57	63-97	120-126	132-155				
BH3b	Bode	638203	3064939	153	56-74	98-104	115-146						
BH BB1	Chaling	644032	3064255	240	81-87	119-143	201-231						
BB3	Budhanilkantha	633601	3072622	145	06-93	102-123	132-142						
BB0	Dhapasi	632065	3070581	239	63-85	118-123	129-134	151-156	167-178	184-189	222-233		
DK3a	Dhobikhola	634772	3058681	188	22-38	125-142	160-177	177-182					
DK3b	Dhobikhola	635781	3058657	238	121-144	157-168	177-183	215-232					
DK 4b	Dhobikhola	634648	3058367	163	113-159								
BB2	Galfutar	632888	3070953	190	54-86	92-98	100-108	118-129	143-170	179-184			
BB6a	Gangabu	630895	3070559	196	33-38	55-60	85-107	145-196					
Bb6b	Gangabu	630778	3070510	206	84-105	117-120	129-138	145-154	160-169	172-178	181-202		
BB7	gangabu	630396	3069513	253	85-189	211-217	223-250						
BB5	gangabu	630417	3069835	206	92-104	132-139	146-200						
BB3	gangabu	631156	3071464	101	24-30	39-50	51-57	73-77	77-95				
BB4	gangabu	630878	3070980	235	20-31	39-50	84-90	94-99	120-165	170-175	188-229		
BB5	gangabu	630564	3070149	250	78-102	140-152	161-167	170-215	133-244				
BB AW	gangabu	630077	3069112	198	110-151	185-191							
DK2	kapan	633804	3067731	36	11-22	22-33							
DK9	Kapan	634209	3068307	54	12-18	38-49							

Appendix B: Pumping wells details

ID	Location	X	Y	Depth (m)	screen (mbgl)								
DK6	kapan	633776	3068701	35	13-24								
DK8	kapan	633745	3067704	34									
BH2b	madhyapur	637648	3064520	217.6	25-41	81-85	88-96	99-109	188-197	203-208			
MK1	mahadev Khola	628719	3069781	177	106-109	120-123	129-133	136-160	164-170				
MK2	mahadev Khola	629444	3070115	250	85-108	125-146							
MK3	mahadev Khola	628393	3070305	224	99-107	129-132	146-172	185-202	212-215				
DK1	mahankalchaur	633708	3067757	72	37-42	46-64							
DK3	Mahankal chaur	633804	3067731	65	43-59								
DK7	Mahankal chaur	633945	3067989	55	35-46								
MH2	Mulpani	636250	3067116	306	41-46	61-73	75-102	125-131	138-212	224-264	270-289	295-302	
MH6a	Mulpani	637353	3065837	196	22-39	56-78	81-93	98-104	110-116	118-149	170-192		
MH5b	Mulpani	637361	3065830	194	79-91	106-112	120-126	133-145	167-173	176-188			
MH4	Mulpani	637539	3066570	237	20-26	30-41	58-63	72-83	94-148	155-161	169-174	185-234	
MH5	Mulpani	637772	3066170	202	53-75	75-114	114-125	129-141	148-164	174-195			
MH3a	Mulpani	637545	3066923	323	45-50	70-92	107-123	130-148	158-169	174-180	202-235	246-252	263-314
MH3b	Mulpani	637536	3066932	287	81-93	131-149	163-169	174-180	220-235	275-282			
MH7	Mulpani	638803	3067042	267	20-37	42-81	120-165	176-187	190-210	219-225	247-258	258-263	
GK5	Nayapati	639494	3070029	105	36-42	47-53	53-59	80-85	89-95	95-100			
GK3a	Nayapati	639457	3070753	259	50-81	91-104	109-120	130-137	140-153	170-180	200-218	220-237	250-259
Gk4	Nayapati	639770	3070183	249	40-57	107-116	151-156	172-180	200-241	241-247			
GK2b	Nayapati	639080	3070292	199	51-54	57-65	69-87	96-105	110-134	137-140	154-176	186-192	
GK3	Nayapati	639186	3070175	251	37-43	48-59	70-125	125-138	138-143	143-161	161-222	222-234	234-246
JW1	Panipokhari	630788	3068453	246	138-168	234-240							
KV200	Jorpati	636583	3067891	136									
kv201	Jorpati	636567	3067901	55									
H34	Baudha	634131	3067910	267	210-225	227-264							

Central Groundwater District

ID	Location	X	Y	Depth (m)	screen (mbgl)								
P11	Lainchaur	629580	3067246	245	175-178	207-222	225-235	237-241					
kv6	Naradevi	628980	3056161	258									
kv7	Gwarko	631406	3061441	213									
kv13	Chhauni	627575	3066501	161									
kv17	Newroad	629364	3065758	306	214-220	224-235	242-248	253-265	274-285	288-300			
kv18	BID	628608	3066498	300									
kv19	BID	628507	3068495	260									
kv22	lainchaur	630053	3067616	275									
P18a	Tahachal	627470	3065609	312	191-204	215-228	243-256	264-278	285-289	295-305			
kv32	Naxal	630627	3066695	277	192-210	214-227	231-234	236-239	242-245	254-268	268-273		
kv37	Tripureshwor	629592	3064878	305									
kv39	Sanothimi	635885	3063260	300									
kv41	lainchaur	629918	3067218	260	200-242								
kv43	Tripureshwor	630006	3064771	260	193-199	210-213	217-226	232-257					
kv44	Sanothimi	635581	3063741	250									
DMG01	Tripureshwor	629622	3064747	260	209-227	233-257							
DMG02	Pachali	628941	3064858	302	190-201	207-229	235-246	257-296					
DMG03	Teku	628537	3064608	302	171-174	180-189	191-216	220-227	234-253	258-297			
DMG04	Hyumat tole	628556	3065253	300	190-196	201-204	209-229	234-253	265-282	286-299			
DMG05	Hyumat tole	628549	3065258	451	296-338	345-354	364-424	430-450					
DMG06	Bhrikutimandap	630250	3065300	570									
DMG07	Teku	628518	3064492	359	186-214	216-228	236-254	260-280	297-339				
DMG08	Sankhamul	631578	3063054	455	183-230	244-360	388-443						
DMG09	Koteswor	632194	3063054	305									
DMG10	Tinkune	633088	3063054	305									
DMG11	Herbs	633762	3062703	305									
DMG12	Tikathali	633395	3061705	300									
DMG13	Balkumari	632412	3062051	300									
DMG14	Imadol	632756	3062226	300									
kv47	Pulchowk	630130	3062924	250	118-124	130-136	142-166	172-178	184-190	196-208			
kv50	battisputali	632527	3065897	270	202-211	219-231	234-240	243-255	258-265				
kv64	Kupandol	629951	3064050	226									
kv72	Kalimati	627942	3064546	252	218-243	252-276							
kv73	kirtipur	627605	3062361	300	130-136	202-208	217-220	240-243	249-252	262-292			
P13	Darbarmarg	630013	3066597	293									
PR03	Darbarmarg	630010	3066582	303	193-205	217-223	227-233	236-242	245-251	268-274	276-274	276-288	294-300
P12	Bijeswari	628415	3066778	67									
AG34	Tripureshwor	630226	3064439	220									
kv75	Darbarmarg	630045	3066553	360	192-210	216-222	240-258	297-303	324-330	336-342			
kv76	Darbarmarg	630040	3066547	303	193-205	217-223	227-233	236-242	245-251	268-274			
H35	battisputali	632608	3065813	258	202-214	219-231	234-241	244-258	259-265				
kv77	Lazimpat	630348	3067710	260	206-248								
PR04	Lainchaur	629730	3067240	299	202-214	217-229	237-267	273-291					
PR06	Lazimpat	630587	3067687	211	106-118	196-211							
kv79	Lazimpat	630524	3067523	270	204-215	219-231	240-249	252-258	261-264				
H30	Laldurbar	630339	3066490	262	198-208	217-223	231-239	245-253					
AG35	Lazimpat	630463	3067301	220									
NA01	Lazimpat	630466	3067782	170									
P15	Darbarmarg	630229	3065467	262	190-197	221-224	229-259						
P17	Kalimati	627389	3065516	318	191-204	215-228	243-258	264-268	286-289	295-308			
P18	Tahachal	627423	3065491	300	207-244	270-273	278-299						
P140	Darbarmarg	630642	3066623	293	190-208	214-220	226-229	238-250	253-265	277-280			
kv89	Minbhawan	632310	3063711	253									
kv86	Lainchaur	630057	3067916	275									

Appendix B: Pumping wells details

ID	Location	X	Y	Depth (m)	screen (mbgl)								
kv97	Subidanagar	632913	3063740	250									
kv98	Hariharbhawan	629961	3063060	130									
kv99	Dhobighat	628891	3062057	245									
kv116	Sanepa	629015	3063253	75									
kv126	Kamalpokhari	631032	3066456	272									
AG37	Newroad	629564	3065535	240									
kv127	Thapathali	630225	3064123	300	207-225	234-240	246-252	260-266	270-276				
kv131	bagdarbar	629539	3065231	300	206-214	220-229	236-244	247-260	274-287	293-296			
M3	Thaiba	634000	3056000	46									
M4	Lubhu	635000	3059000	225									
kv135	Putalisadak	630558	3065225	265	203-228	234-259							
kv137	Naradevi	628941	3066177	258	213-219	225-255							
kv138	Thimi	635478	3062480	250	187-193	205-211	224-230	236-248					
kv144	NEA	630108	3065851	310	212-219	226-232	236-244	260-272	279-291	294-306			
kv146	Pulchowk	630392	3063230	250	186-198	206-244							
kv147	Patan Dhoka	630359	3062806	300									
kv153	Tripureshwor	629815	3064461										
kv155	Bhadrakali	300	630230	3E+06	225-261	365-277	281-293						
kv156	Singhdurbar	631042	3064672	306	226-232	237-243	247-261	266-300					
kv158	Thapathali	630323	3064200	256									
JW4	Jadibuti	633804	3062724	230	200-212	215-227							
KM1	Kalimati	627772	3064875	260	202-230	233-253							
BH-LK1	Lokanthali	634015	3062463	251	172-176	185-194	200-212	215-245					
P32	Dhobighat	626777	3062099	220	132-205								
kv181	Lagankhel	630540	3061808	250	176-214	220-244							
P25	Sinamangal	634617	3064158	255	192-210	215-243	249-252						
kv183	Naxal	631322	3067145	250	195-244								
kv184	Naxal	631311	3067142	200									
kv189	Bhadrakali	630491	3065058	300	195-204	208-217	237-255	262-274	282-300				
kv192	Thapathali	631113	3064162	280	196-202	208-214	220-225	231-246	249-255	265-268			
kv193	Babarmahal	631108	3064155	200									
kv196	Gorkha army	629439	3057284	200	209-227	232-257							
kv197	Pulchowk	630211	3063054	250	151-170	181-193	199-238						
kv209	Sanothimi	635423	3063589	257	212-243	248-253							
kv210	Satdobato	631199	3060820	300	181-184	188-191	195-207	211-217	254-290				
kv214	kamaladhi	630246	3068120	262	188-208	217-203	231-239	245-253					
kv215	Sanothimi	636556	3062454	250									
kv216	Teku	628990	3064801	300	203-209	214-217	220-223	232-244	251-269	272-284	288-294		
kv219	Balaju	628716	3068548	31	25-Dec								
kv227	Kalimati	628384	3065281	250									
kv231	Kings way	630385	3066586	300	186-207	214-227	233-248	251-257	268-271				

Southern Groundwater District

ID	Location	X	Y	Depth (m)	Screen (mbgl)								
kv49	satungal	628420	3068219	160	123-138	150-159							
P35	Chobar	627580	3060261	153	119-149								
kv87	Chobar	628081	3061661	130	62-80	88-106	112-130						
M1	Taudaha	627000	3061000	171	M								
M2	Sunakothi	630000	3058000	230	M								
M6	kalanki	625500	3062000										
M7	Balanbhu	624000	3064000	147	M								
PH2	Bungmati	628993	3054932	90	37-55	65-84							
PH1a	Pharping	627490	3055707	178	71-173								
JW3	Sundarighat	627758	3062547	284	234-246	252-258	268-280						
kv220	Kirtipur	626606	3062945	300	156-174	202-214	270-294						

APPENDIX

C

WATER LEVEL MEASUREMENT DATA

Appendix C: Static water level measurement data

Static water Level Measurement data (March 2001)

Well Id	Location	Depth	X Coord	Y Coord	Well Alt	mgbl	masl
M1	Taudaha	171	627000	3061000	1299.5	5.42	1294.08
M3	Thaiba	46	634000	3056000	1399	43.06	1355.94
M4	Lubhoo	225	636000	3059000	1372	30.21	1341.79
G 17	Patan Hospital	250	630540	3061808	1319	11.16	1307.84
G 16	Tripureswor		629815	3064461	1282	1.12	1280.88
G 13	Baluwatar	250	631221	3068112	1324.6	22.73	1301.87
H 17	Hotel soltee	304	627423	3065491	1298	6.65	1291.35
P 22	BID, Balaju	253	628615	3068509	1306.3	13	1293.3
P15	Naikap	262	626600	3063850	1309.1	2.14	1306.96
BB hal	Halchowk		626646	3067518	1309	0	1309
DO 137	PID, patan	302	630905	3061121	1322	32.8	1289.2
M6	kalanki		625500	3062000	1294	0	1294
DK 1	Mahankal	92	633708	3057757	1335	30.18	1304.82
DK 2	Kapan	62	633804	3067731	1335.4	0.02	1335.38
DK 8	Kapan	34	633745	3067707	1336	2.71	1333.29
MH 6a	Mulpani	198	637361	3065830	1314.4	1.1	1313.3
GK 2a	Nayapati	149	639083	3072297	1342	17.62	1324.38
GK 5	Nayapati	164	638494	3070029	1351	25.85	1325.15
GK 4	Nayapati	248	638776	3070183	1341.6	19.13	1322.47
M5	Duwakot	200	640000	3065000	1392.8	93.3	1299.5
M11	Dhanchi	125	640000	3068000	1313.1	16.8	1296.3

Appendix C: Static water level measurement data

Static water Level Measurement data (March 2002)

Well Id	Location	Depth	X	Y	Well Alt	mgbl	masl
M1	Taudaha	171	627000	3061000	1299.5	8.17	1291.33
M3	Thaiba	46	634000	3056000	1399	42.25	1356.75
M4	Lubhoo	225	636000	3059000	1372	30.25	1341.75
G 17	Patan Hospital	250	630540	3061808	1319	10.57	1308.43
G 16	Tripureswor		629815	3064461	1282	1.08	1280.92
G 13	Baluwatar	250	631221	3068112	1324.6	29.57	1295.03
H 17	Hotel soltee	304	627423	3065491	1298	6.64	1291.36
P 22	BID, Balaju	253	628615	3068509	1306.3	15.63	1290.67
P15	Naikap	262	626600	3063850	1309.1	1.76	1307.34
BB hal	Halchowk		626646	3067518	1309	0	1309
DO 137	PID, patan	302	630905	3061121	1322	29.12	1292.88
M6	kalanki		625500	3062000	1294	0	1294
DK 1	Mahankal	92	633708	3057757	1335	29.47	1305.53
DK 2	Kapan	62	633804	3067731	1335.4	0	1335.4
DK 8	Kapan	34	633745	3067707	1336	2.84	1333.16
MH 6a	Mulpani	198	637361	3065830	1314.4	1.27	1313.13
GK 2a	Nayapati	149	639083	3072297	1342	21.11	1320.89
GK 5	Nayapati	164	638494	3070029	1351	28.33	1322.67
GK 4	Nayapati	248	638776	3070183	1341.6	22.5	1319.1
M5	Duwakot	200	640000	3065000	1392.8	92.5	1300.3
M11	Dhanchi	125	640000	3068000	1313.1	16.28	1296.82

APPENDIX

D

METEOROLOGICAL DATA

Appendix D: Meteorological data

Precipitation (mm)

Month	Jan	Feb	Mar	Apr	May	Jun	Jul	Aug	Sep	Oct	Nov	Dec	Total
Thankot	20.28	25.30	40.17	70.99	146.52	292.57	512.93	444.58	276.49	69.24	10.49	17.72	1927.28
Godavari	19.62	22.59	31.58	62.74	123.18	297.94	508.04	443.13	256.84	65.03	8.15	18.36	1857.22
Khumaltar	15.93	18.93	27.20	52.92	100.84	206.34	312.33	251.27	154.45	59.00	5.76	14.94	1219.91
Kathmandu airport	14.94	18.72	33.84	54.34	115.39	256.77	375.09	324.85	183.87	55.90	7.69	13.07	1454.47
Sakhu	13.74	23.95	30.31	56.06	156.56	312.70	543.79	531.04	284.78	65.87	9.71	11.16	2039.67
Panipokhari	13.14	15.46	27.91	75.75	121.43	265.91	392.59	359.92	196.67	58.05	8.43	11.56	1546.83
Nagarkot	18.41	19.34	30.34	56.10	145.90	317.95	483.59	475.25	280.17	73.18	9.31	11.28	1920.81
Khopasi	17.71	18.67	31.50	53.41	128.79	237.39	354.30	279.45	200.03	59.50	11.28	12.09	1404.11
Bhaktapur	15.18	20.98	32.42	55.69	138.07	247.50	386.37	355.29	188.59	57.89	5.89	14.94	1518.81
Chagunarayan	18.09	21.58	28.70	59.53	151.46	250.27	426.32	404.85	217.03	59.18	8.62	15.25	1660.87
Chapagaun	17.83	17.37	28.43	50.89	95.38	226.77	393.58	326.88	182.85	44.63	4.78	19.11	1408.49
Budhanilkantha	15.55	20.03	38.72	66.94	192.82	339.07	546.23	503.42	239.09	54.68	7.85	9.62	2034.02
Khokana	22.1	20.6	33.1	63.1	118.7	252.3	357.9	298.1	153.1	44.7	9.3	10.2	1383.29
Sundarijal	30.91	16.33	37.90	57.02	197.29	323.75	654.58	614.77	290.20	48.31	12.18	8.42	2291.65
Lele	28.4	21.5	32.8	60.8	125.0	319.4	571.8	474.8	238.7	63.9	13.7	20.1	1970.55
Naikap	17.6	14.5	38.0	58.2	143.0	206.5	413.8	382.6	163.9	41.7	1.9	11.5	1493.2
Sundarijal	10.6	12.3	30.5	54.0	168.9	249.3	586.0	585.6	229.6	43.4	2.3	9.5	1981.9
Nagarjun	18.7	14.1	37.8	64.4	135.9	214.2	454.4	390.5	185.8	46.8	0.0	3.1	1565.40
Tikathali	27.6	20.6	42.5	70.9	138.4	195.4	369.7	330.5	166.4	57.0	3.0	5.6	1427.52
Averall average	18.75	19.10	33.35	60.20	139.14	263.79	454.91	409.31	215.19	56.20	7.38	12.49	1689.79

Potential Evapotranspiration

Month	Jan	Feb	Mar	Apr	May	Jun	Jul	Aug	Sep	Oct	Nov	Dec
Khumaltar	1.72	2.56	3.80	4.38	4.44	4.53	4.07	4.21	3.56	3.06	2.37	1.62
Airport	3.61	4.50	5.39	5.69	5.48	5.08	4.48	5.00	4.09	4.20	3.95	3.23
Avearge (mm/day)	2.67	3.53	4.59	5.03	4.96	4.80	4.27	4.61	3.83	3.63	3.16	2.42
Monthly ET	82.63	98.89	142.38	151.01	153.63	144.08	132.49	142.76	114.79	112.53	94.80	75.10

APPENDIX

E

CALCULATION OF HYDRAULIC HEAD DUE TO ABSTRACTION

Appendix E: Calculation of decline of hydraulic head due to abstraction

Northern Groundwater District

Obs Point	Hydraulic Head at		Decline due to pumping (m)
	2001 pumping	2009 Pumping	
Obs1	1383.56	1383.44	0.12
Obs2	1366	1364.63	1.37
Obs3	1342.01	1338.94	3.07
Obs4	1348.16	1345.71	2.45
G13	1310.41	1295.03	15.38
Obs23	1324.42	1321.26	3.16
Obs13	1326.57	1325.95	0.62
Obs14	1314.62	1314.28	0.34
GK5	1314.78	1322.67	-7.89
GK4	1315.04	1314.92	0.12
GK2	1315.43	1315.3	0.13
Obs22	1317.36	1317.25	0.11
Obs24	1316.33	1316.22	0.11
MH6	1312.7	1313.13	-0.43
Obs12	1310.19	1308.2	1.99
M5	1319.44	1318.25	1.19
Obs26	1317.99	1315.96	2.03
DK8	1340.32	1338.78	1.54
DK2	1339.95	1338.44	1.51
Obs27	1323.25	1321.82	1.43
Obs28	1326.48	1324.86	1.62
Obs29	1329.13	1327.45	1.68
Obs36	1346.11	1343.51	2.6
		Avearge	1.5

Appendix E: Calculation of decline of hydraulic head due to abstraction

Central Groundwater District

Obs Point	Head at		Decline due to pumping (m)
	2001 pumping	2009 Pumping	
P22	1300	1293.81	6.19
H17	1299.73	1291.68	8.05
Bbhal	1294.45	1287.34	7.11
Obs23	1324.42	1321.26	3.16
Obs5	1323.46	1320.35	3.11
Obs6	1292.38	1285.98	6.4
Obs7	1305.93	1300.57	5.36
M4	1312.85	1308.07	4.78
Do137	1315.29	1309.02	6.27
G17	1309.38	1302.67	6.71
Obs10	1298.82	1291.13	7.69
P15	1296.31	1288.47	7.84
Obs11	1293.37	1285.58	7.79
G16	1279.46	1271.27	8.19
Dk1	1314.95	1305.53	9.42
Obs30	1298.3	1295.82	2.48
Obs31	1317.24	1314.16	3.08
Obs32	1329.58	1326.05	3.53
Obs33	1312.15	1308.37	3.78
Obs34	1329.46	1326.05	3.41
Obs42	1278.78	1270.69	8.09
Obs43	1279.75	1272.09	7.66
Obs44	1298.14	1292.05	6.09
Obs45	1291.07	1284.21	6.86
M11	1320.14	1316.02	4.12
Obs53	1299.34	1292.94	6.4
Obs57	1309.09	1304.1	4.99
		Average	5.87

Appendix E: Calculation of decline of hydraulic head due to abstraction

Southern Groundwater District

Obs Point	Head at		Decline due to pumping (m)
	2001 pumping	2009 Pumping	
Obs 16	1322.91	1318.01	4.9
Obs19	1318.65	1313.49	5.16
Obs9	1320.51	1315.65	4.86
M3	1319.38	1314.54	4.84
Obs8	1315.1	1310.58	4.52
Obs19	1318.65	1313.49	5.16
Obs17	1320.95	1315.98	4.97
Obs18	1312	1305.55	6.45
M6	1306.15	1298.74	7.41
M1	1315.74	1306.73	9.01
Obs38	1324.11	1319.4	4.71
Obs39	1321.89	1317.03	4.86
Obs40	1321.44	1316.53	4.91
Obs46	1317.05	1311.95	5.1
Obs47	1319.12	1314.27	4.85
Obs48	1314.37	1308.87	5.5
Obs49	1325.53	1320.9	4.63
Obs50	1326.01	1321.5	4.51
		Average	5.35